PhD thesis

Alteration in the Wnt microenvironment directly regulates molecular events leading to pulmonary senescence

Tamás Kovács

PhD Supervisors: Prof. Dr. Judit E. Pongrácz

Dr. Krisztián Kvell

PhD Program Leader: Prof. Dr. Péter Németh

University of Pécs

Department of Pharmaceutical Biotechnology

Pécs

2015

Table of contents

1. Abbreviations

αSMA	Alpha smooth muscle actin
Abs-	Antibodies
ADRP-	Adipose differentiation-related protein
AP-1-	Activator protein-1
APC-	Adenomatous polyposis coli
ATI	Alveolar type I cell
ATII	Alveolar type II cell
BAT	Brown Adipose Tissue
BIM	BCL2 like protein 11
BMP-	Bone morphogenetic protein
CaMKII-	Ca-Calmodulin Kinase II
COPD	Chronic obstructive pulmonary disease
Dvl-	Dishevelled
EpCAM	Epithelial cell adhesion molecule
FCS	Fetal calf serum
FGM	Fibroblast growth medium
FITC	Fluorescein iso-thyocianate
Fz-	Frizzled
GFP	Green fluorescent protein
Glut4	Glucose transporter type 4
GMCSF	Granulocyte-Monocyte colony stimulating factor
GSK-3-	Glycogen synthase kinase 3
HE	Hematoxylin-eosin staining
LEF1-	Lymphoid Enhancer-binding Factor 1
LRP5/6-	Low density lipoprotein Related Protein 5 and 6
MMP	Matrix Metalloproteinases
MSC	Mesenchymal stem cell
NAD	Nicotinamid dinucleotide
NFAT-	Nuclear Factor of Activating T- cells
NFκB-	Nuclear Factor kappa B
NHLF	Normal human lung fibroblast
NLK	Nemo like kinase

pAb-	Polyclonal antibody
PCP-	Planar cell polarity pathway
PCR-	Polymerase chain reaction
PPARγ	Peroxisome proliferator-activated receptor
PPRE	PPAR responsive element
PTHrP	Parathyreoid hormone related protein
qRT-PCR-	Quantitative real-time polymerase chain reaction
RT-	Reverse transcription
SAEC	Small airway epithelial cell
SAGM	Small airway growth medium
SEMA-	Semaphorin domain
SHH	Sonic hedgehog
SPC	Surfactant protein C
TAK1-	Transforming growth factor β–Activated Kinase 1
TCF1, TCF3-	T-cell Factor 1, 3
TEP1	Thymus epithelial cell line
TG	Triglycerides
TGFβ	Transforming growth factorβ
Thy-1	Glycosylphosphytidylinositol-linked cell-surface glycoprotein
TNFα	Tumor necrosis factorα
WAT	White Adipose Tissue

2. Introduction

2.1 Aging –an overview

The elderly population is increasing with an unprecedented rate within this century putting an enormous pressure on healthcare, labor market and pension system alike.
The EU27 population is projected to become older with the median age expected to rise from 40.4 years in 2008 to 47.9 years by 2060. The proportion of people aged 65 years or over in the total population is estimated to increase from 17.1% (84.6 million in 2008) to 30.0% (151.5 million) in 2060.
Similarly, the number of people aged 80 years or over is likely to triple by 2060 reaching the number of nearly 62 million (Scherbov *et al.*). To provide at least partial solutions for the increasing problem of aging and age related diseases in developed societies, intensive molecular studies are needed.

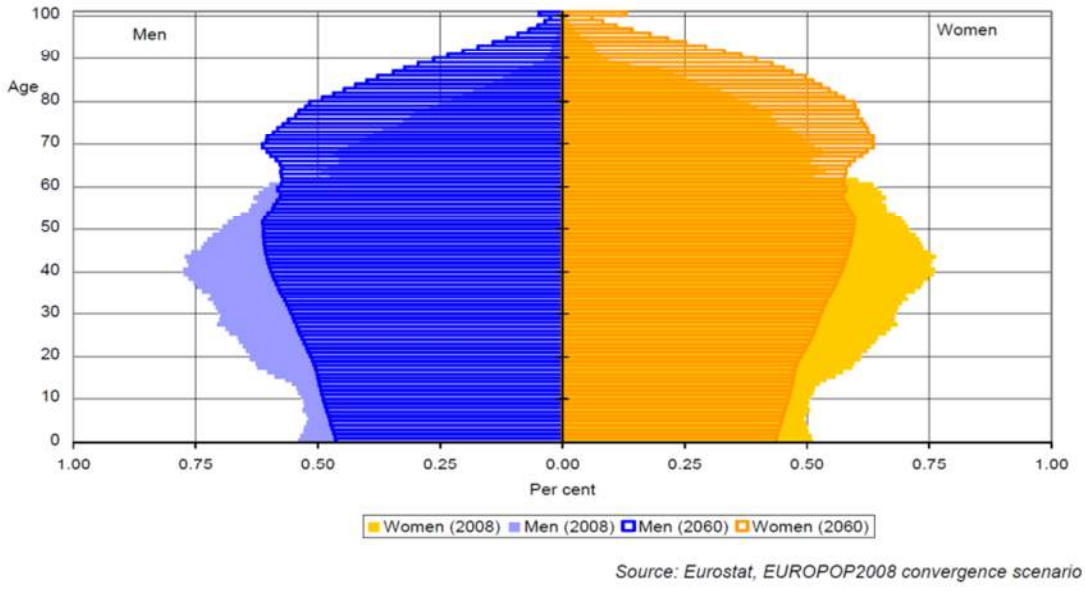

Figure1: Population pyramid in 2008 and in 2060. The population pyramid shows the population distribution by sex and by each year of age or birth. Each bar corresponds to the share of the population at that age, by sex, in the total population.(Scherbov *et al.*)

2.2 Definition of aging

Aging or senescence has been defined as the progressive decline in homoeostasis that occurs after the reproductive phase of life, and leads to an increasing risk of disease and ultimately to death.

Biological aging, although normally linked to chronological age, can occur earlier in life and is thought to result from a failure of organ or cell maintenance and/or repair, particularly a failure to protect DNA against oxidative injury. Thus in general, aging results from an accumulation of molecular damages in the genome and the sustained cellular defects can enhance inflammation, cancer and tissue damage (MacNee 2009).

2.3 Aging in the lung

In the aging lung the total tissue mass decreases along with the number of capillaries. Formation of new alveoli is also limited. Due to decrease in tissue mass as well as muscle weakness, lung capacity declines even in healthy individuals (Tolep *et al.* 1995; Polkey *et al.* 1997). As senescence progresses, lung tissue becomes prone to inflammation, fibrosis and tumors demolishing lung capacity. Infections are frequent in the pulmonary tract of the elderly leading to a chronic cycle of injury and repair that causes significant changes in the structure, function and gene expression of alveolar epithelial cells contributing to the development of chronic pulmonary diseases (Baarsma *et al.* 2011; Chilosi *et al.* 2012). Studies suggest that the senile lung is characterized by airspace enlargement similar to acquired emphysema (Verbeken *et al.* 1992) that is also detected in non-smokers above 50 years of age (Sharma & Goodwin 2006).

While molecular processes of other organs are studied widely, there is relatively limited background knowledge concerning pulmonary senescence. Most studies have been performed in mice and although similarly to humans, aging of the mouse lung is associated with homogeneous airspace enlargement, mice are still not the best model organism to study molecular and micro-environmental changes during pulmonary senescence as not all the physiological processes or responses are identical to humans. Partly, as in mice the aging process initiates earlier and the whole process is faster.

2.4 Normal alveolar function

2.4.1 Main cells in the alveoli

Alveolar type I epithelial cells (ATI): It is also called type I pneumocyte or squamous alveolar cell. ATI cells are very thin (sometime only 25nm) and they cover the 95-97% of the alveoli. ATI cells express several typical markers for example: fibroblast growth factor receptor-activating protein 1, aquaporin 5, purinergic receptor P2X 7 (P2X7), interferon-induced protein, and Bcl2-associated protein. The main physiological role of the ATI cell type is gas exchange (Ward & Nicholas 1984; Chen *et al.* 2004).

Alveolar type II epithelial cells (ATII): It is also called alveolar type II pneumocytes, great alveolar cells or septal cells. ATII cells are granular and they have mostly cuboidal shape. They cover only the 3-5% of the alveolar surface. For the identification of ATII cells, aquaporin 3, and pro-surfactant protein C are the most common markers. They are responsible for the production and secretion of surfactant proteins. Surfactants are phospholipo-proteins and responsible for the lowering of surface tension. It is already confirmed that ATII cells are the facultative stem cells at the alveolar region of the lung. At the place of an injury they are able to renew themselves and in vitro studies showed that they can differentiate into ATI cells (Ward & Nicholas 1984; Chen *et al.* 2004; Barkauskas *et al.* 2013).

Lipofibroblasts are a supportive cell type at the alveolar region of the lung. These cells are capable to take up triglycerides from the blood stream and accumulate it in their cytoplasm. Lipofibroblasts are hard to identify. They are recognizable via their location -adjacent to ATII cells- and expression of PTHrP receptors. Lipofibroblasts also expresses PPARγ and contain accumulated lipid droplets that are visible in their cytoplasm.

Myofibroblasts: The presence of myofibroblasts in alveolar region is well established. Myofiblroblasts play an important role in wound healing processes after injury, but accumulation of these cells can cause pulmonary fibrosis (Hinz *et al.* 2007). The myofibroblasts are more common cells in the alveoli then lipofibroblasts. Myofiblroblasts are easily identified by alpha smooth muscle actin (αSMA) production.

2.4.2 Alveolar function

During development, progenitor cells have been identified to originate from the five putative stem cell niches that were primarily identified in the lungs of mice (Engelhardt 2001). The cells responsible for cellular regeneration in the bronchiolar region are the non-ciliated epithelial cuboid Clara cells (Park *et al.* 2006). At the gas-exchange region of the alveoli there are two types of epithelial cells, Alveolar type I (ATI) and alveolar type II (ATII) cells. The role of ATI cells are quite simple, they provide the gas exchange surface. On the other hand, the role of ATII cells are much more complex. Apart from self-renewal, ATII cells are capable of trans-differentiation into ATI cells (Crosby & Waters 2010; Rock *et al.* 2011; Barkauskas *et al.* 2013). ATII cells are also important in producing surfactant proteins, which are responsible for lowering surface tension in the alveoli aiding gas exchange and stabilizing alveolar structure (Rooney *et al.* 1994). Surfactant proteins are lipo-proteins, therefore triglycerides are essential for their production (Veldhuizen & Possmayer 2004; Maina *et al.* 2010). At the alveolar region of the lung a well-maintained, surfactant producing ATII cell population is essential.

Although surfactants are produced by ATII cells, ATII cells are unable to take up triglycerides directly from the blood stream. Triglycerides are taken up and transported to ATII cells by lipofibroblasts (Torday *et al.* 1995; Rehan & Torday 2012). Lipofibroblasts or lipid laden fibroblasts are fibroblasts adjacent to ATII cells at the alveolar region. They can take up triglycerides directly from the blood stream and accumulate lipid droplets and provide lipids to ATII cells for surfactant production. The lipid accumulation process is regulated by a peroxisome proliferator-activated receptor gamma (PPARγ) (Ferguson *et al.* 2009) and adipose differentiation-related protein (ADRP) (Gao & Serrero 1999; Schultz *et al.* 2002) dependent mechanism. In the absence of PPARγ, lipofibroblasts trans-differentiate into myofibroblasts which cannot maintain lipid accumulation and therefore support normal lung function. A decrease in lipofibroblasts therefore can lead to increased sensitivity to develop lung diseases including chronic obstructive pulmonary disease (COPD) or lung fibrosis. Although lipofibroblasts are capable of taking up triglycerides directly from the blood stream, they also need a signal from ATII cells to initiate the process. The triglyceride uptake

signals include parathyreoid hormone related protein (PTHrP) and prostaglandin E release that activate lipofibroblasts via their PTHrP receptors. Once triglycerides are transported to ATII cells, lipofibroblasts can also stimulate surfactant protein production (Rehan & Torday 2012).

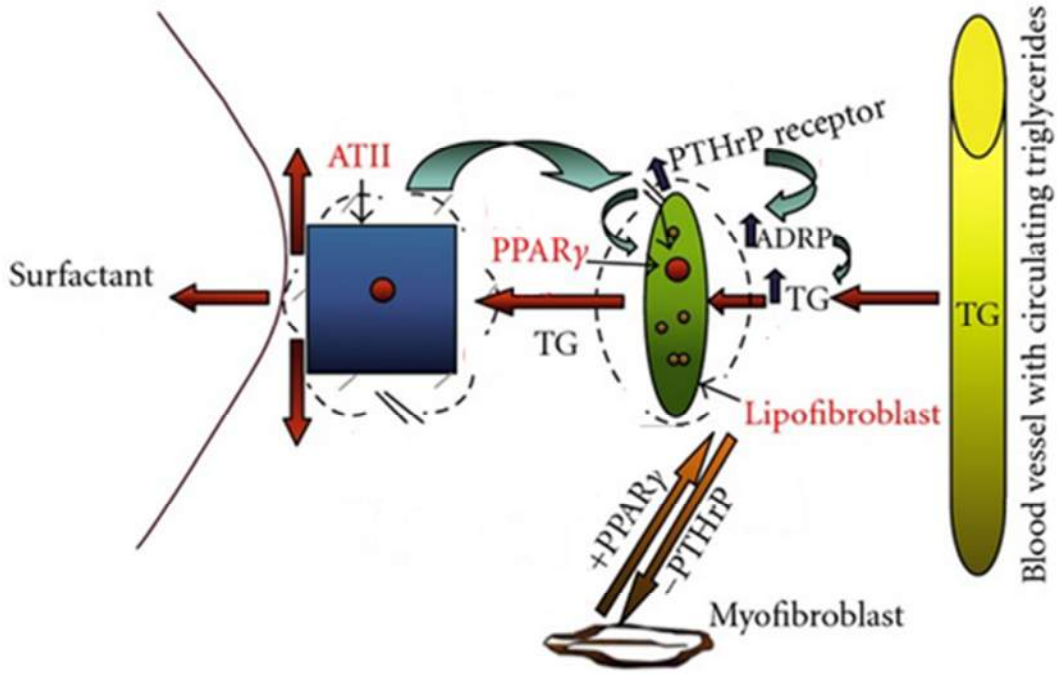

Figure 2: Normal lung function at alveolar level. Lipofibroblasts take up TG (triglycerides) from the blood stream and provide it to ATII cells. In the absence of PPARγ lipofibroblasts differentiate into myofibroblasts (Rehan and Torday 2012).

2.4.2 Epithelial repair mechanisms in the lung

Injuries can be caused by bacterial or viral infections, inflammation, allergic reactions (asthma), exposure to xenobiotics for example cigarette smoke, physical trauma (mechanical ventilation), cancer, or pathology of unknown origin (idiopathic fibrosis). Depending on the nature of the injury, lung repair mechanisms are initiated immediately following the insult and include an acute inflammatory response involving cytokine release, immune cell recruitment and activation of the coagulation cascade (Crosby & Waters 2010).

Epithelial restitution involves spreading and migration or neighboring epithelial cells to cover the denuded area and this is followed by migration and proliferation of progenitor cells to restore cell numbers and to restore tissue function (Puchelle *et al.* 2006; Stripp & Reynolds 2008).

Progenitor cells in other organs for example in the eye, gut, and skin epithelia are constantly renew by proliferation and migration of stem cells. In contrast, lung stem cells renew slowly after an injury (Evans *et al.* 1978; Reynolds *et al.* 2007).

The regeneration process in vivo is hard to investigate therefore in vitro studies provide guidance. In vitro studies have confirmed the role of ATII cells in alveolar regeneration (Kheradmand *et al.* 1994; Panos *et al.* 1995; Yee *et al.* 2006; Rawlins *et al.* 2007) and there are some in vivo (Rock *et al.* 2011) studies where the differentiations of ATII cells into ATI cells are confirmed. Barkauskas et al have shown for example that ATII cells are capable to maintain themselves. Moreover it is also confirmed in alveosphere experiments that alveolar fibroblasts and lipofibroblasts are clearly able to support both proliferation and differentiation of ATI (type I alveolar epithelial cell, responsible for gas exchange) cells (Barkauskas *et al.* 2013).

2.5 Molecular regulation of lung regeneration and aging

2.5.1 PPARγ in general

Peroxisome proliferator- activated receptors (PPARs) are members of the nuclear hormone receptor superfamily, which function at the transcriptional level to regulate a wide range of physiological activities. Upon activation by an appropriate ligand, PPARs form an obligate heterodimer with RXRs (cis-retinoic acid receptors) to recruit nuclear receptor coactivators to specific promoter elements, termed peroxisome proliferator response elements, and modulate gene transcription (Berger & Moller 2002). There are three mammalian PPAR genes: PPARα, PPARβ/δ and PPARγ, each with unique though overlapping tissue distributions, activating ligands and regulatory activities. PPARγ is expressed in a broad range of tissues, including adipose, heart, skeletal muscle, liver, small and large intestine, kidney, pancreas, spleen, and lung (Berger & Moller 2002; Daynes & Jones 2002). PPARγ is also expressed in a wide range of blood cells,

including murine and human macrophages (Chinetti *et al.* 1998), T and B lymphocytes (Clark *et al.* 2000; Yang *et al.* 2003) and eosinophils (Woerly *et al.* 2003; Simon *et al.* 2006a).

PPARγ is most highly expressed in white adipose tissue (WAT) and brown adipose tissue (BAT), where it is a master regulator of adipogenesis as well as a potent modulator of lipid metabolism and insulin sensitivity of the entire body (Ahmadian *et al.* 2013).

PPARγ and RXR form a heterodimer transcription factor and bind the PPRE (PPAR responsive elements on DNA) and induce the expression of several genes. PPARγ is crucial for controlling gene networks involved in glucose homeostasis, including increasing the expression of glucose transporter type 4 (Glut4) and c-Cbl–associated protein (CAP). Moreover, PPARγ controls the expression of numerous factors secreted by adipose tissue, such as adiponectin, resistin, leptin and tumor necrosis factor-α (TNF-α) (Ahmadian *et al.* 2013).

2.5.2 PPARγ in the lung

Within the lung, PPARγ expression has been reported in the epithelium, smooth muscle, endothelium, macrophages, eosinophils, and dendritic cells as well as in fibroblasts.

PPARγ molecule also plays a very important role lung development and maintenance. For example, glycosyl-phosphytidyl-inositol-linked cell-surface glycoprotein (Thy-1) stimulates lipofibroblast differentiation through the activation of PPARγ. Thy-1 positive fibroblasts contain lipid droplets and 2.5 times higher PPARγ activity. Increased PPARγ -a lipofibroblast marker- expression leads to elevated ADRP levels and consequently to increased lipid content. These findings confirm that Thy-1 and PPARγ signaling promotes the lipofibroblast phenotype and this cell type can increase the onset of alveolarization (Varisco *et al.* 2012).

While PPARγ is a very important molecule in the maintenance of the lipofibroblast phenotype (see above), epithelial PPARγ is necessary for the establishment and maintenance of normal lung structure, through regulation of epithelial cell differentiation and control of lung inflammation. PPARγ is also important for postnatal lung maturation. Targeted deletion of PPARγ in epithelial cells changed the epithelial

structure of the lung but not the maturity and the SPC production of alveolar epithelial cells (Simon *et al.* 2006a; Simon *et al.* 2006b).

2.5.3 The Wnt β-catenin pathway

The Wnt family of 19 secreted glycoproteins controls a variety of developmental processes including cell fate specification, cell proliferation, cell polarity and cell migration. The name Wnt is results from fusion of Drosophila segment polarity gene "wingless" and the name of its vertebrate homolog, "integrated" or "int-1" gene. There are two main signaling pathways involved in the signal transduction process from the Wnt receptors called Frizzleds: the canonical or β-catenin dependent, and the non-canonical pathways. Based on their ability to activate a particular Wnt pathway, Wnt molecules have been grouped as canonical (Wnt1, Wnt3, Wnt3a, Wnt7a, Wnt7b, Wnt8) (Torres *et al.* 1996b) and non-canonical pathway activators (Wnt5a, Wnt11) (Torres *et al.* 1996a).

Generally, in the absence of canonical Wnt-s, glycogen synthase kinase-3β (GSK-3β) forms an active complex with adenomatous polyposis coli (APC) and axin and phosphorylates β-catenin (Ikeda 1998; Yamamoto *et al.* 1999). The phosphorylated β-catenin is targeted for ubiquitination and proteasome-mediated degradation. Proteosomal degradation of β-catenin decreases the cytosolic level of β-catenin (Aberle 1997; Akiyama 2000) (Figure 3). In the presence of Wnt-s, signals from the Wnt-Fz-LRP6 complex lead to the phosphorylation of three domains of Dishevelled (Dvl), a family of cytosolic signal transducer molecules (Noordermeer 1994). Activation of Dvl leads to phosphorylation and consequently inhibition of GSK-3β-APC-axin complex. Inhibition of GSK-3β-APC-axin complex results in the stabilization and finally cytosolic accumulation of β-catenin, which then translocate to the nucleus, where is required to form active transcription complexes with members of the T-Cell Factor (LEF1, TCF1, TCF3, TCF4) transcription factor family (Staal & Clevers 2003) and transcription initiator p300 (Labalette *et al.* 2004; Varecza 2011) (Figure 3).

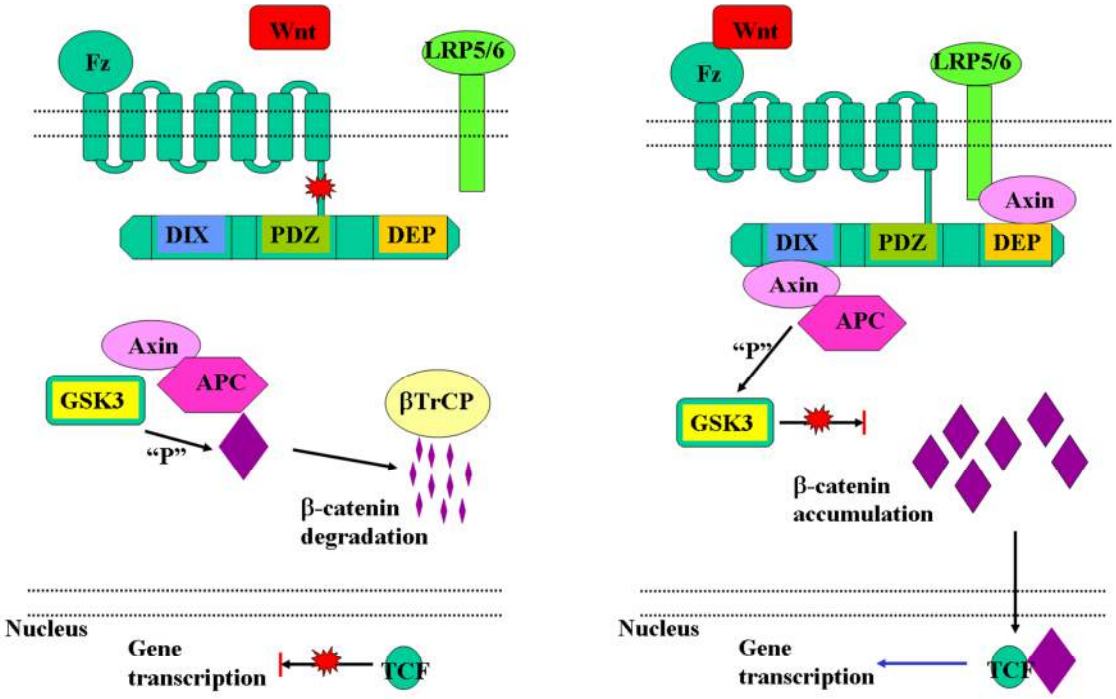

Figure3: Canonical Wnt pathway in the absence (left) and presence (right) of Wnt molecule (Pongracz & Stockley, 2006).

2.5.4 Non-canonical Wnt pathways

Generally, the two non-canonical signaling pathways (Figure 4) are considered as regulators of canonical Wnt signaling and gene transcription. The two non-canonical Wnt pathways, the JNK/AP1 dependent, PCP (Polar cell polarity pathway) (Yamanaka *et al.* 2002) and the PKC/CAMKII/NFAT dependent Ca^{++} pathway (Wang & Malbon 2003), just like the canonical Wnt pathway, become activated following the formation of Wnt-Fz-LRP6 complex.

The Ca^{2+} dependent pathway activates several downstream targets including protein kinase C (PKC), Ca-Calmodulin Kinase II (CaMKII), and the calcium sensitive phosphatase, Calcineurin. Finally, the NFAT transcription factors are activated to stimulate the transcription of many immunologically important genes including interleukin 2 (IL-2), interleukin 4 (IL-4), tumor necrosis factor alpha (TNFα). Wnt5a is a prominent member of the non-canonical Wnt pathway, which activates the calcium

dependent pathway (Kim *et al.* 2010), but there are some recent articles which described that Wnt5a can activate the β-catenin dependent canonical pathway as well (Popp *et al.* 2014).

In the PCP pathway, activation of Dvl leads to JNK and in turn AP1 activation. AP1 is a protein complex, composed of several small proteins for example cJun, JunB, JunD, cFos, FosB, Fra1, Fra2, ATF2, and CREB. As the canonical Wnt pathway can trigger the expression of some AP1 proteins, that transcription factor can be activated by PCP pathway activator Wnt ligands, the canonical Wnt pathway also regulates non-canonical Wnt signals via influencing the composition of AP1 protein complexes. As AP1 also regulates the production of Cyclin D1, matrix metalloproteinases (MMP), Bcl2 like protein 11 (BIM) and Granulocyte-Monocyte Colony Stimulating Factor (GMCSF) (Pongracz & Stockley 2006; Varecza 2011) of canonical Wnt targets, cross-talk amongst Wnt pathways is further emphasized.

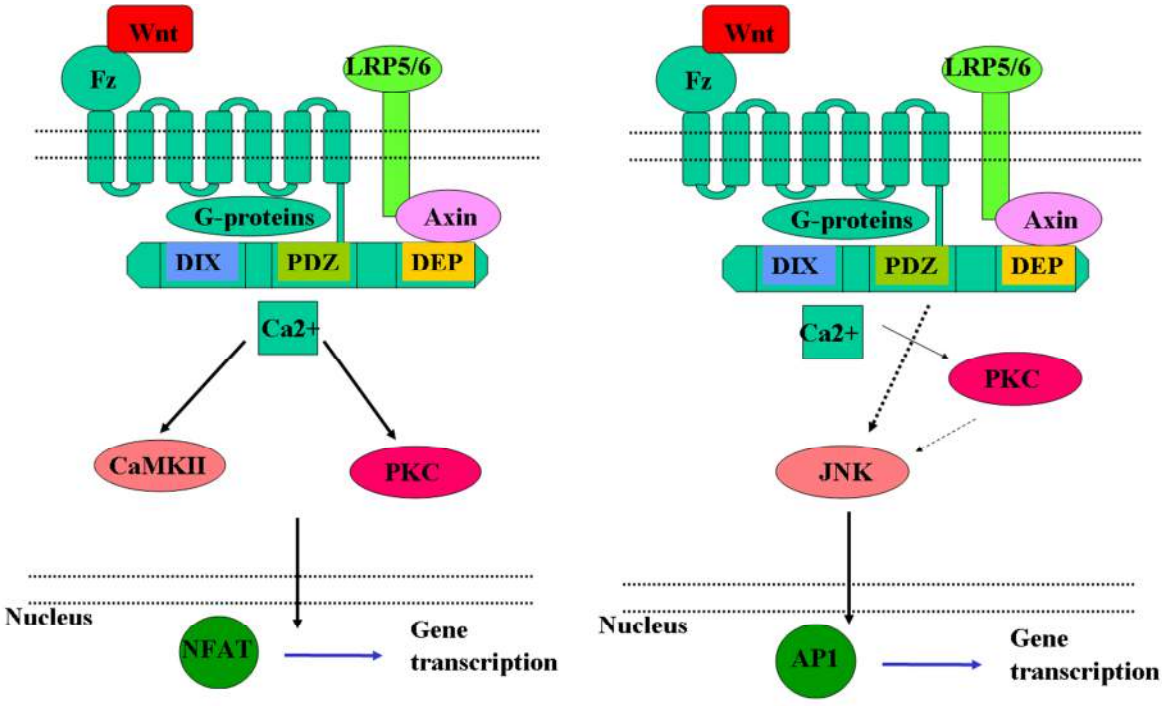

Figure 4: Non-canonical pathways of Wnt signaling. The picture on the left represents the Ca^{2+} pathway, and on the right represents the PCP pathway (Pongracz & Stockley, 2006).

2.5.5 The inhibitory Wnt pathway

Beside the canonical and non-canonical Wnt pathways, inhibitory Fz pathways have also been described (Roman-Roman *et al.* 2004). Fz1 and Fz-6 have both been described to transduce inhibitory Wnt signals. While Fz1 inhibits Wnt signal transduction via a G-protein dependent manner (Roman-Roman *et al.* 2004; Zilberberg *et al.* 2004), Fz-6 (Golan *et al.* 2004) inhibits Wnt dependent gene transcription by activating the Transforming growth factor β–activated kinase 1 (TAK1), a member of the MAPK family, and Nemo-Like Kinase (NLK) (Ishitani *et al.* 2003; Smit *et al.* 2004) via a Ca++ dependent signaling cascade. NLK phosphorylates TCF that as a result unable to bind to β-catenin, consequently formation of an active transcription complex is inhibited (Smit *et al.* 2004; Varecza 2011).

2.5.6 Wnts in aging

As Wnts are important regulators of proliferation, differentiation and even regulation of stem cell survival, recent studies have suggested a role for Wnt family members in aging. It has already been confirmed that drastic Wnt levels alterations can trigger aging as tissue specific stem cells have been shown to be depleted as a result of either low or high Wnt signals (Brack *et al.* 2007).

A decline in tissue regenerative capacity is a hallmark of mammalian aging and is attributed to the impairment of tissue progenitor cell function. It was previously shown that the age-related decline in tissue-specific progenitor cell activity is modulated by factors that are present in the serum (Conboy *et al.* 2005). In line with this study, Brack et al (Brack *et al.* 2007) provided evidence that systemic factors in the serum of aged mice activate canonical Wnt signaling and contribute to age-related decline in skeletal muscle regeneration. The authors showed that skeletal muscle stem cells (satellite cells) convert from a myogenic to a fibrogenic lineage when exposed to aged serum. In parallel canonical Wnt signaling is enhanced in skeletal muscle of aged mice as well as in cultured satellite cells exposed to aged serum. These observations suggest that the Wnt molecules are present in the old serum and can trigger to the decline of tissue functions.

Fibrosis is another feature of aged tissues that is linked for example to the pathogenesis of atrial fibrillation and dyastolic dysfunction of the aging heart (Burstein & Nattel 2008), which process regulated by Wnt signaling. Similarly, in the lung Wnt signaling pathways are over-activated in ATII cells (Chilosi *et al.* 2003) leading to pulmonary fibrosis. More recently the following mechanism was suggested: Wnt signals can induce transformation of fibroblast into activated fibroblasts or myofibroblasts that process leads to fibrosis of the heart or lung (Naito *et al.* 2010).

2.5.7 Wnts in the lung

The Wnt signaling pathways influence many processes in both fetal and adult lungs including development, maintenance of normal homeostasis, as well as influencing disease occurrence (Pongrácz & Stockley).

During development, the lung arises from a small diverticulum in the anterior foregut endoderm at the laryngotracheal groove. The respiratory epithelium then invades the surrounding mesenchyme, followed by the process of branching morphogenesis regulated by a wide array of interacting signaling pathways. Amongst many others, the fibroblast growth factor (FGFs), transforming growth factor beta (TGF-β), bone-morphogenic protein (BMP), sonic hedgehog (SHH), or Wnt (Königshoff & Eickelberg 2010) dependent signals have been listed to be the most important ones.

Zhang et al. have described most extensively the role of Wnt molecules in the developing human lung. The Wnt/β-catenin signaling cascade for example is essential for patterning of the early lung morphogenesis. Expression patterns of canonical Wnt/β-catenin signaling components, including Wnt ligands (Wnt2, Wnt7B), receptors (Fzd4, Fzd7, LRP5, LRP6), transducers (Dvl2, Dvl3, GSK-3β, β-catenin, APC, AXIN2), transcription factors (TCF4, LEF1) were analyzed using quantitative real time PCR. In situ hybridization showed that the canonical Wnt ligands and receptors were predominantly located in the peripheral epithelium, whereas the canonical Wnt signal transducers and transcription factors were not only detected in the respiratory epithelium, but some were also scattered at low levels in the surrounding mesenchyme in the developing human lung (Zhang *et al.* 2012)

In the adult lung, most Wnt components, including canonical and non-canonical Wnt ligands are expressed at detectable levels. Recently, it has been demonstrated that Wnt1 and Wnt3a are mainly localized to bronchial and alveolar epithelium, along with expression of Wnt1 in pulmonary endothelial and smooth muscle cells (Königshoff *et al.* 2008). Quantification of the mRNA levels of canonical Wnt/β-catenin signaling components in lung tissue samples of transplant donors revealed that Wnt ligands, Wnt1, Wnt2, Wnt3a, and Wnt7b, were expressed at similar levels in normal adult lung tissue, whereas Wnt10b exhibited low expression. In support of this, Winn and colleagues (Winn *et al.* 2005) demonstrated the expression of several Wnt proteins in lung epithelial cell lines. Thus, it has become evident that the adult lung expresses all required components for active Wnt signaling but functional studies are still largely missing (Königshoff & Eickelberg 2010).

The role of Wnts in lung diseases is a highly researched area. For example, in pulmonary fibrosis, the role of Wnts has been vigorously investigated both in murine and in human lung tissues. Idiopathic pulmonary fibrosis or IPF (Selman *et al.* 2008) that is a progressive and lethal disease with limited responsiveness to currently available therapies (Martinez *et al.* 2005; Walter *et al.* 2006) has been reported to be regulated by overexpression of canonical Wnts (Königshoff *et al.* 2008) and consequent accumulation of β-catenin in the nucleus (Chilosi *et al.* 2003).

2.5.8 Connection between Wnt β-catenin pathway and PPARγ

In recent studies the secreted Wnt glycolipoprotein ligand family (Pongracz & Stockley 2006) have been reported to regulate both aging (Brack *et al.* 2007) and PPARγ activity (Takada et al. 2009; Talaber et al. 2011). Interestingly the effector molecule of the canonical Wnt pathway, β-catenin, antagonizes PPARγ function (Takada *et al.* 2009), while non-canonical Wnts have not been reported to affect PPARγ transcription or activity. Takada have described that during development mesenchymal stem cells choose the adipoid differentiation lineage but in the presence of Wnts and activation of β-catenin they become osteoblasts. Our research group has also shown that in a Wnt4 overexpressing cell line PPARγ production was suppressed making the cell line less sensitive to steroid induced aging (Talaber *et al.* 2011). Recent studies conducted in

lungs of aging mice have connected PPARγ to lipofibroblast differentiation (Willis & Borok 2007; Paxson *et al.* 2011) (Figure 5). If PPARγ is reduced, lipofibroblasts differentiate into myofibroblast not supporting the maintenance of "stemness" of ATII cells and surfactant synthesis (Königshoff & Eickelberg 2010; Paxson *et al.* 2011).

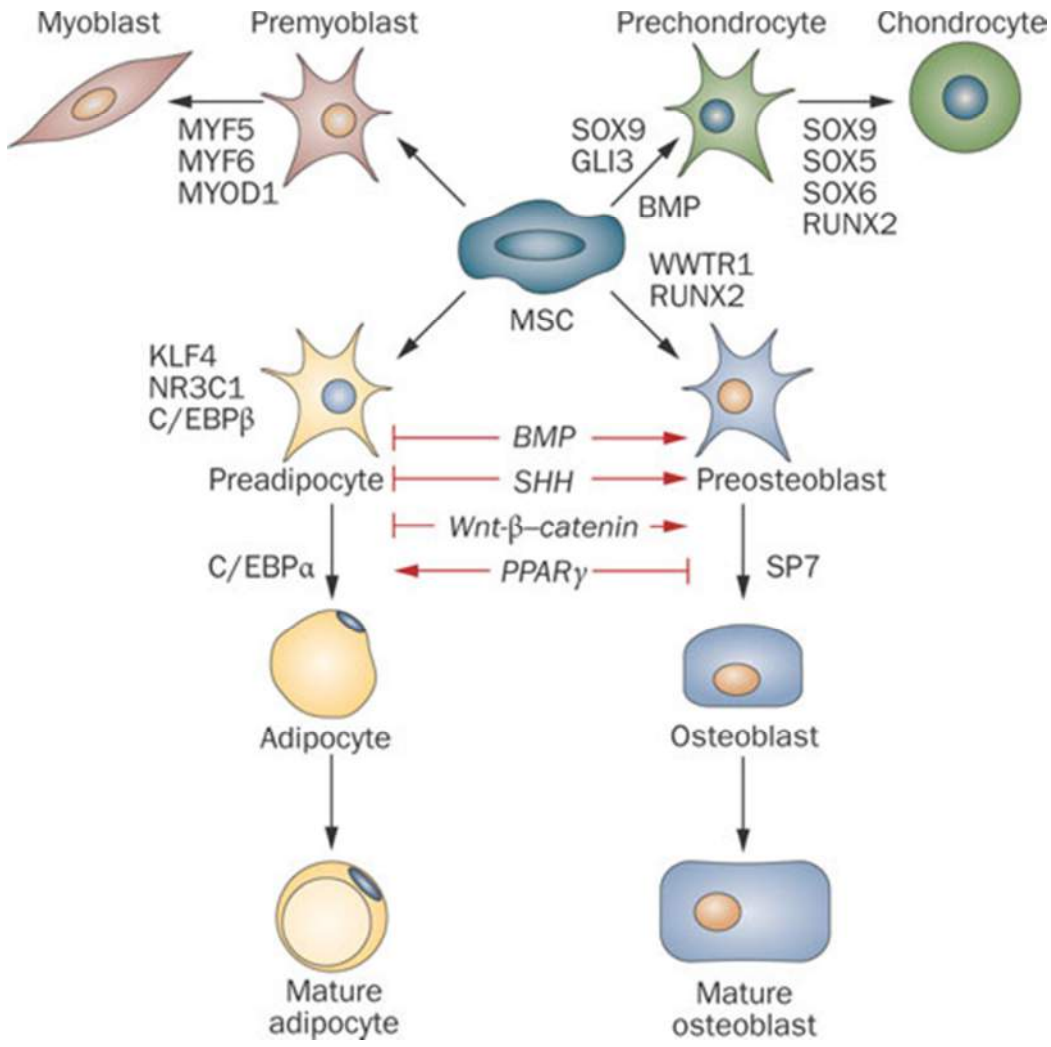

Figure 5: The connection between Wnt/β-catenin pathway and PPARγ. In the development of the mesenchymal stem cells Wnt/β-catenin support the osteoblast development and PPARγ has opposite effect, facilitate the adipogenesis (Takada *et al.* 2009).

2.5.9 Epigenetic regulation of aging - Sirtuin molecules

Studies of aging in yeast led to the discovery of a family of conserved enzymes known as Sirtuins (Silent Information Regulator2-Sir2), which affect multiple signaling pathways that increase the life-span of several organisms. Since the discovery of the first known mammalian Sirtuin, Sirt1, our understanding of the enzymology of Sirtuins, their regulation, and their ability to broadly improve mammalian physiology and health-span (Haigis & Sinclair 2010) has greatly improved. In short, Sirtuins regulate epigenetic mechanisms as they can carry out nicotinamide adenine dinucleotide (NAD^+) dependent deacetylation reactions (Imai *et al.* 2000; Haigis & Sinclair 2010).

Mammals contain seven Sirtuins, Sirt1–7, which are categorized by their highly conserved central NAD^+-binding and catalytic domain, termed the Sirtuin core domain (Frye 2000; Haigis & Guarente 2006). Although these Sirtuins are relatively conserved, their N and C terminal parts differ, and they are likely to have highly divergent biological functions owing to different enzymatic activities, unique binding partners and substrates, and distinct sub-cellular localization and expression pattern (Haigis & Guarente 2006; Haigis & Sinclair 2010).

Mammalian Sirtuins are found in numerous compartments within the cell. Sirt1, -6, and -7 are found predominantly in the nucleus (Michan & Sinclair 2007); Sirt3–5 reside in mitochondria; and Sirt2 is primarily cytoplasmic. The sub-cellular localization of these proteins probably depends upon cell type, stress status, and molecular interactions. For instance, Sirt1 and -2 were found to localize in both the nucleus and the cytoplasm and to interact with both nuclear and cytosolic proteins (Haigis & Guarente 2006).

Regulation of Sirtuin expression and function is modulated by various small molecules. Howitz et al for example have screened a library of NAD+ analogs and plant polyphenols to identify small molecules that modulate the activity of Sirt1 and its homologs and came to a conclusion that several plant polyphenols including resveratrol activate Sirt1 (Howitz *et al.* 2003) indicating a direct link between environmental factors and longevity regulators.

2.5.10 Sirtuin and the epigenetic regulation of PPARγ

Recent studies have described the connection between Sirtuins and PPARγ in different aspects. For example Sirt1 represses PPARγ, therefore up-regulation of Sirt1 triggers

lipolysis and leads to the loss of fat in white adipose tissue (Picard *et al.* 2004). The above process has also been confirmed in an *in vitro* model of 3T3-L1 fibroblast cell-line, where adipogenesis is promoted by the PPARγ nuclear receptor. The cells were cultured in adipogenic differentiation medium containing insulin, dexamethasone and isobutyl-methylxanthine. Normally, insulin can induce the production of Sirt1 but this is not sufficient to modulate PPARγ expression because of the other two components, dexamethasone and isobutyl-methylxanthine. However, following over-expression of Sirt1, Sirt1 could halt the accumulation of lipid droplets in 3T3-L1 cells (Picard *et al.* 2004) indicating PPARγ inhibition.

Interestingly, and in contrast to Sirt1, Sirt7 has an opposite effect, it promotes adipogenesis via an interesting mechanism. Sirt7 can bind to Sirt1 and consequently suppresses Sirt1 activation by direct protein-protein interaction (Bober *et al.* 2012).

Sirt1 and PPARγ connection can also regulate the expression of Sirt1 itself in a negative feedback loop. The process is associated with senescence, as the Sirt1-PPARγ complex inhibits Sirt1 gene expression (Han *et al.* 2010).

2.5.11 Connection between Sirtuins and Wnts

Previous studies described that Wnt/β-catenin signaling and the Sirtuin molecules can both prevent adipogenesis through inhibition of PPARγ (Picard *et al.* 2004; Takada *et al.* 2009), but less is known about the connection between Sirtuins and Wnt pathways. Holloway et al suggest that loss of Sirt1 protein leads to a significant decrease in the level of Dvl proteins, one the signal transducer molecules from Wnt receptors. But if Sirt1 is over-expressed it renders Dvl proteins constitutively active leading to β-catenin accumulation in the cell nucleus and transcription of β-catenin dependent genes (Holloway *et al.* 2010). Another report suggests that Sirt1 promotes osteogenesis over adipogenesis in mesenchymal stem cells (MSC) also via modulation of the canonical Wnt pathway molecule, β-catenin. In MSCs Sirt1 deacetylates β-catenin to trigger its accumulation in the nucleus and activation of gene transcription. This process leads to differentiation towards bone tissue (Simic *et al.* 2013).

In contrast to previous publications Firestein et al have suggested that Sirt1 interacts with β-catenin and suppresses its localization to the nucleus significantly attenuating its ability to activate gene transcription (Firestein *et al.* 2008).

3. Aims of the study

The overall aim of the study was to investigate the molecular background of pulmonary senescence focusing on three well defined target areas:

1. Wnt pathways are deregulated during aging in many tissues, therefore to understand the molecular background of pulmonary aging mechanisms,
    - Wnt ligand expression levels were investigated in the aging lung,
    - as well as cell type specific distribution of Wnts were studied in pulmonary tissue
2. Lipofibroblast are proposed to be essential in maintenance of alveolar type II cells, the stem cells of the alveolar region of the lung.
    - As lipofibroblast function is PPARγ dependent it was investigated whether PPARγ expression changes with age, and
    - whether de-regulation of specific Wnt pathways affect PPARγ expression and activity
    - as well as whether modulation of PPARγ can affect ATII cell function
3. It has been established that aging is regulated by epigenetic factors. Sirtuins are well known epigenetic regulators of longevity, therefore
    - Sirtuin (NAD dependent deacetylases) levels were investigated in the aging process of the lung
    - and it was also the aim to investigate whether Sirtuin activation modulates the pulmonary senescence program?

4. Experimental Procedures

4.1 Ethical Statement

Lung tissue samples were collected during lung resections at the Department of Surgery, University of Pécs, Hungary. The project was approved by the Ethical Committee of the University of Pécs. All collected samples were treated anonymously.

4.2 Animals

For the experiments Balb/C inbred, albino mice were used from both genders. Mice were kept under standardized conditions, where tap water and food was provided ad libitum. They were let to age till 1, 3, 6, 12, 18, 24 months before sacrifice.

4.3 Sky scan microCT

Mice anesthetized intraperitoneally with sodium pentobarbital (eutazol), were placed in the SkyScan 1176 microCT (Bruker, Kontich, Belgium) machine equipped with a large format 11 megapixel camera. Pictures were taken from the lung in 180°. The reconstitution was performed with Skyscan software, which integrates a physiological monitoring subsystem providing breathing and heart-beat gating for thoracic image improvement through synchronized acquisition. Then the pictures were calibrated with CtAn software (Bruker). The 3D pictures were generated from the calibrated images by CtVox (Bruker). Colors were based on the Hounsfield scale. The values of the scale range between -1000 and +1000. The +1000 is the value for bones, zero is the water and -1000 is the air. Red color was placed at -1000 and represents free air inside the lung, while blue color represents lung tissue.

4.4 Lung cell isolation

Mice were anesthetized with 1% of sodium pentobarbital through intraperitoneal injection (70µl/10g). Then abdominal aorta was intersected and mice were perfused through right ventricle with 10 ml of phosphate buffer saline (PBS) to reduce lung blood content. 3 ml trypsine (%) to initiate the fine digestion, 10 ml PBS to wash out trypsine, 3 ml collagenase-dispase (3 mg/ml collagenase (Sigma-Aldrich, St. Louis, MO, USA) 1mg/ml dispase (Roche F. Hoffmann-La Roche Ltd. Basel, Switzerland) 1µg/ml DNAse I (Sigma-Aldrich). Finally, the lung was filled up with the collagenase-dispase solution trough the trachea. Lungs were removed from the chest and separated from the heart and thymus and cleaned from connective tissue. Pulmonary lobes were dissected into smaller pieces and digested in 10 ml collagenase-dispase for 50 minute with continuous stirring. Digested lung tissues were filtered with 70µm cell-strainer (BD Becton, Dickinson and Company Franklin Lakes, New Jersey, U.S.) to create single cell suspension.

4.5 Cell sorting

Single cell suspensions of mouse lungs were labeled with anti CD45-FITC produced at the University of Pécs, Department of Immunology and Biotechnology (Balogh *et al.* 1992) and anti EpCAM1 (G8.8 clone (ATCC) anti-rat-PE) antibodies. Cell sorting was performed using FACSAria III (BectonDickinson) cell sorter. The following populations were collected: $EpCAM^{-}CD45^{-}$ $EpCAM^{+}CD45^{-}$ $EpCAM^{+}CD45^{+}$ and $EpCAM^{+}CD45^{-}$. The purity of sorting was above 99%. The CD45+ populations were further analyzed using anti-CD3, anti-CD5, anti-CD19 and anti-CD64 cell surface markers to differentiate amongst T-, B-cells and macrophages.

4.6 Cell lines

For in vitro experiments TEP1 and Wnt4 over-expressing TEP1 cell line supernatants were used. The TEP1 cell line was created at UCSD and characterized by Beardsley et

al (Beardsley *et al.* 1983). The TEP1 cells were cultured in DMEM (Dulbecco's Modified Eagle's medium Lonza) supplemented with 10% FCS, penicillin, streptomycin and β-mercapto-ethanol. They were kept at 37°C in a humidified thermostat where the CO_2 concentration was 5%.

Normal Human Lung Fibroblast (NHLF) cells were exposed to TEP1 Wnt4 over-expressing supernatant and to normal TEP1 cell normal supernatant as control (Talaber *et al.* 2011) for 7 days. Fibroblast cells (NHLF) were also treated with the β-catenin pathway activator LiCl at the concentration of 10 mM for 7 days and the β-catenin pathway inhibitor, IWR at 1 μM (Sigma) for two days. After RNA isolation and cDNA synthesis, PPARγ levels were measured by qRT-PCR using PPARγ and β-actin specific primers.

4.7 Three dimensional (3D) human lung tissue cultures

Three dimensional (3D) human lung tissue cultures were set up using the protocol (Figure 6) patented by Pongracz (J.E. ; Pongrácz). Briefly, Primary Small Airway Epithelial cells (SAEC) and NHLF cells were purchased from Lonza. All cell types were isolated from lungs of multiple random donors of different sexes and ages. Small Airway Epithelial Growth medium (SAGM) or fibroblast growth medium (FGM) medium were used for the initial expansion of SAEC or NHLF respectively, as recommended by the manufacturer (Lonza). All types of cell cultures were incubated in an atmosphere containing 5% CO2, at 37 ^{o}C. For 3D culturing, cells were mixed at 1:1 ratio, dispensed onto V-bottom 96-well plates (Sarstedt Nümbrecht, Germany) and were immediately pelleted at 600xg for 10 minutes at room temperature. Then 3D lung tissues were kept in 24 well plate (Sarstedt) in mixed SAGM:FGM (1:1 ratio) medium. They were exposed to rhWnt5a or Wnt4 supernatant for 7 days; or to 10nM of resveratrol or Wnt4 for 7 days under standardized cell culture conditions.

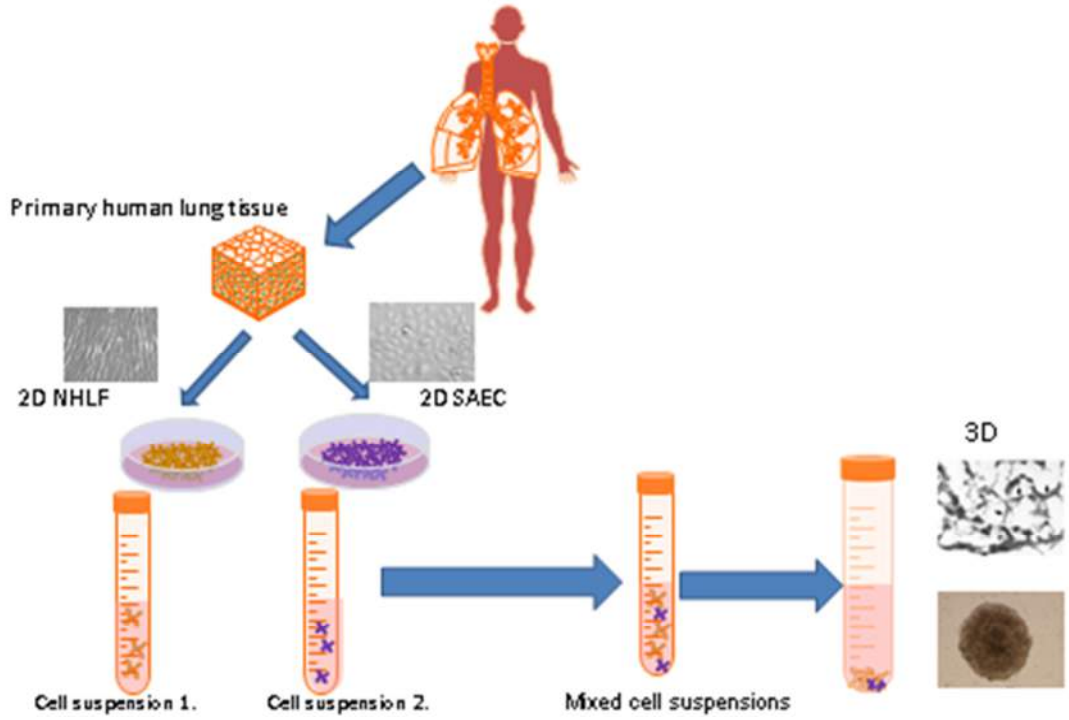

Figure 6: Summary of the procedure to make a human lung tissue spheroids. Isolated primary human cells are cultured in a 2D environment according to the manufacturer's instruction. Cell suspensions are made and mixed in the pre-determined proportions, spun and cultured until the 3D tissue is formed.

4.8 Recombinant Adeno (rAd) and Lenti (L) viral constructs and rAd and L-viral infection of pulmonary epithelium (SAEC) and fibroblasts (NHLF)

ICAT sequence was amplified by PCR reaction using forward (5') 5'-ATGAACCGCGAGGAGCA-3' and reverse (3') 5'-CTACTGCCTCCGGTCTTCC-3' primer sequences and cloned into the bi-cistronic GFP (green fluorescence protein) Adeno Shuttle and Lenti pWPTS vectors. The Shuttle vector was cloned by homologous recombination into the adenoviral vector. Adenovirus was produced by transfecting the linearized plasmid DNA into the 293 packaging cell line (American Type Culture Collection, Rockville, MD) using Lipofectamine 2000 (Invitrogen). The resulting plaques were amplified; the adenovirus purified and concentrated using the adenoviral purification kit (BD Biosciences).

Late second generation lentiviral vectors were prepared by co-transfection of three plasmid constructs (envelope construct pMD.G, packaging construct R8.91 and transfer construct pWPTS) into 293T cells using the calcium-phosphate method as described

previously (Bovia *et al.* 2003). Biological titration was performed with HeLa cells. Viral particles were concentrated 1000-fold in volume; biological titers reached 10^8 TU/ml. The HIV-1 derived lentiviral system was kindly provided by Prof. Didier Trono (CMU, Geneva, Switzerland).

For ICAT delivery to epithelial cells, complete SAEC-NHLF spheroids were incubated in the rAd virus containing media for 1 hour, then the SAEC-(ICAT-GFP)-NHLF and SAEC-(GFP)-NHLF spheroids were washed and incubated for 7 days before RNA isolation. For ICAT delivery to fibroblasts, NHLF cells were exposed to L-virus containing media for 1 hour, then cells were washed and incubated for 2 days in 2D monocultures. NHLF cells were then harvested and spheroids were produced as described above. SAEC-NHLF-(ICAT-GFP) and SAEC-NHLF-(GFP) spheroids were cultured for an additional 5 days before RNA isolation.

4.9 Western blot analysis

Lung tissues of young (1 months) and old (24 months) lysed in lysis buffer (20mM HEPES pH 7.4, 1mM $MgCl_2$, 1mM $CaCl_2$ 137mM NaCl, 50mM β-glycerophosphate, 2mM EGTA, 1% Triton X100 supplemented with 1mM DTT, 2mM PMSF, 2 μg/ml leupeptin, 1 μg/ml aprotinin, 1 μg/ml pepstatine) on ice for 20 min, then snap frozen in liquid nitrogen and stored at 70 °C until used. Ju st before loaded on 10% SDS-PAGE, the samples were boiled in 2× SDS sample buffer. Protein concentrations of lung extracts were measured with bicinchoninic-acid kit (Sigma), then the same amount of proteins were loaded to polyacrylamide gels then transferred to nitrocellulose membrane. The membrane was blocked with TBS buffer containing 1% of BSA and 0.05% of Tween and incubated with primary antibodies (anti-β-catenin, anti-Wnt4 both purchased from Santa Cruz, both at 1:1000 dilution) overnight. HRP conjugated anti-Mouse (Sigma) and anti-Goat (Sigma) were used as secondary antibodies (both at 1:1000 dilution). Blots were visualized using the chemiluminescent Supersignal kit (Pierce) and densitometrically scanned for quantification (LAS 4000 GE Healthcare Life Sciences, Little Chalfont, UK).

4.10 RNA isolation

Cell samples were homogenized in RA1 reagent, and RNA was isolated using the NucleospinII RNA isolation kit (Macherey-Nagel, Dueren, Germany). DNA digestion was performed on column with RNase free DNase. The concentration of RNA samples was measured using Nanodrop (Thermo Scientific, Waltham, MA, USA).

4.11 Real-Time quantitative PCR

cDNA was synthesized with high capacity RNA to cDNA kit (Life technologies Inc., Carlsbad, CA, USA) using 1µg of total RNA according to manufacturer's recommendation. Reverse transcription was performed in 20µl total volume using random hexamer primers. RT-PCR was used for gene expression analysis. Gene expression levels were determined by gene specific RT-PCR using ABsolute QPCR SYBR Green Low ROX master mix (ABGene, Thermo Scientific) and 100 nM primers on the Applied Biosystems 7500 thermal cycler system. For normalization β-actin was used as housekeeping gene. The primer sequences are shown in the table below. PCR conditions were set as follows: one cycle 95°C for 15 minutes, 40 cycles 95°C for 15 seconds, annealing temperature was 58°C and 72°C for 1 minute for elongation. Specification of the PCR reaction was determined by using a dissociation stage. The calculation of the RT-PCR results was performed as follows: The mean Ct values are determined by calculating the average of the parallel samples. ΔCt is calculated by subtracting the mean Ct of the housekeeping gene from the mean Ct of the gene of interest. ΔΔCt is constituted by the difference between the old sample Ct and the young sample as a control Ct values Finally, the relative quantity (RQ), which is presented in the diagrams, can be calculated by applying the formula: $RQ=2^{-\Delta\Delta Ct}$

4.12 Primer sequences (Table 1)

Primers	Forward	Reverse
mouse primers		
mouse β-Actin	TGGCGCTTTTGACTCAGGA	GGGAGGGTGAGGGACTTCC
mouse PTHrPR	GGCGAGGTACAAGCTGAGAT	ACACTTGTGTGGGACACCAT
mouse Wnt4	CTCAAAGGCCTGATCCAGAG	TCACAGCCACACTTCTCCAG
mouse Wnt5a	AAGCAGGCCGTAGGACAGTA	CGCCGCGCTATCATACTTCT
mouse Wnt11	GCTCCATCCGCACCTGTT	CGCTCCACCACTCTGTCC
mouse PPARγ	CCCAATGGTTGCTGATTACAAA	AATAATAAGGTGGAGATGCAGG TTCT
mouse ADRP	CGCCATCGGACACTTCCTTA	GTGATGGCAGGCGACATCT
mouse Sirt1	GACGATGACAGAACGTCACA	GATCGGTGCCAATCATGAGA
mouse Sirt7	TGAGACAGAAGAGGCTGTCG	TGGATCCTGCCACCTATGTC
human primers		
human β-Actin	GCGCGGCTACAGCTTCA	CTTAATGTCACGCACGATTCC
human PPARγ	GGTGGCCATCCGCATCT	GCTTTTGGCATACTCTGTGATCTC
human S100A4	TGGAGAAGGCCCTGGATGT	CCCTCTTTGCCCGAGTACTTG
human IL1β	TCAGCCAATCTTCATTGCTCAA	TGGCGAGCTCAGGTACTTCTG

4.13 Immunofluorescence

Mice were anaesthetized with sodium pentobarbital intraperitoneally and then they were perfused through the right ventricle with PBS solution as described above. Then lungs were filled up with 1:1 ratio of PBS:cryostate embedding media (TissueTek Alphen an den Rijn, Netherland), and frozen down at -80 °C.

The human samples were kept in PBS containing 1% of FCS at room temperature till processing. The filling, freezing and sectioning steps were performed as described above.

At the endpoint of the treatment the 3D microtissues were carefully removed from the 24 well plates and embedded into TissueTek embedding media and immediately frozen down at -80°C.

For histological observations, cryostat sections (7-9 μm) were fixed in cold acetone for 10 minutes.

4.14 Antibodies, Fluorescent staining

Following rehydration and blocking step (for 20 minutes in 5% BSA in PBS) immunofluorescent staining was performed. Anti-Wnt5a (Santa Cruz, Santa Cruz, CA, USA) antibodies Sirt1 and Sirt7 (Santa Cruz, Santa Cruz, CA, USA) were used as primary antibodies, and anti EpCAM1-FITC (clone G8.8, American Type Culture Collection (ATCC) directly labeled antibody was used as a control staining for 1 hour for mouse samples. For human samples anti pro-SPC antibody (Millipore Billerica, MA, USA) and anti-Wnt5a (Santa Cruz, Santa Cruz, CA, USA) were used. For the spheroids anti-KRT7 (DAKO, Agilent, Santa Clara, CA, USA) antibodies and anti E-cadherin (AbCam, Cambridge, UK) antibodies were applied.

The secondary antibodies were northern light anti-mouse NL-493 and northern light anti-rabbit NL-557 (R&D systems, Minneapolis, MO, USA). The nuclei were counterstained with DAPI (Serva, Heidelberg, Germany). Pictures were captured using Olympus IX81 fluorescence microscope equipped with CCD camera and analysis software. Images were processed and analyzed with ImageJ.

Fluorescent images were analyzed, and the mean intensity was calculated with StrataQuest software (Biotech-Europe, Prague, Czech Republic).

4.15 Hematoxylin-eosin staining

Following sectioning (see details above), samples were immediately stained with hematoxylin and eosin. Pictures were scanned with Pannoramic Desk machine (3D Histech, Budapest, Hungary) then analyzed by Pannoramic viewer software (3D Histech).

4.16 Neutral lipid staining

Mouse lung sections were fixed in cold acetone fixed stained with anti-EpCAM1 antibody directly conjugated with FITC (ATCC clone G8.8), then the LipidTox (Life

Technologies Inc.) staining was performed. Fluorescent images were captured and analyzed as described above.

4.17 Statistical analysis

If applicable, data are presented as mean ± standard deviation (SD), and the effects between various experimental groups were compared with the Student t-test. $p<0.05$ was considered as significant. The normal distribution was tested with Kolmogorov-Smirnoff test.

5. Results

5.1 Morphological changes in the aging lung

During aging, pulmonary function degenerate due to pulmonary inflammation and structural changes described as senile emphysema. Micro computed tomography (Figure 7A, 7B) and hematoxilyn-eosin staining (Figure 8A-D) of lung sections confirm such changes in Balb/c mice and human samples, respectively. Both techniques highlighted enlarged airspace both in old mice and in aging human lungs (Figure 7 Figure 8). The 2.5-fold increase in airspace (21 years old; mean alveolar diameter: 222.19 ± 113.12 μm and old 73 years old human; mean alveolar diameter: 317.03 ± 130.22 μm) in the distal lung coincides with decreased gas-exchange surface (Figure 8C, 8D).

To confirm degeneration of the epithelial surface layer during aging, single cell suspensions were generated from the pulmonary tissues of mice and cells were sorted based on EpCAM-1 and CD45 cell surface antigens. Analysis of density plots revealed a significant increase in CD45+ leukocyte level showing a marked increase in both macrophage and lymphocyte populations (Figure 9A, 9B), whereas the number of epithelial cells significantly decreased in the senescent lung (Figure 9A).

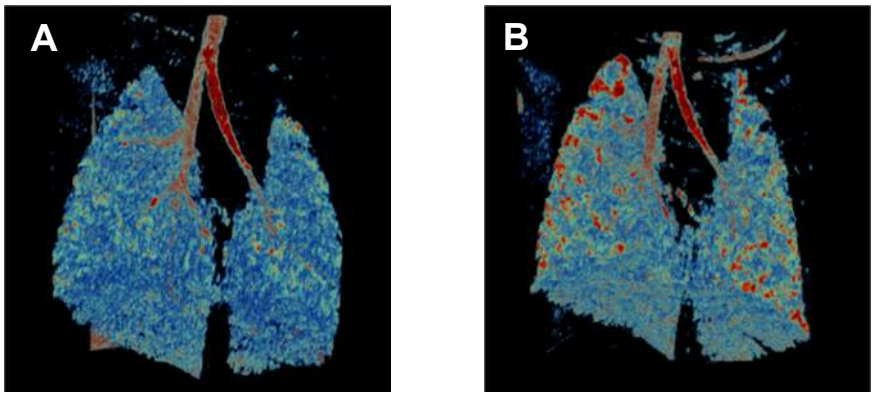

Figure 7: The structure of the lung during aging presented by SkyScan micro Computed Tomograph; photos of lungs of **A:** 1 month and **B:** 24 months old Balb/c mice were obtained in 180 degree, and converted to 3D by CTVol software (Skyscan). The pictures were colored using density based Hounsfield scale (values between -1000 and +1000, where -1000 represents the free air inside lung tissues).

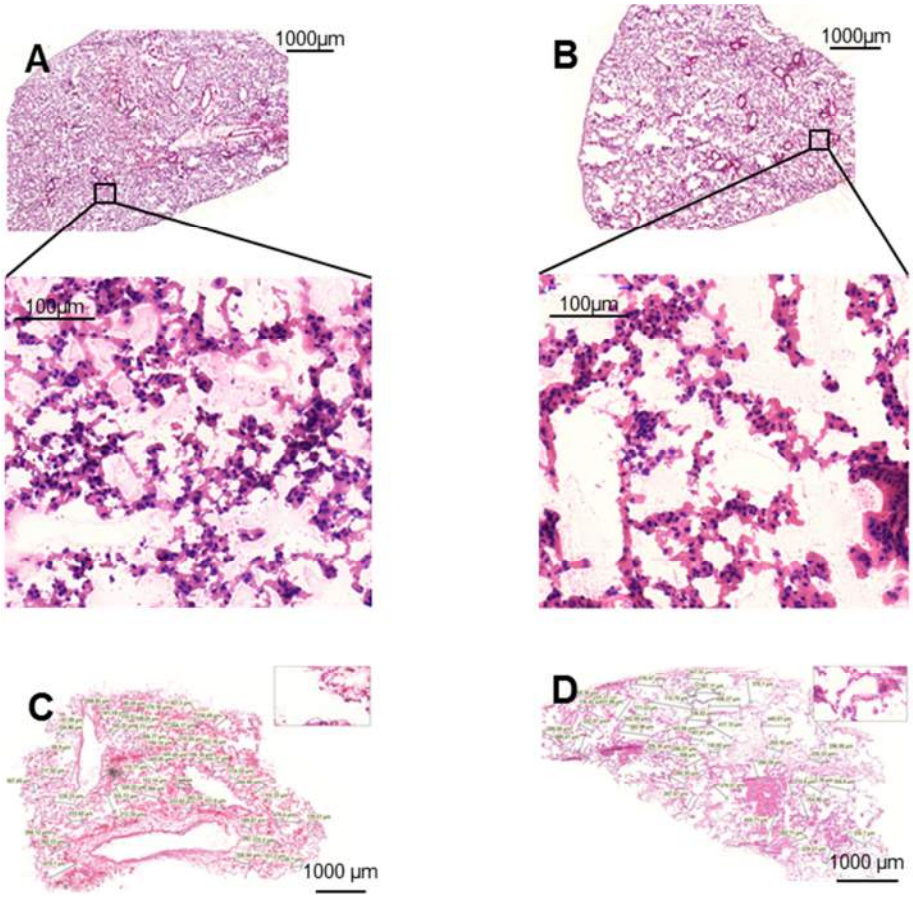

Figure 8: Hematoxylin-Eosin staining of **A:** young (1 month) and **B:** old (24 months) Balb/c mouse lung sections. Hematoxylin-Eosin staining of **C:** young (21 years) and **D:** old (73 years) human lung sections

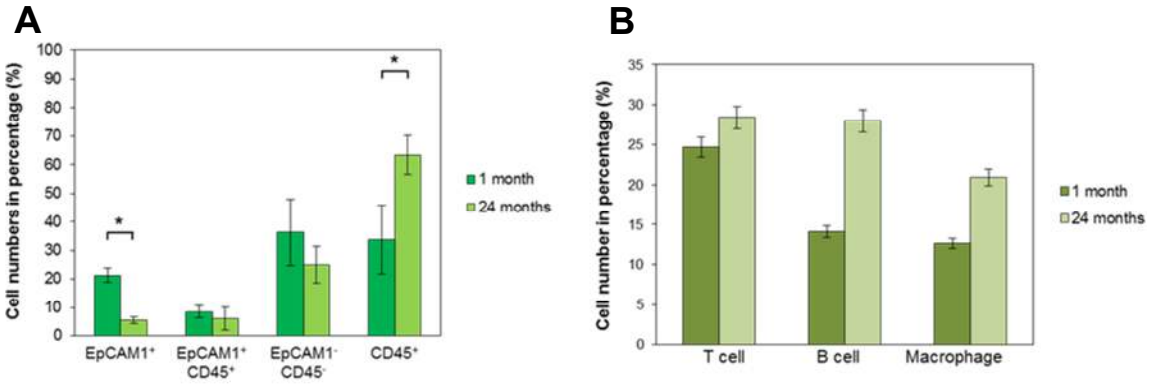

Figure 9**: A:** Flow cytometric analysis of cell population in young (1 month) and old (24 months) mouse lung. **B**: Bar chart of the infiltrating CD45+ immune cell populations using CD3 and CD5 for T-cell, CD5 and CD19 for B-cell and CD64 cell surface marker for macrophage identification.

5.2 Both PPARγ expression and lipid levels decrease with age

While senescence-associated low level chronic inflammation could explain tissue destruction, the reasons for ineffective regeneration are not so easily explained. As lipofibroblasts are essential for maintenance of ATII-s molecular studies were designed to identify molecules involved in lipid production to define the presence and activity of lipofibroblasts during pulmonary senescence. PPARγ mRNA as well as its down-stream target, adipose differentiation-related protein (ADRP) were measured in purified EpCAM-1^+ epithelial and EpCAM-1^- non-epithelial cells using qRT-PCR (Figure 10A). Compared to 1 month old Balb/c mice, both PPARγ and ADRP levels decreased at 24 months of age in both cell populations indicating reduced ability for surfactant synthesis and triglyceride uptake in the aging lung. To confirm the qRT-PCR data, lipid levels were assessed in pulmonary tissues using neutral lipid staining of 1 month and in 24 months old mouse lung sections (Figure 11A, 11B). While lipid staining co-localized with nuclear staining in young (1 month old) mice (Figure 11A), lungs of old (24 months) mice contained enlarged lipid droplets not associated with nuclear staining (Figure 11B). Western blots were performed using protein extracts of 1 month and 24 months mouse lungs (Figure 10B). The results show an age associated reduction in PPARγ protein levels indicating a loss of lipofibroblasts.

According to Torday et al. (Torday *et al.* 2003) parathyroid hormone-related protein (PTHrP) expression is necessary for differentiation of mesenchymal lipofibroblasts, which induce ATII cell differentiation making PTHrP receptor transcript levels indicative of alterations in lipofibroblast differentiation. Quantitative RT-PCR analysis revealed a drastic reduction in PTHrP receptor mRNA levels within the EpCAM1^-/CD45^- cell population (Figure 12) due to loss of lipofibroblasts in the aging lung.

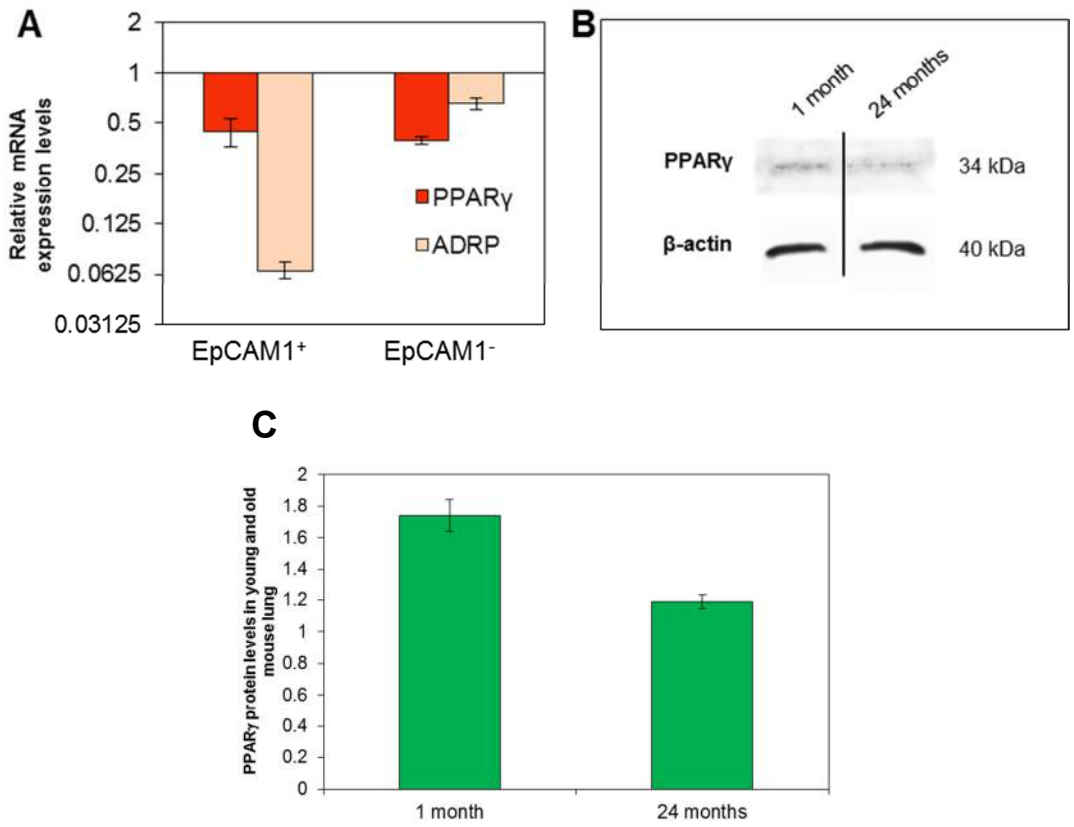

Figure 10: **A**: mRNA expression levels of adipose differentiation markers in 24 months Balb/c mouse lung epithelial and non-epithelial cells, compared to 1 month. Both the PPARγ and the ADRP are decreased at 24 months compared to the 1 month old lung cell types. B: PPARγ protein levels were detected in 1 month and 24 months old lung extracts by Western blotting. Equal protein loading was tested using anti-β-actin antibody. The blot is a representative of two individual experiments. **C**: The blots were then densitometrically analyzed and plotted against the controls.

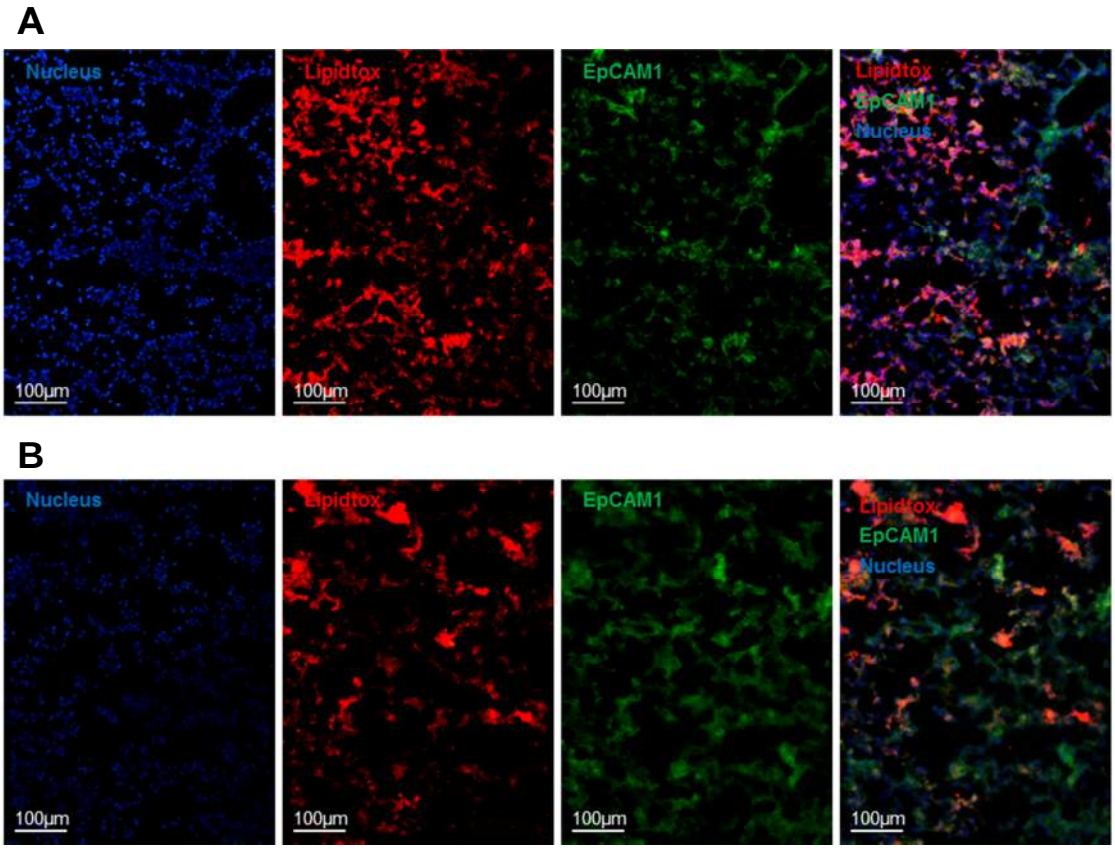

Figure 11: LipidTox staining of **A:** 1 month and **B:** 24 months old Balb/c mouse lung sections showing nuclei staining, lipid staining (LipidTox), and EpCAM1-FITC staining individually then in a merged picture

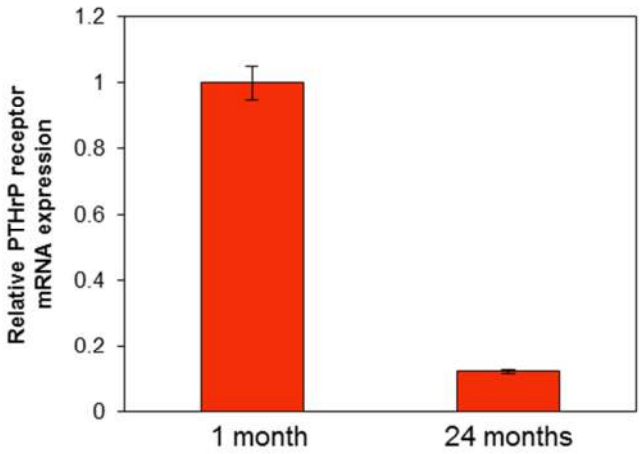

Figure 12: PTHrP receptor mRNA levels were measured in EpCAM-/CD45- cell populations of 1 month and 24 months old Balb/c mouse lungs using qRT-PCR analysis. (The graph is a representative of three individual experiments).

5.3 Alteration of the Wnt microenvironment during pulmonary senescence

Recent studies have highlighted the importance of Wnt signaling in the regulation of PPARγ activity. Takada reviewed (Takada *et al.* 2009) that canonical Wnts antagonize the effect of PPARγ in osteoblast-adipocyte differentiation. Moreover Talabér et al (Talaber *et al.* 2011) have shown that overexpression of Wnt4 in TEP1 thymic epithelial cell line results in reduced PPARγ expression and consequent inhibition of thymic adipose involution indicating a strong involvement of Wnts in pulmonary senescence also.

When measured, several Wnts, including Wnt4 as well as the inflammatory mediator, Wnt5a were expressed in both epithelial and non-epithelial cells of mouse lungs. While Wnt4 mRNA levels increased (Figure 13A) during aging in both epithelial (EpCAM-1^{+}) and non-epithelial (EpCAM-1^{-}) cells, both Wnt5a and Wnt11 expression decreased in epithelial (EpCAM-1^{+}) and increased in non-epithelial (EpCAM-1^{-}) (Figure 13A) cells with age. Western blot analysis of protein extracts of 1 month and 24 months mouse lungs supported the age associated increase in Wnt4 levels (Figure 13B). Protein studies performed on human lung samples using Wnt5a staining of 73 years old (Figure 14A) and 21 years old (Figure 14B) supported similarities between the mouse and human pulmonary senescence program. Corresponding to mouse qRT-PCR data, Wnt5a staining intensity increased with age in the human lung and Wnt5a was detected in the non-epithelial, cytokeratin-7 negative cell population (Figure 10C).

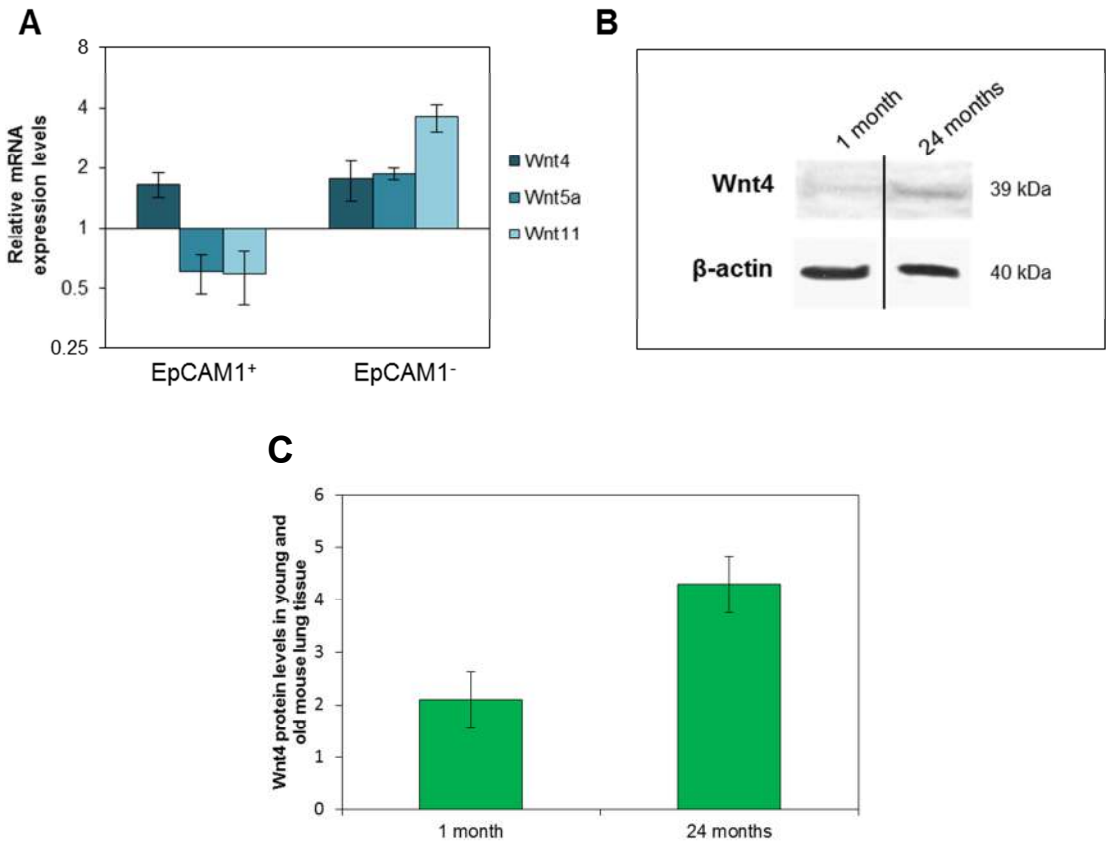

Figure 13: **A:** mRNA expression levels of different Wnt molecules in 24 months Balb/c mouse lung epithelial and non-epithelial cells were measured using qRT-PCR analysis and relative expression was determined to β-actin, then compared to Wnt expression in 1 month test animals. **B:** Wnt4 protein levels were detected in 1 month and 24 months old lung extracts by Western blotting. Equal protein loading was tested using anti-β-actin antibody. (The blot is a representative of two individual experiments). **C**: The blots were then densitometrically analyzed and plotted against the controls.

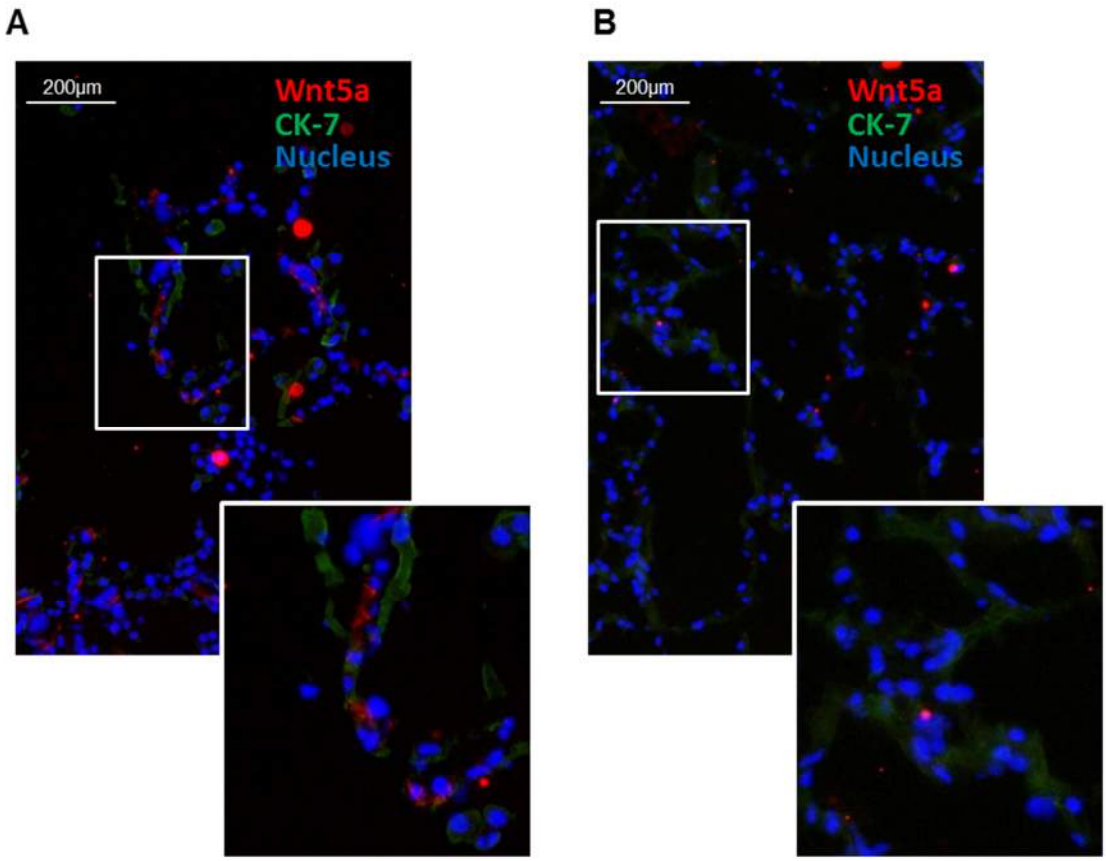

Figure 14: Immunofluorescent staining of Wnt5a in **A:** 73 years and **B:** 21 years human lung sections (The staining is representative of three separate experiments).

5.4 β-catenin dependent regulation of PPARγ expression

Our previous data (Talaber *et al.* 2011) as well as Takada's results (Takada *et al.* 2009) designated the canonical Wnt signaling pathway as regulator of PPARγ expression. As Wnt4 but not Wnt5a or Wnt11 can act via the canonical Wnt signaling pathway (Pongracz & Stockley 2006), our attention was focused on Wnt4. To be able to investigate molecular changes triggered by Wnt molecules in human lung tissue *in vitro*, 3D lung spheroids were exposed to control and Wnt4 supernatants of TEP1 cells for 7 days. Using qRT-PCR analysis, reduced mRNA expression levels of PPARγ were detected. Thereafter canonical Wnt pathway activity was modified using chemical activators and inhibitors of the β-catenin pathway. LiCl was used as an activator of the β-catenin pathway that inhibits the activity of GSK3-β, and therefore protects β-catenin from phosphorylation and consequent proteosomal degradation. IWR is an inhibitor of

the β-catenin pathway that acts via stabilization of Axin protein complexes aiding β-catenin destruction (Pongracz & Stockley 2006).

To investigate our theory, initially primary human lung fibroblasts (NHLF) were used and treated with LiCl at 10 mM, IWR at 1 μM concentration and a Wnt4 enriched supernatant for 7 days, then PPARγ mRNA levels were measured using qRT-PCR. The expression of PPARγ was drastically reduced after LiCl and Wnt4 treatment (Figure 15A and Figure 15B), while inhibition of β-catenin signaling increased PPARγ levels. β-catenin levels were also assessed by Western blot analysis after treatment of NHLF cells with LiCl, Wnt4 and IWR. While LiCl and Wnt4 treatment increased, IWR treatment reduced β-catenin protein levels (Figure 16A) indicating that amplified Wnt4 production during aging is likely to initiate reduction of lipofibroblast differentiation via a β-catenin dependent mechanism. To examine the possibility that Wnt4 induced reduction of PPARγ levels affect SPC production, the 3D in vitro tissue culture was applied, as 3D culture conditions stimulate surfactant production of SAEC. The lung tissue model was treated with Wnt4-enriched supernatants and rhWnt5a, respectively. Following 7 days of incubation, Wnt4 reduced pro-SPC expression demonstrating that Wnt4 can regulate pro-SPC levels (Figure 17A, 17B and 17C).

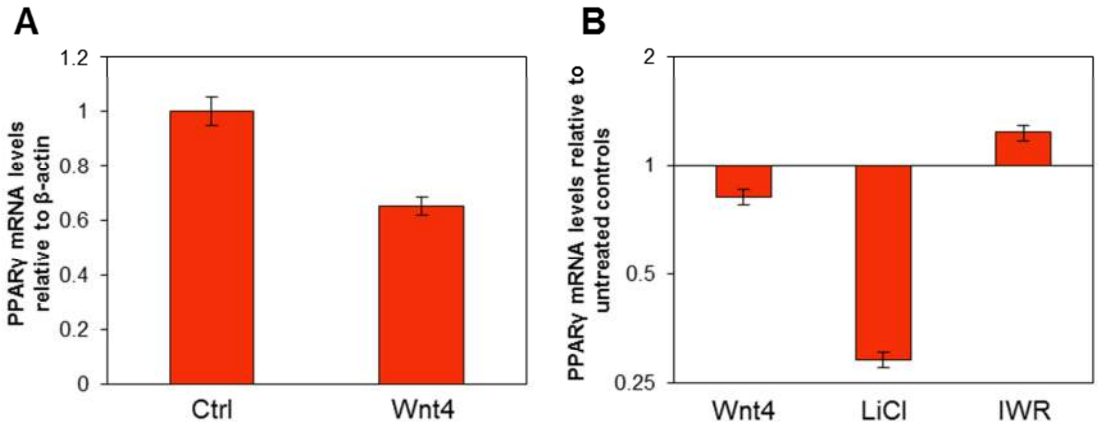

Figure 15: **A:** PPARγ expression levels in 3D spheroids, following 7 day exposure to control (ctrl) and Wnt4 supernatants of thymic epithelial cells (TEP1). PPARγ mRNA expression levels determined by qRT-PCR analysis following 7 day exposure to control (ctrl) and Wnt4 enriched supernatants of TEP1, to 10 mM LiCl and to 1 μM IWR in **B:** primary human lung fibroblast (NHLF) cells.

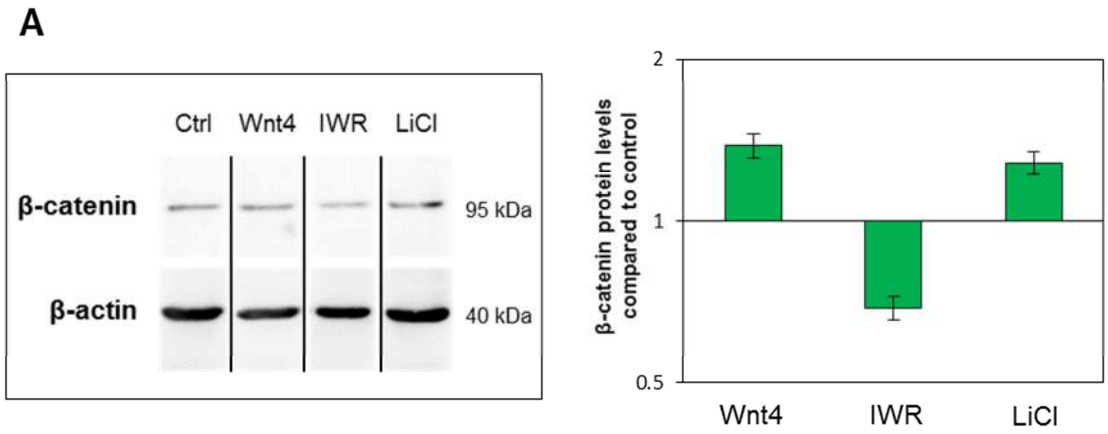

Figure 16: **A:** β-catenin protein levels were determined in NHLF cells after exposure to Wnt4 enriched supernatants of TEP1, 10 mM LiCl and 1 μM IWR for 7 days. Equal protein loading was determined using anti-β-actin antibody. (The blot is a representative of two individual experiments). The blots were then densitometrically analyzed and plotted against the controls.

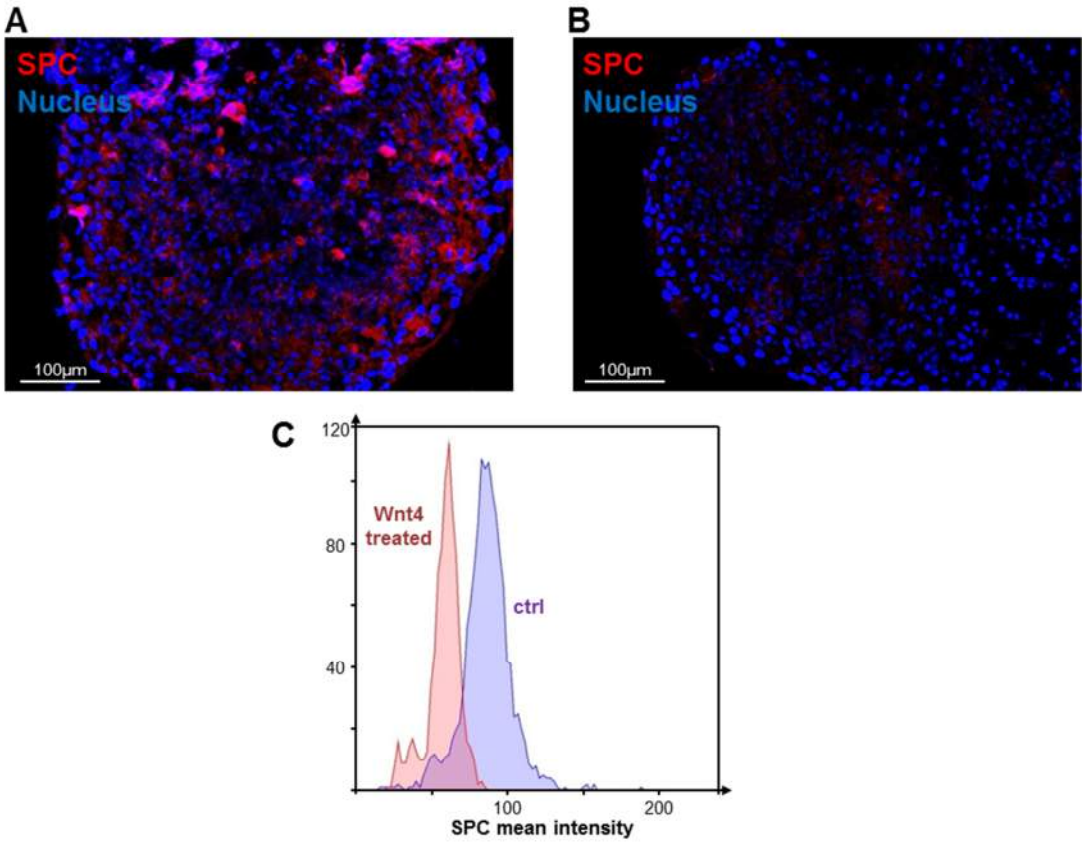

Figure 17: Pro-SPC staining on **A:** ctrl and **B:** Wnt4 enriched supernatant treated human 3D lung tissue spheroids (red: pro-SPC, blue: DAPI stained nuclei) (The staining is representative of three separate experiments). **C:** Mean intensity differences in pro-SPC staining in Wnt4 treated and Ctrl lung tissues. (The graph is a representative of three individual experiments).

5.5 Reduced β-catenin activity is necessary in pulmonary epithelial cells to produce pro-SPC

While the above data support that PPARγ levels in fibroblasts are necessary for lipofibroblast-like differentiation and maintenance of surfactant production in ATII-type cells, it is still not clear whether PPARγ activity is needed within the ATII cell population for surfactant synthesis. It is an important question as age associated decline of PPARγ mRNA affected not only fibroblasts but epithelial cells also (Figure 10A). As the aging process in the human lungs was associated with reduced pro-SPC levels (Figure 18A and 18B) the presence and activity of PPARγ in pulmonary epithelium might be equally important to that in lipofibroblasts.

β-catenin activity was modulated therefore using the physiological inhibitor of the β-catenin dependent Wnt signaling pathway, ICAT. ICAT (Graham *et al.* 2002) was introduced into epithelial as well as fibroblast cells using recombinant viral gene delivery methods in the 3D human lung model. To specifically target epithelial cells (SAEC), recombinant Adeno viruses (rAd-GFP and rAd-ICAT-GFP) were used, while fibroblasts (NHLF) were transfected using lentiviruses (rL-GFP and rL-ICAT-GFP). For lentiviral gene delivery, NHLF cells were infected before the generation of 3D lung tissue spheroids to avoid parallel transfection of the epithelial components. Following 7 days of exposure to ICAT, PPARγ expression was measured. Inhibition of β-catenin activity either in epithelium or in fibroblasts drastically increased PPARγ expression (Figure 19A and 19B) indicating that inhibition of β-catenin signaling modulates lipid metabolism of both cell types. Pro-SPC staining increased drastically in rAd-ICAT-GFP infected tissues (Figure 20A and 20B) identifying a β-catenin regulated and PPARγ dependent mechanism as an important element of pro-SPC production in ATII cells.

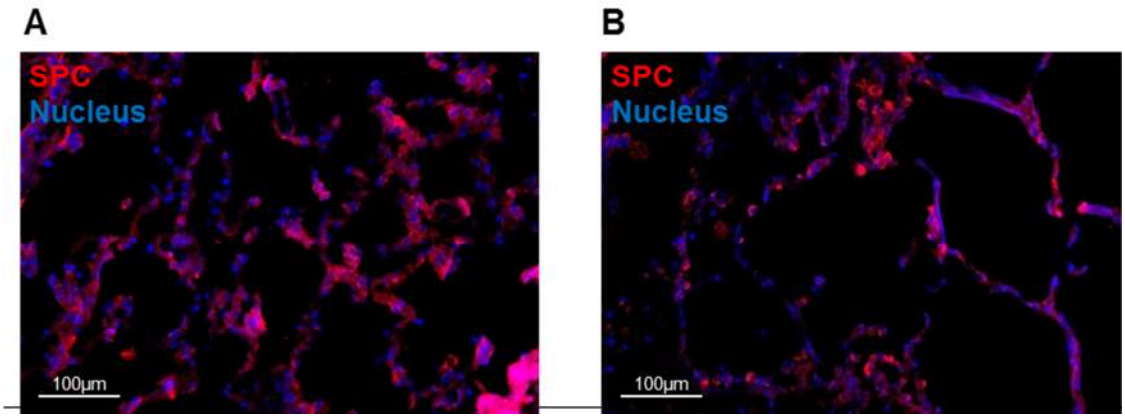

Figure 18: Immunofluorescent staining of pro-surfactant protein C (pro-SPC) in **A:** 21 years old and **B:** 73 years old human lung tissue sections.

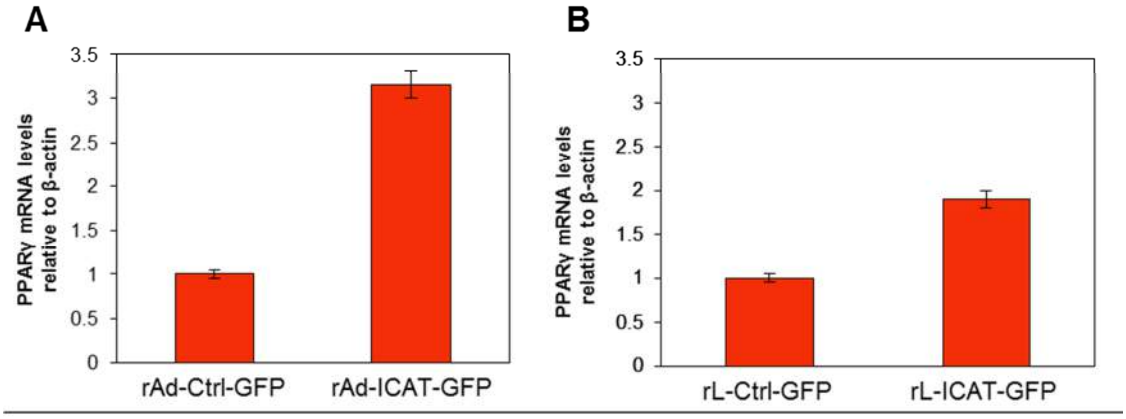

Figure 19: **A:** PPARγ mRNA expression levels were determined by qRT-PCR analysis in 3D human lung tissue model following 7 day suppression of β-catenin activity by ICAT specifically within the SAEC population using rAd gene delivery. **B:** PPARγ mRNA expression levels were determined by qRT-PCR analysis in 3D human lung tissue model following suppression of β-catenin activity by ICAT specifically within the NHLF cell population using rL gene delivery.

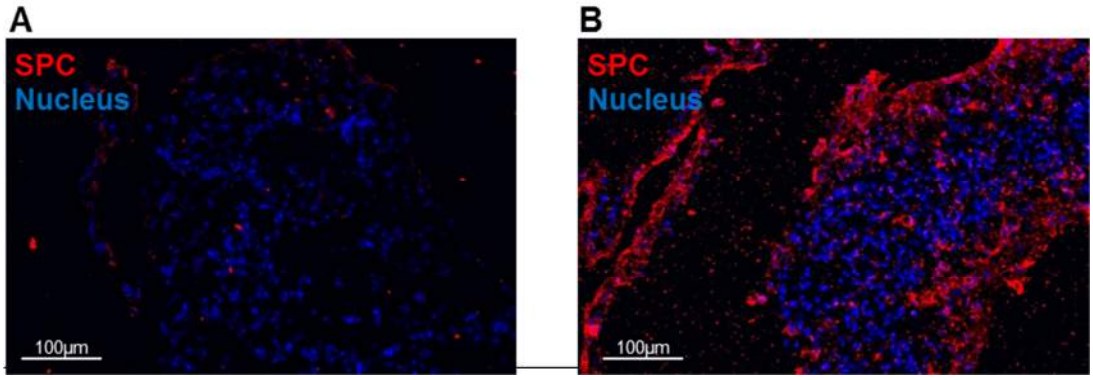

Figure 20: Immunofluorescence staining of pro-SPC in **A:** control 3D human lung tissue model containing rAd-Ctrl-GFP SAEC and **B:** ICAT overexpressing 3D human lung tissue model containing rAd-ICAT-GFP SAEC (the staining is representative of three separate experiments).

5.6 Wnt signaling in myofibroblast-like differentiation

According to a previous study (Torday et al 2003) transdifferentiation of lipofibroblasts to myofibroblasts is characterized by loss of PTHrP receptor expression and triglyceride content. Our results support previous findings as PTHrP mRNA levels decreased with age in the non-epithelial cell population (Figure 12). To investigate if changes in the Wnt microenvironment are responsible for increased myofibroblast differentiation, the myofibroblast marker S100A4 mRNA was measured after exposure of NHLF cells and the 3D lung tissue spheroids to Wnt4 and Wnt5a, respectively. Interestingly, both Wnt4 and Wnt5a were able to increase S100A4 transcript levels (Figure 21A and 21B) indicating involvement in the regulation of myofibroblast- differentiation.

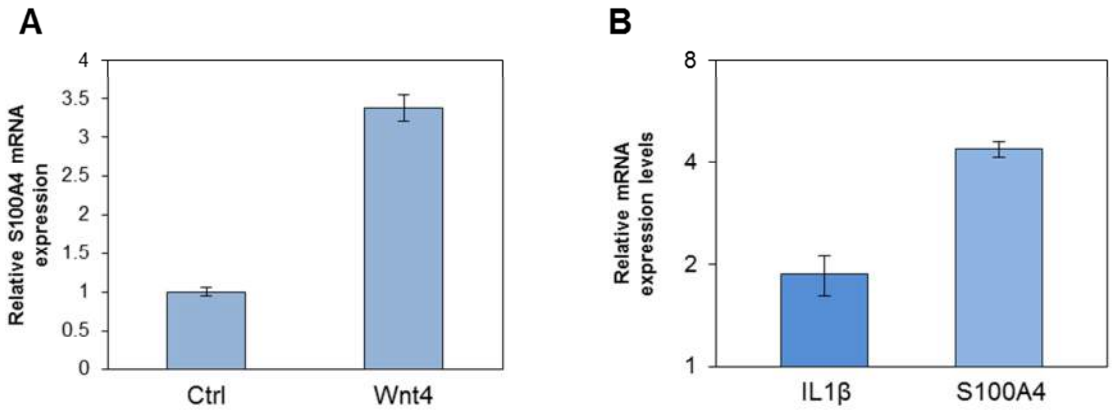

Figure 21: **A:** Relative gene expression levels of S100A4 in Wnt4 enriched supernatant treated human lung tissue spheroids. qRT-PCR analysis of gene expression is presented as relative to controls (data is representative of two separate experiments). **B:** Relative gene expression levels of IL1β and S100A4 in rhWnt5a treated human lung tissue spheroids. qRT-PCR analysis of gene expression is presented as relative to un-treated controls (data is representative of three separate experiments).

5.7 Epigenetic regulation of the pulmonary aging mechanism

As it is accepted that environmental factors affect aging in general, it was predicted that epigenetic mechanisms can modulate pulmonary senescence. Sirtuins are often connected with aging and different senescent mechanisms. In order to unveil their function in pulmonary senescence, an initial screening of Sirtuin expression was performed. mRNA level was measured in both $EpCAM^{+}$ (epithelial) and $EpCAM^{-}$ (fibroblast like, non-epithelial) pulmonary cells of young and old mouse lung samples.

Interestingly, both Sirt1 and Sirt7 message levels were increased with age, although Sirt7 showed a higher, nearly two fold increases in both cell types (Figure 22). At protein level the difference between the young and old lungs was more pronounced. While Sirt1 protein expression increased significantly in old human lungs supporting mRNA data (Figure 23), Sirt7 protein remained undetectable both in young and old lungs. Based on the general view of the anti-aging function of Sirt1, it was difficult to explain our findings. Recent studies, however, have revealed that Sirt1 acts against adipogenesis and inhibits PPARγ protein function. To investigate whether Sirt1 can inhibit PPARγ activity in lung tissues, experiments were set up using 10 nM concentration of resveratrol, a small molecule that mimics Sirt1 function, and Wnt4 that was able to activate the β-catenin pathway and inhibit PPARγ in previous experiments. As both resveratrol and Wnt4 act as inhibitors of PPARγ expression, a synergistic effect was expected that was supported by experiments, as both resveratrol and Wnt4 down-regulated PPARγ expression and their effects were additive in co-treatment (Figure 24).

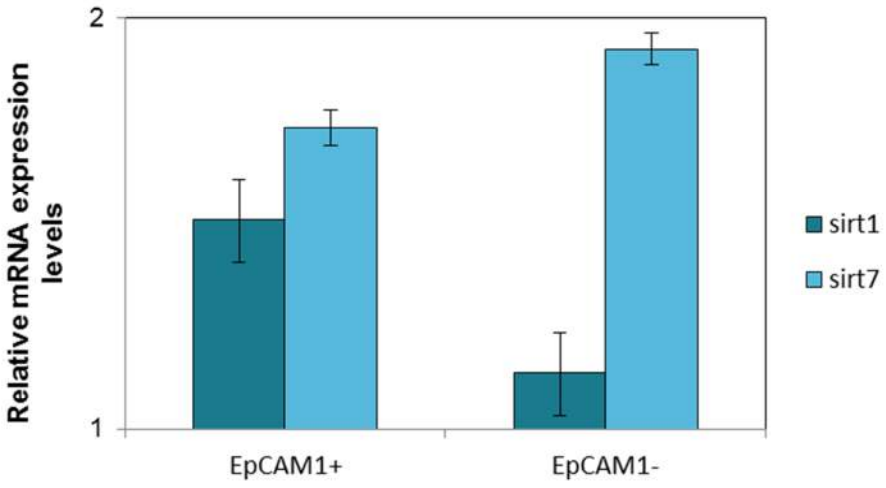

Figure 22 A: mRNA expression levels of Sirt1 and Sirt7 molecules in 24 months Balb/c mouse lung epithelial and non-epithelial cells were measured using qRT-PCR analysis and relative expression was determined to β-actin, then compared to Sirt1 and Sirt7 expression in 1 month test animals.

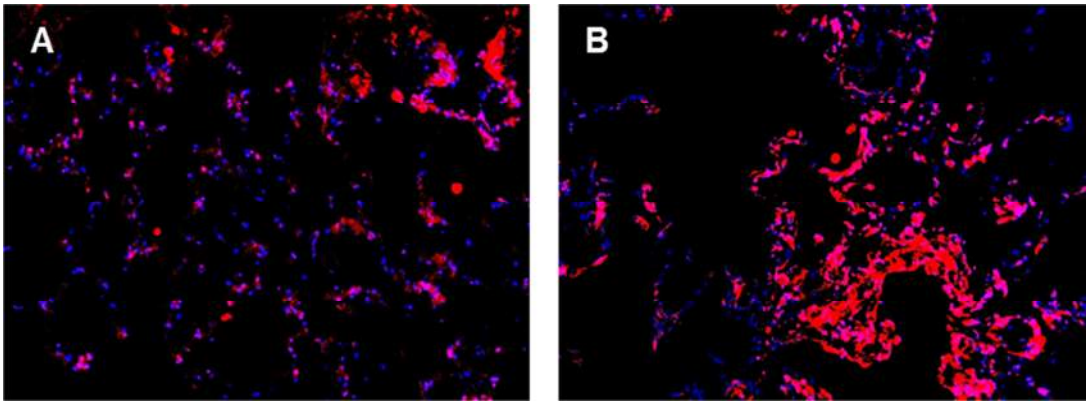

Figure 23: Immunofluorescent staining ofSirt1 in **A:** 21 years old and **B:** 73 years old human lung tissue sections.

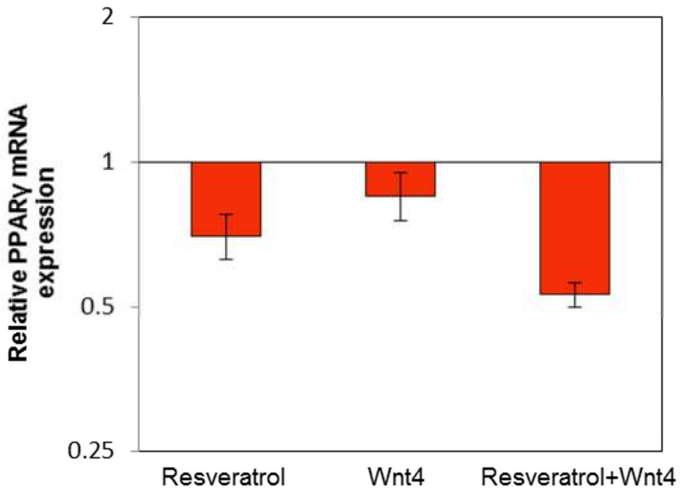

Figure 24: Relative PPARγ mRNA expression levels in 3D lung tissues following 1 week of 10 nM Resveratrol and Wnt4 supernatant exposure.

6. Discussion

During senescence, changes in the structure and cellular composition of the lung leads to airspace enlargement and to decrease of useful alveolar surface area (Tolep *et al.* 1995). The enlarged alveoli can be visualized in micro CT pictures of mice as well as in HE staining of both mouse and human lung sections. Investigation of the RNA expression levels of Wnt4, Wnt5a Wnt11 and other molecules PPARγ, ADRP of the pulmonary aging process has highlighted that both in test animals and in humans the structural differences are triggered by very similar molecular alterations in Wnt signaling, as Wnt4 and Wnt5a were differentially up-regulated in the aging lung.

Pinpointing the initial molecular trigger, however, is difficult. Increased Wnt5a levels have been reported to regulate accumulation of leukocytes and increased inflammatory cytokine production (Li *et al.* 2011; Briolay *et al.* 2013) as well as senescence (Florian *et al.* 2013) in many tissues. Previous studies have also described Wnt5a to increase fibroblast proliferation (Vuga *et al.* 2009), increased inflammatory cytokine production (Rauner *et al.* 2012) and epithelial cell migration (Bartis *et al.* 2013) providing further insight into the molecular environment favoring fibrosis and cancer development in the elderly lung.

Based on the physiological effects of Wnt5a, increased Wnt5a secretion in the aging lung can stimulate inflammation and maintain a damaging environment that affects the gas-exchange surface. If the damaging microenvironment is prolonged and coincides with a reduced regenerative capacity, the outcome can be fatal. Decreased number of the alveolar progenitor or ATII cells (Torday *et al.* 2003; Yee *et al.* 2006) could explain such age associated reduction in the regenerative capacity. As ATII cells serve not just as alveolar stem cells, but they are also the source of surfactants, reduction in pro-SPC levels can also indicate weakened functionality of ATII-s and decreased stability of alveolar structure and function as well as vulnerability to infections. But why would ATII-s produce less surfactants with age?

In parallel with increased Wnt5a levels, Wnt4 expression also increases in the lung with age. The highly conserved Wnt4 molecule that has been reported to maintain homeostasis and regulate regeneration in many organs shows imbalance with age that can lead to diseases in various organs (He *et al.* 2009; DiRocco *et al.* 2013) although specific mechanisms have not been described yet. Our studies perhaps are amongst the first ones that can provide explanation for consequences of age-associated alterations in

Wnt4 levels. Wnt4 and down-stream activation of β-catenin can affect the lipid metabolism at PPARγ level. The PPARγ is an essential molecule for the triglyceride uptake of lipofibroblasts. As lipofibroblasts provide triglycerides for ATII cells and indirectly support SPC production, Wnt4 induced reduction in PPARγ levels can have far reaching consequences. PPARγ and its down-stream target, ADRP are responsible for the uptake of triglycerides from the blood stream (Varisco *et al.* 2012) that is essential for surfactant production in ATII cells. If PPARγ levels are reduced, then triglyceride uptake is reduced that directly leads to down-regulation of surfactant production. As surfactant lining of the alveoli is essential to uniform inflation, and to protect against chemical or particulate injury of the distal lungs, the reduced surfactant level makes the lung prone to infections and chronic inflammation. Because ATII cells are facultative stem cells of the alveolar region, the change in the microenvironment damages the regenerative capacity and accelerates aging.

Up-regulation of Wnt4 and Wnt5a has an additional impact on the aging lung tissue. Both Wnt4 and Wnt5a can increase myofibroblast (S100A4) marker expression indicating that ATII cells are left without their essential support mechanism (lipofibroblast) (Torday *et al.* 2003; Rehan & Torday 2012) during senescence. Additionally, Wnt4 induced myofibroblast differentiation might also be linked to modulation of tissue damage control, as when tissue or parenchymal repair is needed myofibroblasts function as elemental emergency cells. It might sound good at first, but the presence of myofibroblast are often related to fibrosis (DiRocco *et al.* 2013). Data in the literature and our results point more directly towards development of fibrosis (DiRocco *et al.* 2013) once Wnt4 levels are higher. As Wnt4 reduces PPARγ expression, Wnt4 aids lipofibroblast to myofibroblast transdifferentiation that process can cause emphysema like structures in aged lungs.

While modification of Wnt expression in absolute protein levels are relatively little, the distal lung seems unable to adapt to shifts in the molecular microenvironment (Figure 25). Especially, as changes taking place are simultaneously magnified at several levels. An increase in Wnt4 expression both in epithelial and non-epithelial cells leads to PPARγ down-regulation that paralyses lipofibroblast differentiation and facilitates myofibroblast production and quite possibly reduces the ability of ATII cells for surfactant production. As in the absence of lipofibroblasts ATII-s can no longer replenish their triglyceride sources from the blood, surfactant production can become

drastically reduced. In the absence of surfactants, the lung tissue becomes prone to infections (LeVine *et al.* 2002; Kazi *et al.* 2010). During the course of infection, alveolar epithelial cells also start to produce Wnt5a that adds to the already increased Wnt5a levels produced by the aging non-epithelial elements of the distal lung. The simultaneous increase in inflammatory cytokines produced by the infiltrating immune cells that attack the site of infection can increase Wnt5a levels even further (Rauner *et al.* 2012). Meanwhile, the damaged alveolar epithelial lining is unable to regenerate as the number of functional ATII cells is decreasing leaving the damaged tissue in need of myofibroblasts to close the wound.

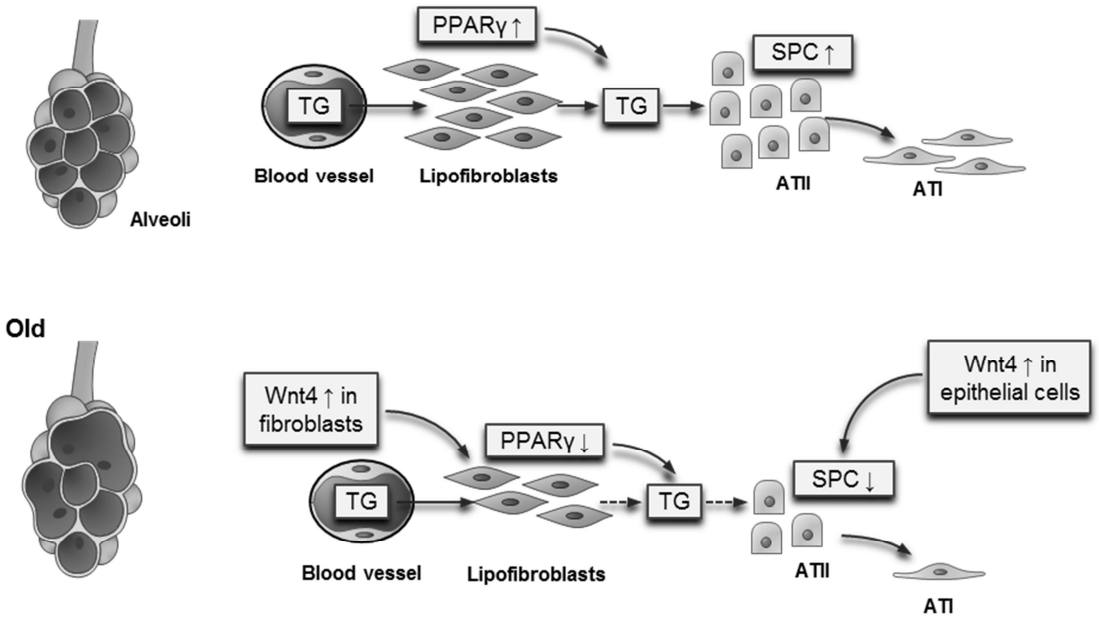

Figure 25: Schematic summary of molecular changes in the distal lung during senescence (TG: triglyceride; SPC: pro-surfactant protein C, PPARγ: peroxisome proliferator-activated receptor gamma).

Environmental factors also modulate the process of pulmonary senescence. While Sirtuins, the NAD dependent deacetylases have been proposed to protect tissues against senescence (Imai *et al.* 2000), our data concerning pulmonary aging mechanisms don't unequivocally support such statements. Our theories are aided by the literature. For example, Sirt1 and Sirt7 act antagonistically on PPARγ. While Sirt1 controls lipolysis and physiological differentiation processes leading away from adipogenesis (Haigis & Sinclair 2010; Yang *et al.* 2014), Sirt7 has often been described to have an opposite

effect. Sirt7 can form a direct protein-protein bond with Sirt1 changing Sirt1 function and promoting adipogenesis (Bober *et al.* 2012). In the lung, lipofibroblasts that support ATII maintenance and function are dependent of PPARγ activity that is regulated by Sirtuins. In the absence of PPARγ lipofibroblasts differentiate into myofibroblast that no longer support triglyceride uptake and normal epithelial microenvironment of the alveolar region. Sirt1 can suppress PPARγ and as increased levels of Sirt1 at both message and protein levels were detected in the aging lung suppression lipofibroblast-type differentiation is hardly surprising during pulmonary senescence. Simultaneously, Sirt7 protein was undetectable in aged lung tissues indicating that PPARγ expression can be suppressed by Sirt1 while the effect of Sirt7 message is unlikely to be substantial in this physiological setting.

Interestingly, Sirt1 is also connected to Wnt signaling via activation of Dvl proteins and accumulation (Holloway *et al.* 2010) and deacetylation of β-catenin (Simic *et al.* 2013; Gao *et al.* 2014) that leads to suppression of PPARγ expression and activity.

Although there are some contradicting experiments on cell lines (Firestein *et al.* 2008), our work using the Sirt1 activator (Howitz *et al.* 2003; Pervaiz & Holme 2009) resveratrol revealed that similarly to Wnt4, Sirt1 can suppress PPARγ, and therefore can accelerate lipofibroblast to myofibroblast differentiation leading to inability to repair lung damage in aging individuals.

In conclusion we can also state, that while resveratrol/Sirt1, might effectively protects longevity in certain single cell organisms, the lung may not benefit from activation of Sirt1 at all and “cost-benefit” has to be analyzed carefully before encouraging the general public to take the Sirt1 activator -resveratrol- in high dosage.

7. Conclusions

The alveolar region of the lung changes during aging and the useful lung surface decreases.

The Wnt microenvironment changes with age and while Wnt4 mRNA is elevated in both $EpCAM^+$ (epithelial) and in $EpCAM^-$ (non-epithelial cells), Wnt5a levels only increase in non-epithelial cells.

In contrast to Wnts, PPARγ and its downstream target molecule ADRP are decreased both in the EpCAM+ (epithelial) and in EpCAM- (non-epithelial) cell populations. These molecules are very important in adipogenesis in general and in the life of lipofibroblasts, the regulators of ATII maintenance in the lung.

Regulation of PPARγ expression is a canonical or β-catenin dependent process.

Wnt4 and Wnt5a both increase the mRNA level of S100A4 myofibroblasts marker and decrease PTHrP lipofibroblast marker. These results suggest activation of a lipofibroblast to myofibroblasts transdifferentiation mechanisms during pulmonary senescence.

Increased myofibroblast presence in the aging lung can result in emphysema like structures, decreased respiratory surface are and in consequent breading difficulty.

Sirt1 and Sirt7 have elevated at mRNA level in mice, but only Sirt1 proteins were detected at increased levels in aged human lung tissues supporting our proposed mechanism of aging in the lung.

Additionally, human lung tissues exposed to resveratrol and/or Wnt4 resulted in PPARγ suppression and changes detected during pulmonary senesce.

8. Acknowledgement

I would like to express my deepest gratitude to my supervisor Prof. Judit E. Pongrácz for her excellent guidance, caring, patience, and for providing an excellent research atmosphere. Without her, I would have never been able to finish my PhD thesis.

I also would like to bow my thanks to my other supervisor Dr. Krisztián Kvell who helped me a lot during my laboratory work and his advices always helped me to solve problems.

I would like to thank my colleagues, especially Dávid Ernszt and Diána Feller who were always next to me in the lab and we had great discussions during late night experiments.

I would also like to thank all the colleagues in the Department of Pharmaceutical Biotechnology and the Department of Immunology and Biotechnology.

Finally, I would like to thank my family and friends who always supported and encouraged me during my studies.

9. List of publications

Total impact factor: 9.669

Total citations: 4

The thesis based on the following publications

Kovacs, T., Csongei, V., Feller, D., Ernszt, D., Smuk, G., Sarosi, V., Jakab, L., Kvell, K., Bartis, D. and Pongracz, J. E. (2014), Alteration in the Wnt microenvironment directly regulates molecular events leading to pulmonary senescence. Aging Cell, 13: 838–849. doi: 10.1111/acel.12240 (IF: 5.939)

Kovacs, T., Feller, D., Ernszt, D. Rapp J., Sarosi, V., Kvell, K., and Pongracz, J. E. Epigenetic regulation of pulmonary senescence. To be submitted to Mechanisms of Aging (IF: 3.510).

The thesis based on the following conference presentations and posters

Presentations:

Kovács T, Kvell K, Willert K, Pongrácz J.E: The functional test of Wnt protein. First International Doctoral Workshop in Natural Sciences 2012.

Kovács T., Csöngei V., Ernszt D., Feller D., Pongrácz J.E.: Wnt4 promotes tissue destruction during lung aging via inhibiting PPARγ expression. Second International Doctoral Workshop in Natural Sciences 2013. ISBN: 978-963-08-7403-8 (First prize winner in oral presentation section)

Posters

Kovács T, Ernszt D, Pongrácz JE: The molecular pattern of aging lung. 9th János Szentágothai Interdisciplinary Conference and Student Competition, Pécs, Hungary, 3-4 May 2013 ISBN 978-963-642-519-7 (First prize winner in Medical Poster section)

Kovacs T, Csongei V, Feller D, Ernszt D, Bartis D, Pongrácz JE: Altered Wnt microenvironment during pulmonary senescence leads to drastic decline of the alveolar epithelial surface. ERS Lung Science Conference 2014 Estoril, Portugal. March 21-23, 2014

Csongei V, Feller D, **Kovacs T**, Bartis D, Helyes Z, Pongrácz JE: Three-dimensional human lung micro-cultures for in vitro studies of COPD. ERS Lung Science Conference 2014 Estoril, Portugal. March 21-23, 2014

Other publications

Bartis D, Csongei V, Weich A, Kiss E, Barko S, **Kovacs T**, Avdicevic M, D'Souza VK; Rapp R, Kvell K, Jakab L, Nyitrai M, Molnar TF, Thickett DR, László T, Pongrácz JE (2013): Down regulation of Canonical and Up-Regulation of Non-Canonical Wnt signalling int he carcinogenic process of Squamous Cell Lung Carcinoma. PLoS ONE 8(3):e57393. doi:10.1371/journal.pone.0057393 (IF: 3.730)

Ernszt D, Pap A, **Kovacs T**, Keller Zs, Fejes V.A. Gaál P, Werry JE, Nagy L, Pongracz JE, Kvell K: The missing link of thymic senescence (2014) Submitted to Nature Communications (IF: 10.742)

Lecture note

Miskei Gy, Rapp J, Kiss E, **Kovacs T**, Pongracz JE (2014): Basic and Complex Cell and Tissue Culture Techniques for Biotechnology Students. University of Pécs

Other posters

Feller D., Helyes Zs., Rapp J., Kun J., Ernszt D., Kovács T., Pongracz E. J.: Changes inexpression levels of Wnt signalling molecules in cigarette smoke- induced experimental model systems. 9th János Szentágothai Interdisciplinary Conference and Student Competition, Pécs, Hungary, 3-4 May 2013ISBN 978-963-642-519-7

Sípos G, Csöngei V, Kovács T, Kvell K, Pongrácz JE: Development of an in vitro 3D lung tissue model containing activated T-cells to study chronic obstructive pulmonary disease (COPD).9th János Szentagothai Inrterdisciplinary Conference and Student Competition, Pécs, Hungary, 3-4 May 2013 ISBN 978-963-642-519-7

10. References

Aberle H, Bauer, A., Stappert, J., Kispert, A., and Kemler, R. (1997). b-Catenin is a target for the ubiquitin-proteosome pathway. *EMBO J.* **16**, 3797-3804.

Ahmadian M, Suh JM, Hah N, Liddle C, Atkins AR, Downes M , Evans RM (2013). PPARγ signaling and metabolism: the good, the bad and the future. *Nat Med*. **19**, 557-566.

Akiyama T (2000). Wnt/b-catenin signaling. *Cytokine&Growth Factor Rev.* **11**, 273-282.

Baarsma HA, Spanjer AI, Haitsma G, Engelbertink LH, Meurs H, Jonker MR, Timens W, Postma DS, Kerstjens HA , Gosens R (2011). Activation of WNT/β-catenin signaling in pulmonary fibroblasts by TGF-β_1 is increased in chronic obstructive pulmonary disease. *PLoS One*. **6**, e25450.

Balogh P, Bebök Z , Németh P (1992). Cellular enzyme-linked immunocircle assay. A rapid assay of hybridomas produced against cell surface antigens. *J Immunol Methods*. **153**, 141-149.

Barkauskas CE, Cronce MJ, Rackley CR, Bowie EJ, Keene DR, Stripp BR, Randell SH, Noble PW , Hogan BL (2013). Type 2 alveolar cells are stem cells in adult lung. *J Clin Invest*. **123**, 3025-3036.

Bartis D, Csongei V, Weich A, Kiss E, Barko S, Kovacs T, Avdicevic M, D'Souza VK, Rapp J, Kvell K, Jakab L, Nyitrai M, Molnar TF, Thickett DR, Laszlo T , Pongracz JE (2013). Down-regulation of canonical and up-regulation of non-canonical Wnt signalling in the carcinogenic process of squamous cell lung carcinoma. *PLoS One*. **8**, e57393.

Beardsley TR, Pierschbacher M, Wetzel GD , Hays EF (1983). Induction of T-cell maturation by a cloned line of thymic epithelium (TEPI). *Proc Natl Acad Sci U S A.* **80**, 6005-6009.

Berger J , Moller DE (2002). The mechanisms of action of PPARs. *Annu Rev Med.* **53**, 409-435.

Bober E, Jian, Smolka C, Ianni A, Vakhrusheva O, Krüger M , Braun T (2012). Sirt7 promotes adipogenesis by binding to and inhibiting Sirt1ed^eds). *BMC Proceedings*.

Bovia F, Salmon P, Matthes T, Kvell K, Nguyen TH, Werner-Favre C, Barnet M, Nagy M, Leuba F, Arrighi JF, Piguet V, Trono D , Zubler RH (2003). Efficient transduction of primary human B lymphocytes and nondividing myeloma B cells with HIV-1-derived lentiviral vectors. *Blood*. **101**, 1727-1733.

Brack AS, Conboy MJ, Roy S, Lee M, Kuo CJ, Keller C , Rando TA (2007). Increased Wnt signaling during aging alters muscle stem cell fate and increases fibrosis. *Science*. **317**, 807-810.

Briolay A, Lencel P, Bessueille L, Caverzasio J, Buchet R , Magne D (2013). Autocrine stimulation of osteoblast activity by Wnt5a in response to TNF-α in human mesenchymal stem cells. *Biochem Biophys Res Commun*. **430**, 1072-1077.

Burstein B , Nattel S (2008). Atrial fibrosis: mechanisms and clinical relevance in atrial fibrillation. *J Am Coll Cardiol*. **51**, 802-809.

Chen Z, Jin N, Narasaraju T, Chen J, McFarland LR, Scott M , Liu L (2004). Identification of two novel markers for alveolar epithelial type I and II cells. *Biochem Biophys Res Commun*. **319**, 774-780.

Chilosi M, Poletti V , Rossi A (2012). The pathogenesis of COPD and IPF: distinct horns of the same devil? *Respir Res*. **13**, 3.

Chilosi M, Poletti V, Zamò A, Lestani M, Montagna L, Piccoli P, Pedron S, Bertaso M, Scarpa A, Murer B, Cancellieri A, Maestro R, Semenzato G , Doglioni C (2003). Aberrant Wnt/beta-catenin pathway activation in idiopathic pulmonary fibrosis. *Am J Pathol*. **162**, 1495-1502.

Chinetti G, Griglio S, Antonucci M, Torra IP, Delerive P, Majd Z, Fruchart JC, Chapman J, Najib J , Staels B (1998). Activation of proliferator-activated receptors alpha and gamma induces apoptosis of human monocyte-derived macrophages. *J Biol Chem*. **273**, 25573-25580.

Clark RB, Bishop-Bailey D, Estrada-Hernandez T, Hla T, Puddington L , Padula SJ (2000). The nuclear receptor PPAR gamma and immunoregulation: PPAR gamma mediates inhibition of helper T cell responses. *J Immunol*. **164**, 1364-1371.

Conboy IM, Conboy MJ, Wagers AJ, Girma ER, Weissman IL , Rando TA (2005). Rejuvenation of aged progenitor cells by exposure to a young systemic environment. *Nature*. **433**, 760-764.

Crosby LM , Waters CM (2010). Epithelial repair mechanisms in the lung. *Am J Physiol Lung Cell Mol Physiol*. **298**, L715-731.

Daynes RA , Jones DC (2002). Emerging roles of PPARs in inflammation and immunity. *Nat Rev Immunol*. **2**, 748-759.

DiRocco DP, Kobayashi A, Taketo MM, McMahon AP , Humphreys BD (2013). Wnt4/β-catenin signaling in medullary kidney myofibroblasts. *J Am Soc Nephrol*. **24**, 1399-1412.

Engelhardt JF (2001). Stem cell niches in the mouse airway. *Am J Respir Cell Mol Biol*. **24**, 649-652.

Evans MJ, Cabral-Anderson LJ , Freeman G (1978). Role of the Clara cell in renewal of the bronchiolar epithelium. *Lab Invest*. **38**, 648-653.

Ferguson HE, Kulkarni A, Lehmann GM, Garcia-Bates TM, Thatcher TH, Huxlin KR, Phipps RP , Sime PJ (2009). Electrophilic peroxisome proliferator-activated receptor-gamma ligands have potent antifibrotic effects in human lung fibroblasts. *Am J Respir Cell Mol Biol*. **41**, 722-730.

Firestein R, Blander G, Michan S, Oberdoerffer P, Ogino S, Campbell J, Bhimavarapu A, Luikenhuis S, de Cabo R, Fuchs C, Hahn WC, Guarente LP , Sinclair DA (2008). The SIRT1 deacetylase suppresses intestinal tumorigenesis and colon cancer growth. *PLoS One*. **3**, e2020.

Florian MC, Nattamai KJ, Dörr K, Marka G, Uberle B, Vas V, Eckl C, Andrä I, Schiemann M, Oostendorp RA, Scharffetter-Kochanek K, Kestler HA, Zheng Y , Geiger H (2013). A canonical to non-canonical Wnt signalling switch in haematopoietic stem-cell ageing. *Nature*. **503**, 392-396.

Frye RA (2000). Phylogenetic classification of prokaryotic and eukaryotic Sir2-like proteins. *Biochem Biophys Res Commun*. **273**, 793-798.

Gao C, Xiao G , Hu J (2014). Regulation of Wnt/β-catenin signaling by posttranslational modifications. *Cell Biosci*. **4**, 13.

Gao J , Serrero G (1999). Adipose differentiation related protein (ADRP) expressed in transfected COS-7 cells selectively stimulates long chain fatty acid uptake. *J Biol Chem*. **274**, 16825-16830.

Golan T, Yaniv A, Bafico A, Liu G , Gazit A (2004). The human Frizzled 6 (HFz6) acts as a negative regulator of the canonical Wnt. beta-catenin signaling cascade. *J Biol Chem*. **279**, 14879-14888.

Graham TA, Clements WK, Kimelman D , Xu W (2002). The crystal structure of the beta-catenin/ICAT complex reveals the inhibitory mechanism of ICAT. *Mol Cell*. **10**, 563-571.

Haigis MC , Guarente LP (2006). Mammalian sirtuins--emerging roles in physiology, aging, and calorie restriction. *Genes Dev*. **20**, 2913-2921.

Haigis MC , Sinclair DA (2010). Mammalian sirtuins: biological insights and disease relevance. *Annu Rev Pathol*. **5**, 253-295.

Han L, Zhou R, Niu J, McNutt MA, Wang P , Tong T (2010). SIRT1 is regulated by a PPAR{γ}-SIRT1 negative feedback loop associated with senescence. *Nucleic Acids Res*. **38**, 7458-7471.

He W, Dai C, Li Y, Zeng G, Monga SP , Liu Y (2009). Wnt/beta-catenin signaling promotes renal interstitial fibrosis. *J Am Soc Nephrol*. **20**, 765-776.

Hinz B, Phan SH, Thannickal VJ, Galli A, Bochaton-Piallat ML , Gabbiani G (2007). The myofibroblast: one function, multiple origins. *Am J Pathol*. **170**, 1807-1816.

Holloway KR, Calhoun TN, Saxena M, Metoyer CF, Kandler EF, Rivera CA , Pruitt K (2010). SIRT1 regulates Dishevelled proteins and promotes transient and constitutive Wnt signaling. *Proc Natl Acad Sci U S A*. **107**, 9216-9221.

Howitz KT, Bitterman KJ, Cohen HY, Lamming DW, Lavu S, Wood JG, Zipkin RE, Chung P, Kisielewski A, Zhang LL, Scherer B , Sinclair DA (2003). Small molecule activators of sirtuins extend Saccharomyces cerevisiae lifespan. *Nature*. **425**, 191-196.

Ikeda S, Kishida, S., Yamamoto, H., Murai, H., Koyama, S., Kikuchi, A. (1998). Axin, a negative regulator of the Wnt signaling pathway, forms a complex with GSK3b and b-catenin and promotes GSK-3b-dependent phosphorylation of b-catenin. *The EMBO J*. **17**, 1371-1384.

Imai S, Johnson FB, Marciniak RA, McVey M, Park PU , Guarente L (2000). Sir2: an NAD-dependent histone deacetylase that connects chromatin silencing, metabolism, and aging. *Cold Spring Harb Symp Quant Biol*. **65**, 297-302.

Ishitani T, Kishida S, Hyodo-Miura J, Ueno N, Yasuda J, Waterman M, Shibuya H, Moon RT, Ninomiya-Tsuji J , Matsumoto K (2003). The TAK1-NLK mitogen-activated protein kinase cascade functions in the Wnt-5a/Ca(2+) pathway to antagonize Wnt/beta-catenin signaling. *Mol Cell Biol*. **23**, 131-139.

Kazi AS, Tao JQ, Feinstein SI, Zhang L, Fisher AB , Bates SR (2010). Role of the PI3-kinase signaling pathway in trafficking of the surfactant protein A receptor P63

(CKAP4) on type II pneumocytes. *Am J Physiol Lung Cell Mol Physiol*. **299**, L794-807.

Kheradmand F, Folkesson HG, Shum L, Derynk R, Pytela R , Matthay MA (1994). Transforming growth factor-alpha enhances alveolar epithelial cell repair in a new in vitro model. *Am J Physiol*. **267**, L728-738.

Kim J, Kim DW, Ha Y, Ihm MH, Kim H, Song K , Lee I (2010). Wnt5a induces endothelial inflammation via beta-catenin-independent signaling. *J Immunol*. **185**, 1274-1282.

Königshoff M, Balsara N, Pfaff EM, Kramer M, Chrobak I, Seeger W , Eickelberg O (2008). Functional Wnt signaling is increased in idiopathic pulmonary fibrosis. *PLoS One*. **3**, e2142.

Königshoff M , Eickelberg O (2010). WNT signaling in lung disease: a failure or a regeneration signal? *Am J Respir Cell Mol Biol*. **42**, 21-31.

Labalette C, Renard C, Neuveut C, Buendia M , Wei Y (2004). Interaction and functional cooperation between the LIM protein FHL2, CBP/p300, and beta-catenin. *Mol. Cell Biol.* **24**, 10689-10702.

LeVine AM, Hartshorn K, Elliott J, Whitsett J , Korfhagen T (2002). Absence of SP-A modulates innate and adaptive defense responses to pulmonary influenza infection. *Am J Physiol Lung Cell Mol Physiol*. **282**, L563-572.

Li B, Zhong L, Yang X, Andersson T, Huang M , Tang SJ (2011). WNT5A signaling contributes to Aβ-induced neuroinflammation and neurotoxicity. *PLoS One*. **6**, e22920.

MacNee W (2009). Accelerated lung aging: a novel pathogenic mechanism of chronic obstructive pulmonary disease (COPD). *Biochem Soc Trans*. **37**, 819-823.

Maina JN, West JB, Orgeig S, Foot NJ, Daniels CB, Kiama SG, Gehr P, Mühlfeld C, Blank F, Müller L, Lehmann A, Brandenberger C , Rothen-Rutishauser B (2010). Recent advances into understanding some aspects of the structure and function of mammalian and avian lungs. *Physiol Biochem Zool*. **83**, 792-807.

Martinez FJ, Safrin S, Weycker D, Starko KM, Bradford WZ, King TE, Flaherty KR, Schwartz DA, Noble PW, Raghu G, Brown KK , Group IS (2005). The clinical course of patients with idiopathic pulmonary fibrosis. *Ann Intern Med*. **142**, 963-967.

Michan S , Sinclair D (2007). Sirtuins in mammals: insights into their biological function. *Biochem J*. **404**, 1-13.

Naito AT, Shiojima I , Komuro I (2010). Wnt signaling and aging-related heart disorders. *Circ Res*. **107**, 1295-1303.

Noordermeer JK, J., Perrimon, N., and Nusse, R. (1994). Dishevelled and armadillo act in the wingless signalling pathway in Drosophila. *Nature*. **367**, 80-83.

Panos RJ, Bak PM, Simonet WS, Rubin JS , Smith LJ (1995). Intratracheal instillation of keratinocyte growth factor decreases hyperoxia-induced mortality in rats. *J Clin Invest*. **96**, 2026-2033.

Park KS, Wells JM, Zorn AM, Wert SE, Laubach VE, Fernandez LG , Whitsett JA (2006). Transdifferentiation of ciliated cells during repair of the respiratory epithelium. *Am J Respir Cell Mol Biol*. **34**, 151-157.

Paxson JA, Gruntman A, Parkin CD, Mazan MR, Davis A, Ingenito EP , Hoffman AM (2011). Age-dependent decline in mouse lung regeneration with loss of lung fibroblast clonogenicity and increased myofibroblastic differentiation. *PLoS One*. **6**, e23232.

Pervaiz S , Holme AL (2009). Resveratrol: its biologic targets and functional activity. *Antioxid Redox Signal*. **11**, 2851-2897.

Picard F, Kurtev M, Chung N, Topark-Ngarm A, Senawong T, Machado De Oliveira R, Leid M, McBurney MW , Guarente L (2004). Sirt1 promotes fat mobilization in white adipocytes by repressing PPAR-gamma. *Nature*. **429**, 771-776.

Polkey MI, Harris ML, Hughes PD, Hamnegärd CH, Lyons D, Green M , Moxham J (1997). The contractile properties of the elderly human diaphragm. *Am J Respir Crit Care Med*. **155**, 1560-1564.

Pongracz JE , Stockley RA (2006). Wnt signalling in lung development and diseases. *Respir Res*. **7**, 15.

Pongrácz J Lung tissue modeled^eds). Hungary.

Popp T, Steinritz D, Breit A, Deppe J, Egea V, Schmidt A, Gudermann T, Weber C , Ries C (2014). Wnt5a/β-catenin signaling drives calcium-induced differentiation of human primary keratinocytes. *J Invest Dermatol*. **134**, 2183-2191.

Puchelle E, Zahm JM, Tournier JM , Coraux C (2006). Airway epithelial repair, regeneration, and remodeling after injury in chronic obstructive pulmonary disease. *Proc Am Thorac Soc*. **3**, 726-733.

Rauner M, Stein N, Winzer M, Goettsch C, Zwerina J, Schett G, Distler JH, Albers J, Schulze J, Schinke T, Bornhäuser M, Platzbecker U , Hofbauer LC (2012). WNT5A is induced by inflammatory mediators in bone marrow stromal cells

and regulates cytokine and chemokine production. *J Bone Miner Res*. **27**, 575-585.

Rawlins EL, Ostrowski LE, Randell SH , Hogan BL (2007). Lung development and repair: contribution of the ciliated lineage. *Proc Natl Acad Sci U S A*. **104**, 410-417.

Rehan VK , Torday JS (2012). PPARγ Signaling Mediates the Evolution, Development, Homeostasis, and Repair of the Lung. *PPAR Res*. **2012**, 289867.

Reynolds SD, Reynolds PR, Snyder JC, Whyte F, Paavola KJ , Stripp BR (2007). CCSP regulates cross talk between secretory cells and both ciliated cells and macrophages of the conducting airway. *Am J Physiol Lung Cell Mol Physiol*. **293**, L114-123.

Rock JR, Barkauskas CE, Cronce MJ, Xue Y, Harris JR, Liang J, Noble PW , Hogan BL (2011). Multiple stromal populations contribute to pulmonary fibrosis without evidence for epithelial to mesenchymal transition. *Proc Natl Acad Sci U S A*. **108**, E1475-1483.

Roman-Roman S, Shi DL, Stiot V, Haÿ E, Vayssière B, Garcia T, Baron R , Rawadi G (2004). Murine Frizzled-1 behaves as an antagonist of the canonical Wnt/beta-catenin signaling. *J Biol Chem*. **279**, 5725-5733.

Rooney SA, Young SL , Mendelson CR (1994). Molecular and cellular processing of lung surfactant. *FASEB J*. **8**, 957-967.

Scherbov S, Mamolo M , Lutz W Probabilistic population projections for the 27 EU member states based on Eurostat assumptionsed^eds).

Schultz CJ, Torres E, Londos C , Torday JS (2002). Role of adipocyte differentiation-related protein in surfactant phospholipid synthesis by type II cells. *Am J Physiol Lung Cell Mol Physiol*. **283**, L288-296.

Selman M, Pardo A , Kaminski N (2008). Idiopathic pulmonary fibrosis: aberrant recapitulation of developmental programs? *PLoS Med*. **5**, e62.

Sharma G , Goodwin J (2006). Effect of aging on respiratory system physiology and immunology. *Clin Interv Aging*. **1**, 253-260.

Simic P, Williams EO, Bell EL, Gong JJ, Bonkowski M , Guarente L (2013). SIRT1 suppresses the epithelial-to-mesenchymal transition in cancer metastasis and organ fibrosis. *Cell Rep*. **3**, 1175-1186.

Simon DM, Arikan MC, Srisuma S, Bhattacharya S, Andalcio T, Shapiro SD , Mariani TJ (2006a). Epithelial cell PPARgamma is an endogenous regulator of normal lung maturation and maintenance. *Proc Am Thorac Soc*. **3**, 510-511.

Simon DM, Arikan MC, Srisuma S, Bhattacharya S, Tsai LW, Ingenito EP, Gonzalez F, Shapiro SD , Mariani TJ (2006b). Epithelial cell PPAR[gamma] contributes to normal lung maturation. *FASEB J*. **20**, 1507-1509.

Smit L, Baas A, Kuipers J, Korswagen H, van de Wetering M , Clevers H (2004). Wnt activates the Tak1/Nemo-like kinase pathway. *J Biol Chem*. **279**, 17232-17240.

Staal FJ , Clevers H (2003). Wnt signaling in the thymus. *Curr. Opin. Immunol.* **15**, 204-208.

Stripp BR , Reynolds SD (2008). Maintenance and repair of the bronchiolar epithelium. *Proc Am Thorac Soc*. **5**, 328-333.

Takada I, Kouzmenko AP , Kato S (2009). Wnt and PPARgamma signaling in osteoblastogenesis and adipogenesis. *Nat Rev Rheumatol*. **5**, 442-447.

Talaber G, Kvell K, Varecza Z, Boldizsar F, Parnell SM, Jenkinson EJ, Anderson G, Berki T , Pongracz JE (2011). Wnt-4 protects thymic epithelial cells against dexamethasone-induced senescence. *Rejuvenation Res*. **14**, 241-248.

Tolep K, Higgins N, Muza S, Criner G , Kelsen SG (1995). Comparison of diaphragm strength between healthy adult elderly and young men. *Am J Respir Crit Care Med*. **152**, 677-682.

Torday J, Hua J , Slavin R (1995). Metabolism and fate of neutral lipids of fetal lung fibroblast origin. *Biochim Biophys Acta*. **1254**, 198-206.

Torday JS, Torres E , Rehan VK (2003). The role of fibroblast transdifferentiation in lung epithelial cell proliferation, differentiation, and repair in vitro. *Pediatr Pathol Mol Med*. **22**, 189-207.

Torres M, Yang-Snyder J, Purcell S, DeMarais A, McGrew L , Moon R (1996). Activities of the Wnt-1 class of secreted signaling factors are antagonized by the Wnt-5A class and by a dominant negative cadherin in early Xenopus development. *J. Cell Biol.* **133**, 1123-1137.

Varecza Z (2011). The role of Wnt signaling in thymic senescence. In *Department of Imunology and Biotechnology*ed^eds). Pécs: University of Pécs, pp. 67.

Varisco BM, Ambalavanan N, Whitsett JA , Hagood JS (2012). Thy-1 signals through PPARγ to promote lipofibroblast differentiation in the developing lung. *Am J Respir Cell Mol Biol*. **46**, 765-772.

Veldhuizen R , Possmayer F (2004). Phospholipid metabolism in lung surfactant. *Subcell Biochem*. **37**, 359-388.

Verbeken EK, Cauberghs M, Mertens I, Lauweryns JM , Van de Woestijne KP (1992). Tissue and airway impedance of excised normal, senile, and emphysematous lungs. *J Appl Physiol (1985)*. **72**, 2343-2353.

Vuga LJ, Ben-Yehudah A, Kovkarova-Naumovski E, Oriss T, Gibson KF, Feghali-Bostwick C , Kaminski N (2009). WNT5A is a regulator of fibroblast proliferation and resistance to apoptosis. *Am J Respir Cell Mol Biol*. **41**, 583-589.

Walter N, Collard HR , King TE (2006). Current perspectives on the treatment of idiopathic pulmonary fibrosis. *Proc Am Thorac Soc*. **3**, 330-338.

Wang H , Malbon C (2003). Wnt signaling, Ca2+, and cyclic GMP: visualizing frizzled functions. *Science*. **300**, 1529-1530.

Ward HE , Nicholas TE (1984). Alveolar type I and type II cells. *Aust N Z J Med*. **14**, 731-734.

Willis BC , Borok Z (2007). TGF-beta-induced EMT: mechanisms and implications for fibrotic lung disease. *Am J Physiol Lung Cell Mol Physiol*. **293**, L525-534.

Winn RA, Marek L, Han SY, Rodriguez K, Rodriguez N, Hammond M, Van Scoyk M, Acosta H, Mirus J, Barry N, Bren-Mattison Y, Van Raay TJ, Nemenoff RA , Heasley LE (2005). Restoration of Wnt-7a expression reverses non-small cell lung cancer cellular transformation through frizzled-9-mediated growth inhibition and promotion of cell differentiation. *J Biol Chem*. **280**, 19625-19634.

Woerly G, Honda K, Loyens M, Papin JP, Auwerx J, Staels B, Capron M , Dombrowicz D (2003). Peroxisome proliferator-activated receptors alpha and gamma down-regulate allergic inflammation and eosinophil activation. *J Exp Med*. **198**, 411-421.

Yamamoto H, Kishida S, Kishida M, Ikeda S, Takada S , Kikuchi A (1999). Phosphorylation of axin, a Wnt signal negative regulator, by glycogen synthase kinase-3beta regulates its stability. *J Biol Chem*. **274**, 10681-10684.

Yamanaka H, Moriguchi T, Masuyama N, Kusakabe M, Hanafusa H, Takada R, Takada S , Nishida E (2002). JNK functions in the non-canonical Wnt pathway to regulate convergent extension movements in vertebrates. *EMBO Rep*. **3**, 69-75.

Yang L, Yan D, Yan C , Du H (2003). Peroxisome proliferator-activated receptor gamma and ligands inhibit surfactant protein B gene expression in the lung. *J Biol Chem*. **278**, 36841-36847.

Yang SJ, Choi JM, Chang E, Park SW , Park CY (2014). Sirt1 and Sirt6 mediate beneficial effects of rosiglitazone on hepatic lipid accumulation. *PLoS One*. **9**, e105456.

Yee M, Vitiello PF, Roper JM, Staversky RJ, Wright TW, McGrath-Morrow SA, Maniscalco WM, Finkelstein JN , O'Reilly MA (2006). Type II epithelial cells are critical target for hyperoxia-mediated impairment of postnatal lung development. *Am J Physiol Lung Cell Mol Physiol*. **291**, L1101-1111.

Zhang M, Shi J, Huang Y , Lai L (2012). Expression of canonical WNT/β-CATENIN signaling components in the developing human lung. *BMC Dev Biol*. **12**, 21.

Zilberberg A, Yaniv A , Gazit A (2004). The low density lipoprotein receptor-1, LRP1, interacts with the human frizzled-1 (HFz1) and down-regulates the canonical Wnt signaling pathway. *J Biol Chem*. **279**, 17535-17542.

Aging Cell (2014) pp1–12 Doi: 10.1111/acel.12240

Alteration in the Wnt microenvironment directly regulates molecular events leading to pulmonary senescence

Tamas Kovacs,[1,2] Veronika Csongei,[1,2] Diana Feller,[1,2] David Ernszt,[1,2] Gabor Smuk,[3] Veronika Sarosi,[4] Laszlo Jakab,[5] Krisztian Kvell,[1,2] Domokos Bartis[6] and Judit E. Pongracz[1,2]

[1]Medical School, Department of Pharmaceutical Biotechnology, University of Pécs, Pécs, Hungary
[2]János Szentágothai Research Centre, University of Pécs, Pécs, Hungary
[3]Medical School, Department of Pathology, University of Pécs, Pécs, Hungary
[4]Medical School, Department of Pulmonology, University of Pécs, Pécs, Hungary
[5]Medical School, Department of Surgery, University of Pécs, Pécs, Hungary
[6]Department of Clinical Respiratory Sciences, Centre for Translational Inflammation Research, University of Birmingham Research Laboratories, Queen Elizabeth Hospital, Birmingham, UK

Summary

In the aging lung, the lung capacity decreases even in the absence of diseases. The progenitor cells of the distal lung, the alveolar type II cells (ATII), are essential for the repair of the gas-exchange surface. Surfactant protein production and survival of ATII cells are supported by lipofibroblasts that are peroxisome proliferator-activated receptor gamma (PPARγ)-dependent special cell type of the pulmonary tissue. PPARγ levels are directly regulated by Wnt molecules; therefore, changes in the Wnt microenvironment have close control over maintenance of the distal lung. The pulmonary aging process is associated with airspace enlargement, decrease in the distal epithelial cell compartment and infiltration of inflammatory cells. qRT–PCR analysis of purified epithelial and nonepithelial cells revealed that lipofibroblast differentiation marker parathyroid hormone-related protein receptor (PTHrPR) and PPARγ are reduced and that PPARγ reduction is regulated by Wnt4 via a β-catenin-dependent mechanism. Using a human *in vitro* 3D lung tissue model, a link was established between increased PPARγ and pro-surfactant protein C (pro-SPC) expression in pulmonary epithelial cells. In the senile lung, both Wnt4 and Wnt5a levels increase and both Wnt-s increase myofibroblast-like differentiation. Alteration of the Wnt microenvironment plays a significant role in pulmonary aging. Diminished lipo- and increased myofibroblast-like differentiation are directly regulated by specific Wnt-s, which process also controls surfactant production and pulmonary repair mechanisms.

Key words: molecular biology of aging; pulmonary senescence; Wnt microenvironment.

Introduction

In the aging lung, the total tissue mass decreases along with the number of capillaries. Formation of new alveoli is also limited. Due to decrease in tissue mass as well as muscle weakness, lung capacity declines with age even in healthy individuals (Tolep *et al.*, 1995; Polkey *et al.*, 1997). As senescence progresses, lung tissue becomes prone to inflammation, fibrosis and tumors demolishing lung capacity. Infections are frequent in the pulmonary tract of the elderly, leading to a chronic cycle of injury and repair that causes significant changes in the structure, function and gene expression of alveolar epithelial cells contributing to the development of chronic pulmonary diseases (Baarsma *et al.*, 2011; Chilosi *et al.*, 2012). Studies suggest that the senile lung is characterized by airspace enlargement similar to acquired emphysema (Verbeken *et al.*, 1992) even detected in nonsmokers above 50 years of age (Sharma & Goodwin, 2006; Calvi *et al.*, 2011). Similarly to humans, aging of the mouse lung is associated with homogeneous airspace enlargement.

The aging process of the lung is complex both in test animals and humans. Apart from decreased ability to withstand infections, low level chronic inflammatory processes are frequently detected (Meyer *et al.*, 1996). The low level chronic inflammation is associated with tissue destruction requiring effective tissue regeneration (Crosby & Waters, 2010) coordinated by epithelial progenitor cells. The progenitor cells originate from the five putative stem cell niches primarily identified in the lungs of mice (Engelhardt, 2001). The cells responsible for cellular regeneration in the bronchiolar region are the nonciliated epithelial cuboid Clara cells (Park *et al.*, 2006) while in the gas-exchange region of the alveoli, ATII cells drive the regenerative process. ATII cells are capable of transdifferentiation into ATI cells (Crosby & Waters, 2010; Rock *et al.*, 2011; Barkauskas *et al.*, 2013) providing the gas exchange surface of alveoli. ATII cells are also important in producing surfactant proteins responsible for lowering surface tension in the alveoli aiding gas exchange and stabilizing alveolar structure (Rooney *et al.*, 1994) Surfactants also have immune-modulatory activity in the host defense system (Veldhuizen & Possmayer, 2004; Maina *et al.*, 2010) making the presence of a well-maintained ATII cell population essential.

Although ATII cells are vitally important, ATII-s are unable to take up triglycerides directly from the blood and need the help of lipofibroblasts (Torday *et al.*, 1995; Rehan & Torday, 2012). Lipofibroblasts can take up triglycerides and accumulate lipid droplets generated by a proliferator-activated receptor gamma (PPARγ) (Ferguson *et al.*, 2009) and adipose differentiation-related protein (ADRP) (Gao & Serrero, 1999; Schultz *et al.*, 2002)-dependent mechanism.

In recent studies, the secreted Wnt glycolipoprotein ligand family (Pongracz & Stockley, 2006) have been reported to regulate both aging (Brack *et al.*, 2007) and PPARγ activity (Takada *et al.*, 2009; Talaber *et al.*, 2011). The two main and best characterized Wnt pathways are the β-catenin-dependent or canonical and the β-catenin-independent or noncanonical pathways (Pongracz & Stockley, 2006). While the canonical Wnts antagonize the PPARγ function (Takada *et al.*, 2009), noncanonical Wnts have not been reported to affect PPARγ transcription or activity. Recent studies conducted in aging mice have connected PPARγ to lipofibroblast differentiation (Willis & Borok, 2007; Paxson

Correspondence
Dr. Judit E. Pongracz, Medical School, Department of Pharmaceutical Biotechnology, Szentágothai Research Centre, University of Pecs, 12 Szigeti Str, Pecs 7624, Hungary. Tel.: +36 30 435 7944; fax: +36 72 501 654; e-mail: pongracz.e.judit@pte.hu

Accepted for publication *22 May 2014*

Aging Cell

et al., 2011). If PPARγ is reduced, lipofibroblasts differentiate into myofibroblast not supporting the maintenance of 'stemness' or surfactant synthesis (Königshoff & Eickelberg, 2010; Paxson *et al.*, 2011).

Based on the above data, we theorized that a well-balanced Wnt microenvironment is essential in the alveolar epithelial maintenance mechanism. To investigate the stability of the Wnt microenvironment and the availability of lipofibroblasts in the aging lung, studies were performed using Balb/c mice, primary human lung tissues as well a three-dimensional (3D) human lung tissue model. Our results demonstrate that increased expression of Wnt4 leads to down-regulation of PPARγ in fibroblasts and epithelials cells increasing myofibroblast and inhibiting lipofibroblast differentiation, resulting in decreased surfactant production.

Results

Morphological changes in the aging lung

During aging, pulmonary function deteriorates due to pulmonary inflammation and structural changes described as senile emphysema. Microcomputed tomography (Fig. S1A,B, Supporting information) and hematoxilyn–eosin staining (Fig. S1C,D, Supporting information) of lung sections confirm such changes in Balb/c mice. Both techniques highlighted enlarged airspace in the distal lung regularly coinciding with decreased gas-exchange surface. Similar airspace enlargement has also been observed in old human lungs measured by a 2.5-fold increase in mean alveolar diameter (Fig. S1E,F, Supporting information).

To confirm degeneration of the epithelial surface layer during aging, single cell suspensions were generated from the pulmonary tissues of mice, and cells were sorted based on EpCAM1 and CD45 cell surface antigens. Analysis of density plots (Fig. 1A,B) revealed a significant increase in CD45+ leukocyte level showing a marked increase in both macrophage and B-cell populations (Fig. S1G, Supporting information), whereas the number of epithelial cells significantly decreased in the senescent lung (Fig. 1C).

Both PPARγ expression and lipid levels decrease with age

While senescence-associated low level chronic inflammation explains tissue destruction, the reasons for ineffective regeneration are not so easily explained. As lipofibroblasts are essential for maintenance of ATII-s, molecular studies were designed to identify molecules involved in lipid production to define the presence and activity of lipofibroblasts. PPARγ mRNA as well as its downstream target, adipose differentiation-related protein (ADRP), were measured in purified $EpCAM1^+$ epithelial and $EpCAM1^-$ nonepithelial cells using qRT–PCR (Fig. 2A). Compared with 1-month-old Balb/c mice, both PPARγ and ADRP levels decreased at 24 months of age in both cell populations indicating reduced ability for lipid synthesis in the aging lung. To confirm the qRT–PCR data, lipid levels were assessed in pulmonary tissues using neutral lipid staining of 1-month-old and in 24-month-old mouse lung sections (Fig. 2B,C). While lipid staining co-localized with nuclear staining in young (1-month-old) mice (Fig. 2B), lungs of old (24-month-old) mice contained enlarged lipid droplets not associated with nuclear staining (Fig. 2C). Western blots were performed using protein extracts of 1-month- and 24-month-old mouse lungs (Fig. 2D). The results show an age-associated reduction in PPARγ protein levels indicating a loss of lipofibroblasts. According to Torday *et al.* (Torday *et al.*, 2003), parathyroid hormone-related protein (PTHrP) expression is necessary for differentiation of mesenchymal lipofibroblasts, which induce ATII cell differentiation making PTHrP receptor transcript levels indicative of alterations in lipofibroblast differentiation. qRT–PCR analysis revealed a drastic reduction in PTHrP receptor mRNA levels within the $EpCAM1^-/CD45^-$ cell population (Fig. 2E) indicating loss of lipofibroblasts in the aging lung.

Alteration of the Wnt microenvironment during pulmonary senescence

Recent studies have highlighted the importance of Wnt signaling in the regulation of PPARγ activity. Takada reviewed (Takada *et al.*, 2009) that canonical Wnts antagonize the effect of PPARγ in osteoblast–adipocyte differentiation. Moreover, Talabér *et al.* (Talaber *et al.*, 2011) have shown that overexpression of Wnt4 in TEP1 thymic epithelial cell line results in reduced PPARγ expression and consequent inhibition of thymic adipose involution.

Several Wnts, including Wnt4 as well as the inflammatory mediator, Wnt5a were measured in both epithelial and nonepithelial cells of mouse lungs. While Wnt4 mRNA levels increased (Fig. 3A) during aging in both epithelial ($EpCAM1^+$) and nonepithelial ($EpCAM1^-$) cells, both Wnt5a and Wnt11 expression decreased in epithelial ($EpCAM1^+$) and increased in nonepithelial ($EpCAM1^-$) (Fig. 3A) cells during senescence. Western blot analysis of protein extracts of 1-month- and 24-month-old mouse lungs supported the age-associated increase in Wnt4 levels (Fig. 3B). Wnt5a staining of 73-year-old (Fig. 3C) and 21-year-old (Fig. 3D) human lungs reinforced similarities between the mouse and human pulmonary senescence program. Corresponding to mouse qRT–PCR data, Wnt5a-staining intensity increased with age in the human lung and Wnt5a was detected in the nonepithelial, cytokeratin-7 negative cell population (Fig. 3C).

β-catenin-dependent regulation of PPARγ expression

Our previous data (Talaber *et al.*, 2011) as well as Takada's results (Takada *et al.*, 2009) designated the canonical Wnt signaling pathway as regulator of PPARγ expression. As Wnt4 but not Wnt5a or Wnt11 can act via the canonical Wnt signaling pathway (Pongracz & Stockley, 2006), our attention was focused on Wnt4. First 3D human lung tissue models were exposed to control and Wnt4 supernatants of TEP1 cells for 7 days. Using qRT–PCR, reduced mRNA expression levels of PPARγ were measured (Fig. 4A). Thereafter, canonical Wnt pathway activity was modified using chemical activators and inhibitors of the β-catenin pathway. LiCl was used as activator inhibiting the activity of glycogen-synthase kinase (GSK)3-β, which enzyme phosphorylates and labels β-catenin for proteosomal degradation. IWR is an inhibitor stabilizing Axin proteins that play a role in β-catenin destruction (Pongracz & Stockley, 2006).

Primary human lung fibroblasts (NHLF) were treated with LiCl at 10 mM, IWR at 1 μM concentration and with Wnt4-enriched supernatant of TEP1 cells for 7 days, then PPARγ mRNA levels were measured using qRT–PCR. The expression of PPARγ was drastically reduced after LiCl and Wnt4 treatment (Fig. 4A,B), while inhibition of β-catenin signaling increased PPARγ levels. β-catenin levels were also assessed by Western blot analysis after treatment of NHLF cells with LiCl, Wnt4 and IWR. While LiCl and Wnt4 treatment increased, IWR treatment reduced β-catenin protein levels (Fig. 4C) indicating that amplified Wnt4 production during aging is likely to initiate reduction of lipofibroblast differentiation via a β-catenin-dependent mechanism. To examine the possibility that Wnt4-induced reduction of PPARγ levels affect SPC production, a distal human lung tissue model was set up using small airways epithelial

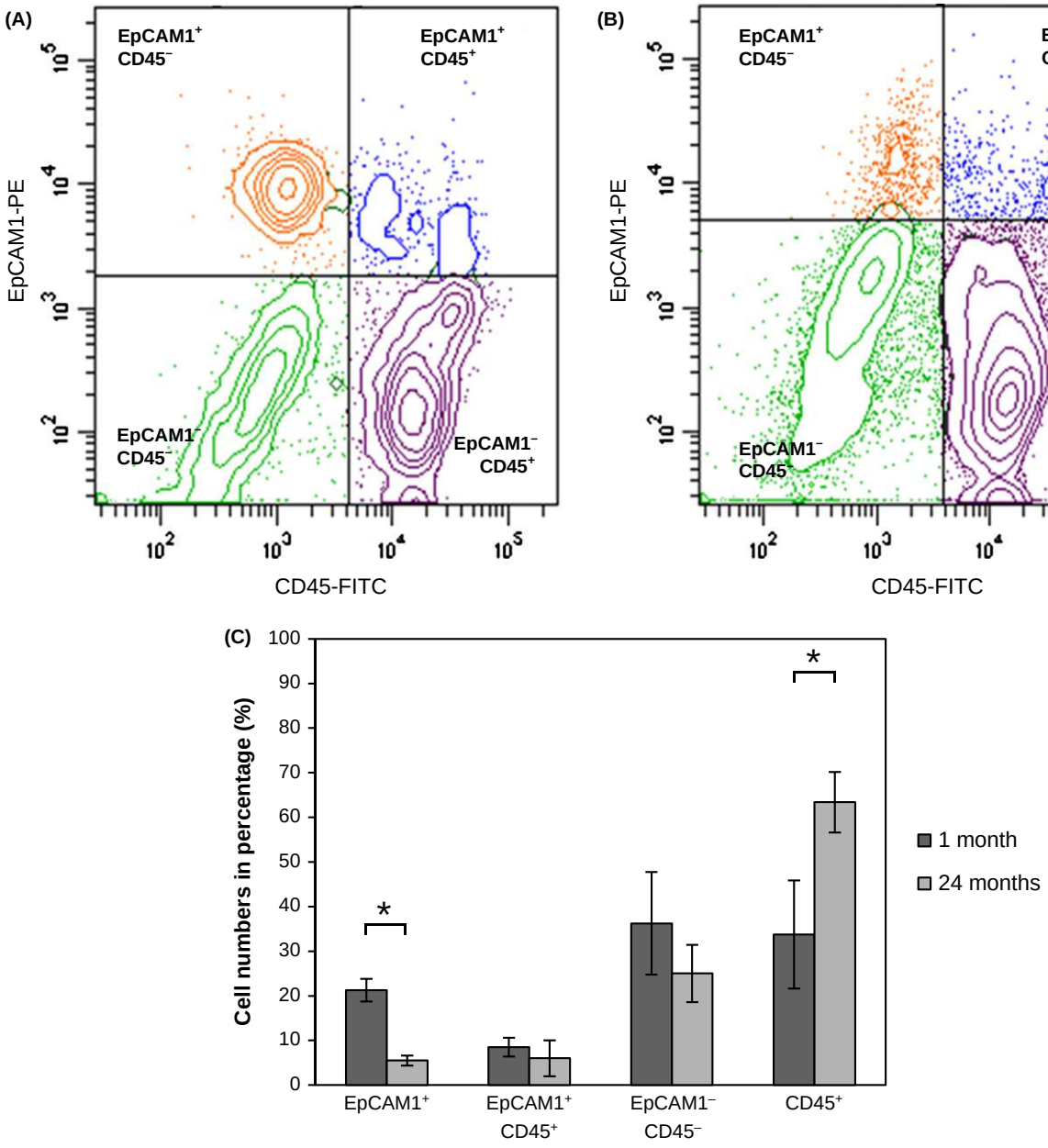

Fig. 1 Flow cytometric analysis of cell populations in (A): 1-month and (B): 24-month lungs of Balb/c mice (EpCAM1$^+$, CD45$^+$, EpCAM1$^-$CD45$^-$, EpCAM1$^+$CD45$^+$) (C): Bar chart of young and old mouse lung cells. The numbers of different cell subsets are shown in percentage (*$P < 0.05$).

cells (SAEC) and NHLF in three-dimensional (3D) human lung tissue models (Fig. S2, Supporting information). As the 3D human lung tissue model showed reduced inflammatory cytokine and increased differentiation marker expression both at levels of pro-SPC and Aquaporins (Fig. S2, Supporting information), it was determined to be a suitable model system for molecular analysis of surfactant regulation. The 3D lung tissue model was treated with Wnt4-enriched supernatants and rhWnt5a, respectively. Following 7 days of incubation, Wnt4 reduced pro-SPC expression, demonstrating that Wnt4 can regulate pro-SPC levels (Fig. 4D–F). In contrast, rhWnt5a treatment had no significant effect on pro-SPC expression (Fig. S4A,B), supporting the theory that Wnt4 is the likely regulator of PPARγ and surfactant expression.

Reduced β-catenin activity is necessary in pulmonary epithelial cells to produce pro-SPC

While the above data support that PPARγ levels in fibroblasts are necessary for lipofibroblast-like differentiation and maintenance of surfactant production in ATII-type cells, it is still not clear whether PPARγ activity is needed within the ATII cell population for surfactant synthesis. It is an important question as age-associated decline of PPARγ mRNA affected not only in fibroblasts but epithelial cells also (Fig. 2A). As the aging process in the human lungs was associated with reduced pro-SPC levels (Fig. 5A,B), the presence and activity of PPARγ in pulmonary epithelium might be equally important to that in lipofibroblasts.

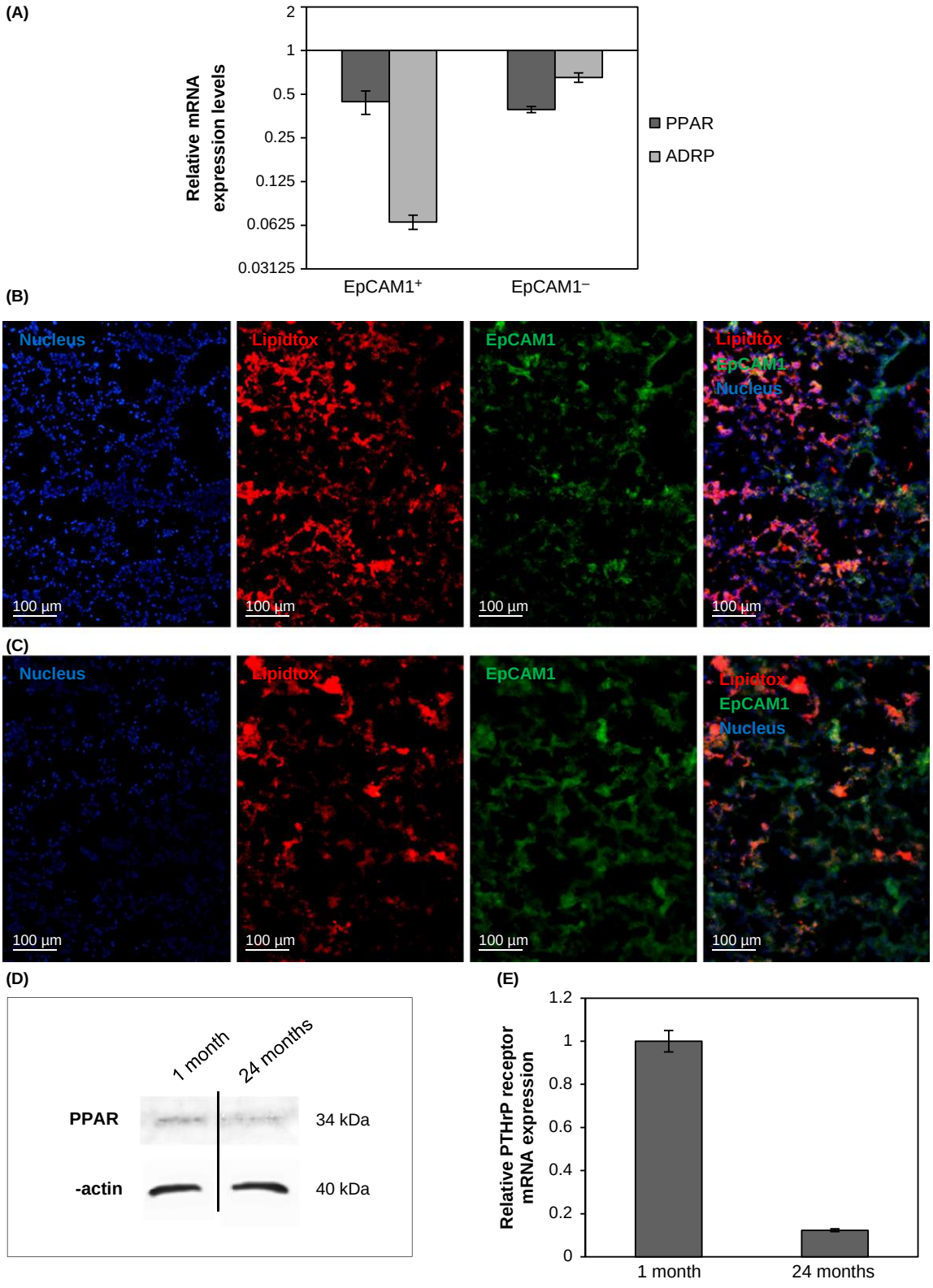

Fig. 2 (A): mRNA expression levels of adipose differentiation markers in 24-month-old Balb/c mouse lung epithelial and nonepithelial cells, compared with 1 month-old. Both the PPARγ and the ADRP are decreased at 24 month-old compared with the 1-month-old lung cell types. LipidTox staining of (B): 1-month-old and (C): 24-month-old Balb/c mouse lung sections showing nuclei staining, lipid staining (LipidTox), and EpCAM1-FITC staining individually then in a merged picture. (D): PPARγ protein levels were detected in 1-month-old and 24-month-old lung extracts by Western blotting. Equal protein loading was tested using anti-β-actin antibody. The blot is a representative of two individual experiments. (E): PTHrP receptor mRNA levels were measured in EpCAM-/CD45- cell populations of 1-month-old and 24-month-old Balb/c mouse lungs using qRT–PCR analysis. (The graph is a representative of three individual experiments).

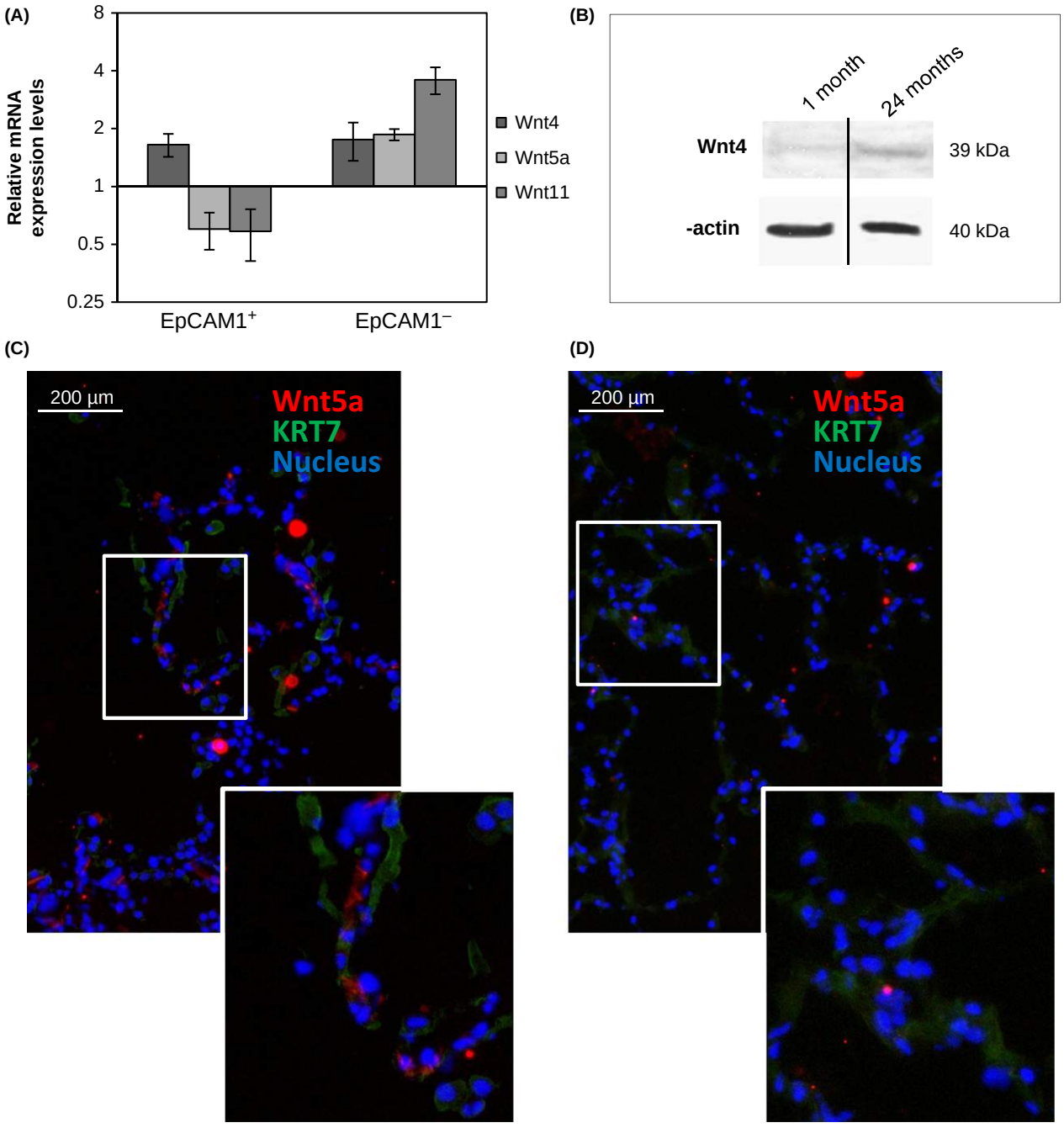

Fig. 3 (A): mRNA expression levels of different Wnt molecules in 24-month-old Balb/c mouse lung epithelial and nonepithelial cells were measured using qRT–PCR analysis and relative expression was determined to β-actin, then compared with Wnt expression in 1-month-old test animals. (B): Wnt4 protein levels were detected in 1-month-old and 24-month-old lung extracts by Western blotting. Equal protein loading was tested using anti-β-actin antibody. (The blot is a representative of two individual experiments). Immunofluorescent staining of Wnt5a in (C): 73-year and (D): 21-year human lung sections (The staining is representative of three separate experiments).

β-catenin activity was modulated therefore using the physiological inhibitor of the β-catenin-dependent Wnt signaling pathway, ICAT. ICAT (Graham *et al.*, 2002) was introduced into epithelial as well as fibroblast cells using recombinant viral gene delivery methods in the 3D human lung tissue model. To specifically target epithelial cells (SAEC), recombinant Adeno viruses (rAd-GFP and rAd-ICAT-GFP) were used (Fig. 5C), while fibroblasts (NHLF) were transfected using lentiviruses (rL-GFP and rL-ICAT-GFP). For lentiviral gene delivery, NHLF cells were infected before the generation of the 3D human lung tissue model to avoid transfection of epithelial components. Following 7 days of exposure to ICAT, PPARγ expression was measured. Inhibition of β-catenin activity either in epithelium or in fibroblasts drastically increased PPARγ expression (Fig. 5D,E), indicating that inhibition of β-catenin signaling modulates lipid metabolism of both cell types.

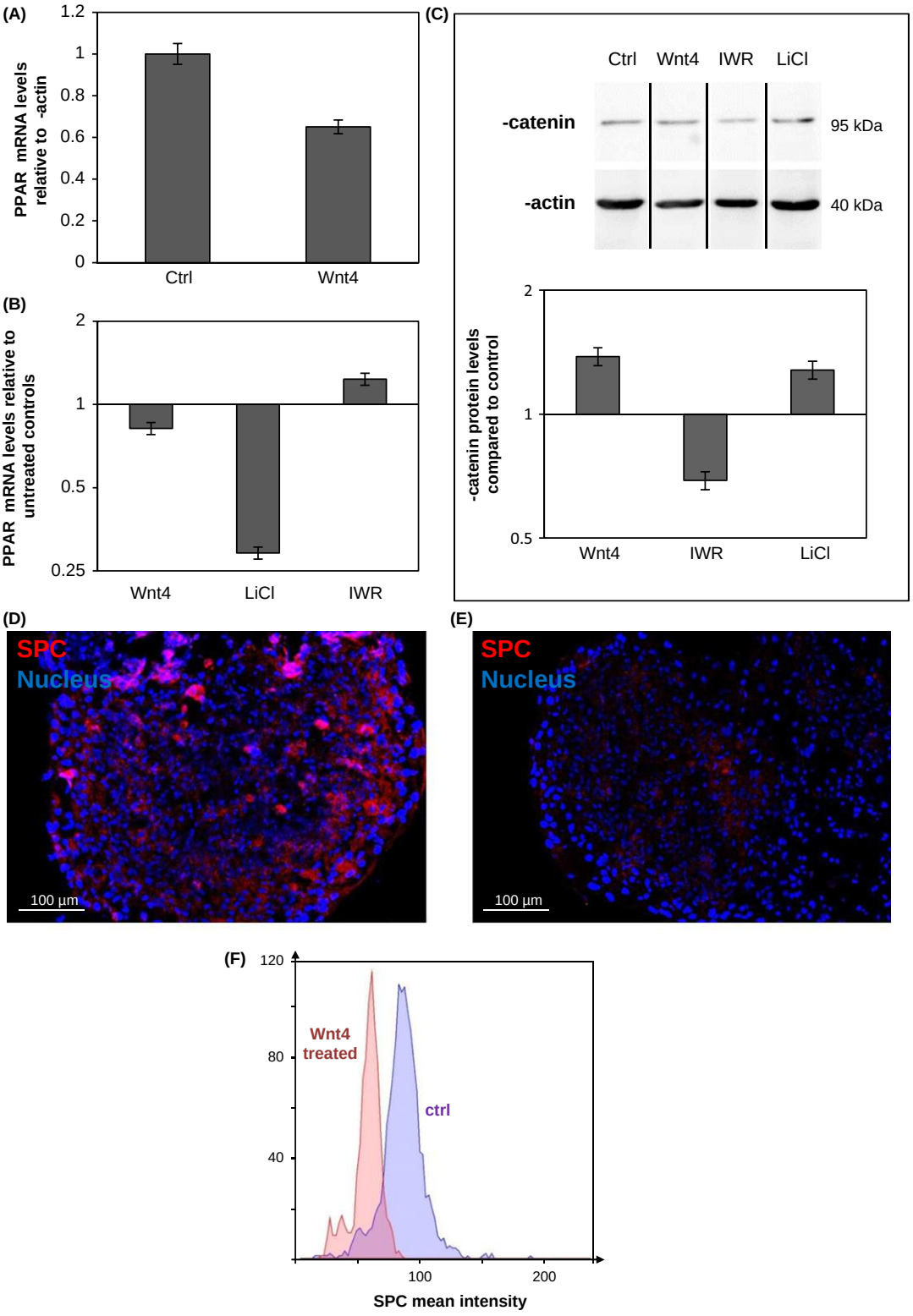

Fig. 4 (A): PPARγ expression levels in 3D human lung tissue models, following 7-day exposure to control (ctrl) and Wnt4 supernatants of thymic epithelial cells (TEP1). PPARγ mRNA expression levels were determined by qRT–PCR analysis following 7-day exposure to control (ctrl) and Wnt4-enriched supernatants of TEP1, to 10 mM LiCl and to 1 µM IWR in (B): primary human lung fibroblast (NHLF) cells. (C): β-catenin protein levels were determined in NHLF cells after exposure to Wnt4-enriched supernatants of TEP1, 10 mM LiCl and 1 µM IWR for 7 days. Equal protein loading was determined using anti-β-actin antibody. (The blot is a representative of two individual experiments). The blots were then densitometrically scanned and plotted against the controls. Pro-SPC staining on (D): ctrl and E: Wnt4-enriched supernatant treated 3D human lung tissue model (red: pro-SPC, blue: DAPI stained nuclei) (The staining is representative of three separate experiments). F: Mean intensity differences in pro-SPC staining in Wnt4-treated and Ctrl 3D human lung tissue models. (The graph is a representative of three individual experiments).

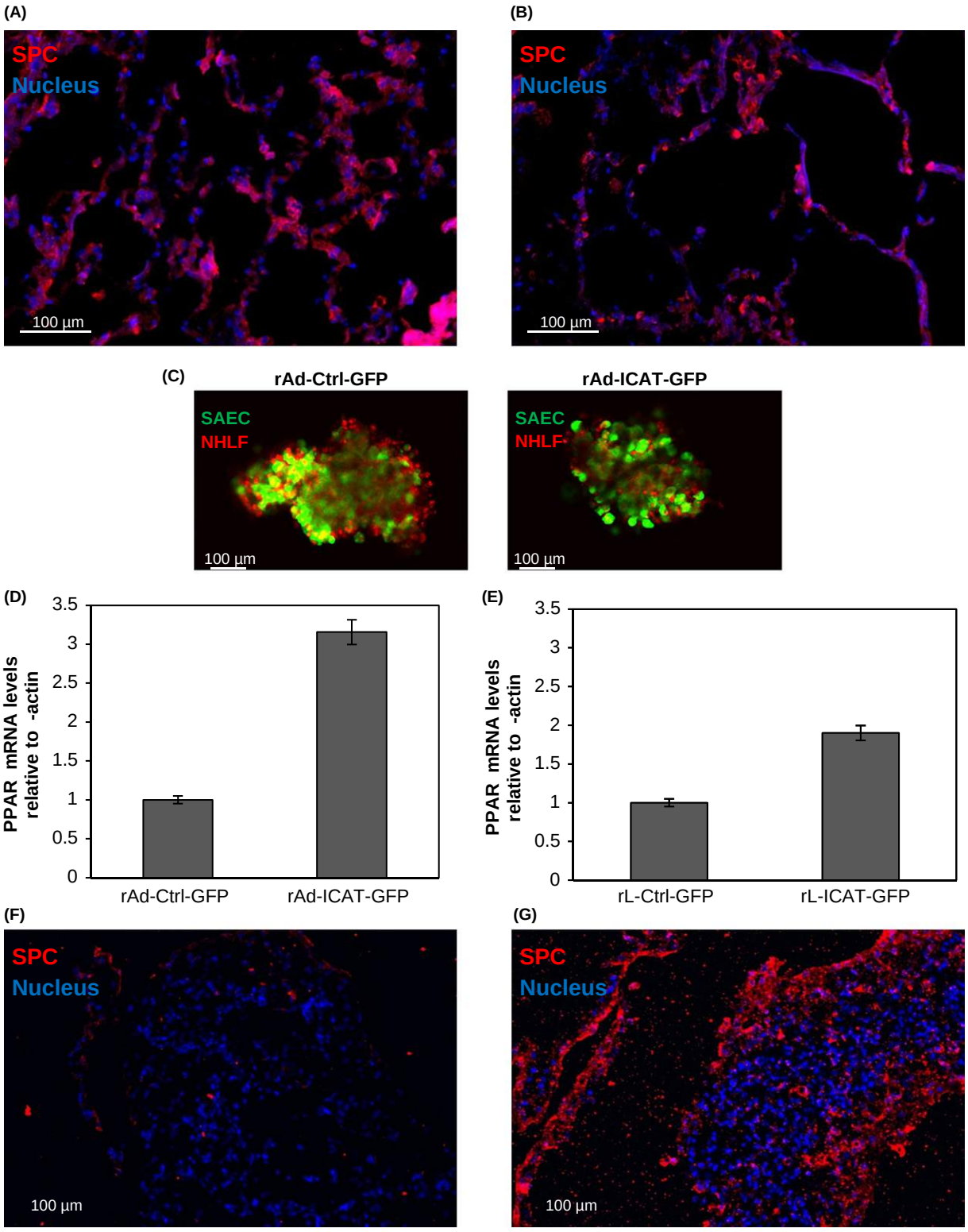

Fig. 5 Immunofluorescent staining of pro-surfactant protein C (pro-SPC) in (A): 21-year-old and (B): 73-years-old human lung tissue sections. (C): Confocal picture of intact 3D human lung tissue models infected with rAd-Ctrl-GFP and rAd-ICAT-GFP. SAEC are expressing GFP (green) within the 3D human lung tissue model. NHLF cells were prestained with DiI (red). (D): PPARγ mRNA expression levels were determined by qRT–PCR analysis in 3D human lung tissue model following 7-day suppression of β-catenin activity by ICAT specifically within the SAEC population using rAd gene delivery. (E): PPARγ mRNA expression levels were determined by qRT–PCR analysis in 3D human lung tissue model following suppression of β-catenin activity by ICAT specifically within the NHLF cell population using rL gene delivery. Immunofluorescent staining of pro-SPC in (F): control 3D human lung tissue model containing rAd-Ctrl-GFP SAEC and (G): ICAT overexpressing 3D human lung tissue model containing rAd-ICAT-GFP SAEC (the staining is representative of three separate experiments).

Pro-SPC-staining increased drastically in rAd-ICAT-GFP-infected tissues (Fig. 5F,G) identifying a β-catenin-regulated and PPARγ-dependent mechanism as an important element of pro-SPC production in ATII cells.

Wnt signaling in myofibroblast-like differentiation

According to Torday *et al.* (Torday *et al.*, 2003), transdifferentiation of lipofibroblasts to myofibroblasts is characterized by loss of PTHrP receptor expression and triglyceride content. Our results support previous findings as PTHrP mRNA levels decreased with age in the nonepithelial cell population (Fig. 2E). To investigate whether changes in the Wnt microenvironment are responsible for increased myofibroblast differentiation, the myofibroblast marker S100A4 mRNA was measured after exposure of NHLF cells and the 3D human lung tissue model to Wnt4 and Wnt5a, respectively. Interestingly, both Wnt4 and Wnt5a were able to increase S100A4 transcript levels (Fig. 6A,B), indicating involvement in myofibroblast-differentiation.

Discussion

During senescence, changes in the structure and cellular composition of the lung leads to airspace enlargement that occur even in nonsmoker, healthy adults (Tolep *et al.*, 1995). Investigating the molecular background of the pulmonary aging process has highlighted that both in test animals and in humans the structural differences are triggered by very similar molecular alterations in Wnt signaling. Up-regulation of Wnt4 in epithelial and nonepithelial cells as well as up-regulation of Wnt5a in nonepithelial tissue compartments can lead to far reaching consequences.

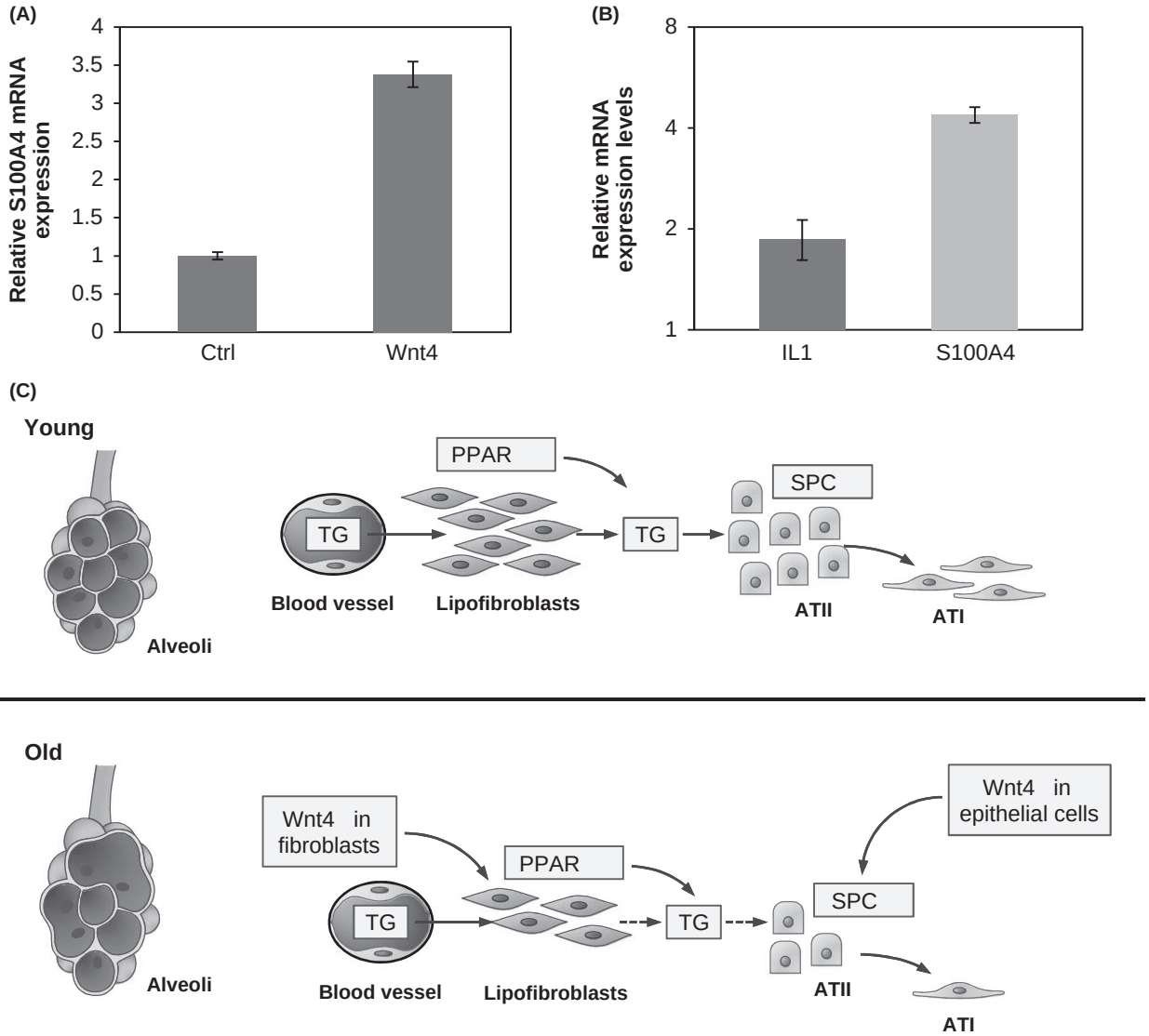

Fig. 6 (A): Relative gene expression levels of S100A4 in Wnt4-enriched supernatant treated human lung tissue spheroids. qRT–PCR analysis of gene expression is presented as relative to controls (data is representative of two separate experiments). (B): Relative gene expression levels of IL1β and S100A4 in rhWnt5a-treated 3D human lung tissue models. qRT–PCR analysis of gene expression is presented as relative to untreated controls (data are representative of three separate experiments). (C): Schematic summary of molecular changes in the distal lung during senescence (TG: triglyceride; SPC: pro-surfactant protein C, PPAR : peroxisome proliferator-activated receptor gamma).

Pinpointing the initial molecular trigger, however, is difficult. Increased Wnt5a levels have been reported to regulate accumulation of leukocytes and increased inflammatory cytokine production (Li *et al.*, 2011; Briolay *et al.*, 2013) as well as senescence (Florian *et al.*, 2013) in many tissues. Previous studies have also described Wnt5a to increase fibroblast proliferation (Vuga *et al.*, 2009), increased inflammatory cytokine production (Rauner *et al.*, 2012) and epithelial cell migration (Bartis *et al.*, 2013) providing further insight into the molecular environment favoring fibrosis and cancer development in the elderly lung.

Increased Wnt5a secretion of fibroblast cells of the aging lung can stimulate inflammation and therefore maintenance of a damaging environment to the gas-exchange surface. If the damaging microenvironment is prolonged and coincides with a reduced regenerative capacity, the outcome can be fatal. Decreased number of the alveolar progenitor or ATII cells (Torday *et al.*, 2003; Yee *et al.*, 2006) could explain such age-associated reduction in regeneration. ATII cells serve not just as alveolar stem cells, but they are also the source of surfactants. Reduction in pro-SPC levels indicates weakened functionality of ATII-s that was documented in both aging test animals as well as in primary human lung tissue.

Our studies have shown that alterations in Wnt secretion and consequent modulation of intracellular signaling interferes with the lipid metabolism at PPARγ level. The Wnt4-induced reduction in PPARγ levels seems especially important as PPARγ and its down-stream target, ADRP are responsible for the uptake of triglycerides from the blood stream (Varisco *et al.*, 2012) that is essential for surfactant production in ATII cells. Our data have also shown that PPARγ is necessary in epithelial cells to regulate surfactant production. As surfactant lining of the alveoli is essential to uniform inflation and to protect against chemical or particulate injury of the distal lungs, a decrease in surfactant production can accelerate and maintain lung tissue damage and speed up aging.

Up-regulation of Wnt4 and Wnt5a has an additional impact on aging lung tissue. Both Wnt4 and Wnt5a can increase myofibroblast (S100A4) marker expression, indicating that ATII cells are left without their essential support mechanism (lipofibroblast) (Torday *et al.*, 2003; Rehan & Torday, 2012) during senescence. Additionally, Wnt-induced myofibroblast differentiation might also be linked to modulation of tissue damage control, as when tissue or parenchymal repair is needed myofibroblasts function as elemental emergency cells.

While modification of Wnt expression in absolute levels are relatively little, the distal lung seems unable to adapt to shifts in the molecular microenvironment (Fig. 6C). Especially, as changes taking place simultaneously are magnified at several levels. An increase in Wnt4 expression leads to PPARγ down-regulation that paralyses lipofibroblast differentiation and quite possibly reduces the ability of ATII cells for surfactant production. As in the absence of lipofibroblasts, ATII-s can no longer replenish their triglyceride sources from the blood, surfactant production can become drastically reduced. In the absence of surfactants, the lung tissue becomes prone to infections (LeVine *et al.*, 2002; Kazi *et al.*, 2010). During the course of infection, alveolar epithelial cells start to produce Wnt5a that adds to the already increased Wnt5a levels produced by the aging nonepithelial elements of the distal lung. The simultaneous increase in inflammatory cytokines produced by the infiltrating immune cells that attack the site of infection can increase Wnt5a levels even further (Rauner *et al.*, 2012). Meanwhile, the damaged alveolar epithelial lining is unable to regenerate as the number of functional ATII cells is decreasing leaving the damaged tissue in need of myofibroblasts to close the wound.

Further studies are necessary and are underway to investigate the above described mechanism *in vivo* and to explore the potential clinical applications of the pulmonary repair mechanism.

Experimental procedures

Ethical statement

Lung tissue samples were collected during lung resections at the Department of Surgery, University of Pécs, Hungary. The project was approved by the Ethical Committee of the University of Pécs. Patients had given written consent to provide samples for research purposes. All collected samples were treated anonymously.

Animals

For the experiments Balb/C inbred, albino mice were used from both genders. The mice were kept under standardized conditions, where tap water and food was provided ad libitum.

Sky scan microCT

Mice anesthetized intraperitoneally with sodium pentobarbitol (eutazol) were placed in the SKYSCAN 1176 microCT (Bruker, Kontich, Belgium) machine equipped with a large format 11 megapixel camera. The pictures were taken from the lung in 180°. The reconstitution was performed with SKYSCAN software, which integrates a physiological monitoring subsystem providing breathing and heartbeat gating for thoracic image improvement through synchronized acquisition. Then the pictures were calibrated with CTAN software (Bruker). The 3D pictures were generated from the calibrated images by CtVox (Bruker). Colors were based on Hounsfield scale, where red was placed at −1000 and represents free air, and through tones, blue represents lung tissue.

Lung cell isolation

Mice were anesthetized with 1% of sodium pentobarbital through intraperitoneal injection (70 μL/10 g). Then abdominal aorta was intersected, and mice were perfused through right ventricle with 10 mL of phosphate-buffered saline (PBS) to reduce lung blood content. 3 mL trypsine (%) to initiate the fine digestion, 10 mL PBS to wash out trypsine, 3 mL collagenase-dispase (3 mg mL^{-1} collagenase (Sigma-Aldrich, St. Louis, MO, USA) 1 mg mL^{-1} dispase (Roche F. Hoffmann-La Roche Ltd. Basel, Switzerland) 1u μL^{-1} DNAse I (Sigma-Aldrich). Finally, the lung was filled up with the collagenase-dispase solution trough the trachea. Lungs were removed from the chest and separated from the heart and thymus and cleaned from connective tissue. Pulmonary lobes were dissected into smaller pieces and digested in 10 mL collagenase-dispase for 50 min with continuous stirring. Digested lung cells were filtered with 70-μm cell-strainer (BD Becton, Dickinson and Company Franklin Lakes, NJ, USA)

Cell sorting

Single cell suspension isolated from mouse lungs were labeled with anti-CD45-FITC produced at the University of Pécs, Department of Immunology and Biotechnology (Balogh *et al.*, 1992) and anti-EpCAM1 (G8.8 anti-rat-PE). Cell sorting was performed by FACSAria III (BectonDickinson) cell sorter. The following populations were collected: $EpCAM^{-}CD45^{-}$ Ep-

CAM^+CD45^- $EpCAM^+CD45^+$ and $EpCAM^+CD45^-$. The purity of sorting was above 99%.

Cell lines

During our experiments, normal human lung fibroblast (NHLF) cells were exposed to TEP1 Wnt4 overexpressing supernatant and to normal TEP1 cell normal supernatant as control (Talaber *et al.*, 2011) for 7 days. Fibroblast cells (NHLF) were also treated with the β-catenin pathway activator LiCl at the concentration of 10 mM for 7 days and the β -catenin pathway inhibitor, IWR at 1 μM (Sigma) for two days. After RNA isolation and cDNA synthesis, PPARγ levels were measured by qRT–PCR using PPARγ- and β-actin-specific primers.

Three-dimensional (3D) human lung tissue model

Primary small airway epithelial cells (SAEC) and normal human lung fibroblasts (NHLF) cells were purchased from Lonza (Walkersville, MD, USA). All cell types were isolated from the lungs of multiple random donors of different sexes and ages. We used Small Airway Epithelial Growth medium (SAGM) or fibroblast growth medium (FGM) for the initial expansion of SAEC or NHLF respectively, as recommended by the manufacturer (Lonza). All types of cell cultures were incubated in an atmosphere containing 5% CO2, at 37 °C. For 3D culturing, cells were mixed at 1:1 ratio, dispensed onto V-bottom 96-well plates (Sarstedt Nümbrecht, Germany) and were immediately pelletted at 600xg for 10 min at room temperature. Then spheroids were kept in 24-well plate (Sarstedt) in mixed SAGM:FGM (1:1 ratio) medium. They were exposed to rhWnt5a and Wnt4 supernatant for 7 days.

Recombinant Adeno (rAd) and Lenti (L) viral constructs and rAd and L-viral infecton of pulmonary epithelium (SAEC) and fibroblasts (NHLF)

ICAT sequence was amplified by PCR using forward (5′) 5′-ATG AACCGCGAGGAGCA-3′ and reverse (3′) 5′-CTACTGCCTCCGGTCT TCC-3′ primer sequences and cloned into the bicistronic GFP (green fluorescence protein) Adeno Shuttle and Lenti pWPTS vectors. The Shuttle vector was cloned by homologous recombination into the adenoviral vector. Adenovirus was produced by transfecting the linearized plasmid DNA into the 293 packaging cell line (American Type Culture Collection, Rockville, MD, USA) using Lipofectamine 2000 (Invitrogen, Carlsbad, CA, USA). The resulting plaques were amplified, the adenovirus purified and concentrated using the adenoviral purification kit (BD Biosciences, Franklin Lakes, NJ, USA).

Late second-generation lentiviral vectors were prepared by co-transfection of three plasmid constructs (envelope construct pMD.G, packaging construct R8.91 and transfer construct pWPTS) into 293T cells using the calcium phosphate method as described previously (Bovia *et al.*, 2003). Biological titration was performed with HeLa cells. Viral particles were concentrated 1000-fold in volume; biological titers reached 10^8 TU mL^{-1}. The HIV-1-derived lentiviral system was kindly provided by Prof. Didier Trono (CMU, Geneva, Switzerland).

For ICAT delivery to epithelial cells, complete SAEC-NHLF spheroids were incubated in the rAd virus containing media for 1 h, then the SAEC-(ICAT-GFP)-NHLF and SAEC-(GFP)-NHLF shpereoids were washed and incubated for 7 days before RNA isolation. For ICAT delivery to fibroblasts, NHLF cells were exposed to L-virus containing media for 1 h, then the cells were washed and incubated for 2 days in 2D monocultures. NHLF cells were then harvested, and spheroids were produced as described above. SAEC-NHLF-(ICAT-GFP) and SAEC-NHLF-(GFP) shperoids were cultered for an additional 5 days before RNA isolation.

Western blot analysis

Lung tissues of young (1 months) and old (24 months) lyzed in lysis buffer (20 mM HEPES pH 7.4, 1 mM $MgCl_2$, 1 mM $CaCl_2$ 137 mM NaCl, 50 mM β-glycerophosphate, 2 mM EGTA, 1% Triton ×100 supplemented with 1 mM DTT, 2 mM PMSF, 2 μg mL^{-1} leupeptin, 1 μg mL^{-1} aprotinin, 1 μg mL^{-1} pepstatine) on ice for 20 min, then snap-frozen in liquid nitrogen and stored at −70 °C until used. Just before loaded on 10% SDS-PAGE, the samples were boiled in 2× SDS sample buffer. Protein concentrations of lung extracts were measured with bicinchoninic-acid kit (Sigma), then the same amount of proteins were loaded to polyacrylamide gels then transferred to nitrocellulose membrane. The membrane was blocked with TBS buffer containing 1% of BSA and 0.05% of Tween and incubated with primary antibodies (anti-β-catenin, anti-Wnt4 both purchased from Santa Cruz, both at 1:1000 dilution) overnight. HRP-conjugated anti-Mouse (Sigma) and anti-Goat (Sigma) were used as secondary antibodies (both at 1:1000 dilution). Blots were visualized using the chemiluminescent Supersignal kit (Pierce) and densitometrically scanned for quantification (LAS 4000).

RNA isolation

Cell samples were homogenized in RA1 reagent, and RNA was isolated using the NucleospinII RNA isolation kit (Macherey-Nagel, Dueren, Germany). DNA digestion was performed on column with RNase-free DNase. The concentration of RNA samples was measured using Nanodrop (Thermo Scientific, Waltham, MA, USA).

Real-Time quantitative PCR

cDNA was synthesized with high-capacity RNA to cDNA kit (Life technologies Inc., Carlsbad, CA, USA) using 1 μg of total RNA according to manufacturer's recommendation. Reverse transcription was performed in 20 μL total volume using random hexamer primers. RT–PCR was used for gene expression analysis. Gene expression levels were determined by gene-specific RT–PCR using ABsolute QPCR SYBR Green Low ROX master mix (ABGene, Thermo Scientific) and 100 nM primers on the Applied Biosystems 7500 thermal cycler system. For normalization, β-actin was used as housekeeping gene. The primer sequences are shown in the Table 1. PCR conditions were set as follows: one cycle 95 °C for 15 min, 40 cycles 95 °C for 15 s, annealing temperature was 58 °C and 72 °C for 1 min for elongation. Specification of the PCR was determined by using a dissociation stage. The calculation of the RT–PCR results was performed as follows: The mean Ct values are determined by calculating the average of the parallel samples. ΔCt is calculated by subtracting the mean Ct of the housekeeping gene from the mean Ct of the gene of interest. ΔΔCt is constituted by the difference between the old sample Ct and the young sample as a control Ct values. Finally, the relative quantity (RQ), which is presented in the diagrams, can be calculated by applying the formula: $RQ = 2^{-\Delta\Delta Ct.}$

Immunofluorescence

Mice were anaesthetized with sodium pentobarbital intraperitoneally and then they were perfused through the right ventricle with PBS solution as described above. Then lungs were filled up with 1:1 ratio of

Table 1 Primer sequences

Primers	Forward	Reverse
Mouse β-Actin	TGGCGCTTTTGACTCAGGA	GGGAGGGTGAGGGACTTCC
Mouse PTHrPR	GGCGAGGTACAAGCTGAGAT	ACACTTGTGTGGGACACCAT
Mouse Wnt4	CTCAAAGGCCTGATCCAGAG	TCACAGCCACACTTCTCCAG
Mouse Wnt5a	AAGCAGGCCGTAGGACAGTA	CGCCGCGCTATCATACTTCT
Mouse Wnt11	GCTCCATCCGCACCTGTT	CGCTCCACCACTCTGTCC
Mouse PPARγ	CCCAATGGTTGCTGATTACAAA	AATAATAAGGTGGAGATGCAGGTTCT
Mouse ADRP	CGCCATCGGACACTTCCTTA	GTGATGGCAGGCGACATCT
Human β-Actin	GCGCGGCTACAGCTTCA	CTTAATGTCACGCACGATTCC
Human PPARγ	GGTGGCCATCCGCATCT	GCTTTTGGCATACTCTGTGATCTC
Human S100A4	TGGAGAAGGCCCTGGATGT	CCCTCTTTGCCCGAGTACTTG
Human IL1β	TCAGCCAATCTTCATTGCTCAA	TGGCGAGCTCAGGTACTTCTG

PBS:cryostate embedding media (TissueTek Alphen an den Rijn, The Netherlands) and frozen down at −80 °C.

The human samples were kept in PBS containing 1% of FCS at room temperature till processing. The filling, freezing and sectioning steps were performed as described above.

At the endpoint of the treatment, the 3D human lung tissue models were carefully removed from the 24-well plates and embedded into TissueTek embedding media and immediately frozen down at −80 °C.

For histological observations, cryostat sections (7–9 μm) were fixed with cold acetone for 10 min.

Antibodies, fluorescent imaging

Following the rehydration and blocking step (for 20 min in 5% BSA in PBS), immunofluorescent staining was performed. Anti-Wnt5a (Santa Cruz, Santa Cruz, CA, USA) antibodies were used as primary antibodies, and anti-EpCAM1-FITC (clone G8.8, American Type Culture Collection (ATCC) directly labeled antibody was used as a control staining for 1 h. For human samples, anti-pro-SPC antibody (Millipore Billerica, MA, USA) was used. For the spheroids, anti-KRT7 (DAKO, Agilent, Santa Clara, CA, USA) antibodies and anti-E-cadherin (AbCam, Cambridge, UK) antibodies were applied.

The secondary antibodies were northern light anti-mouse NL-493 and northern light anti-rabbit NL-557 (R&D systems, Minneapolis, MO, USA). The nuclei were counterstained with DAPI (Serva, Heidelberg, Germany). Pictures were captured using Olympus IX81 fluorescence microscope (Shinjuku, Tokyo, Japan) equipped with CCD camera and analysis software. Images were processed and analyzed with ImageJ.

Fluorescent images were analyzed, and the mean intensity was calculated with STRATAQUEST software (Biotech-Europe, Prague, Czech Republic).

Hematoxylin–eosin staining

Preparation of mouse and human lung sections is described above. Following sectioning, the samples were immediately stained with hematoxylin and eosin. Pictures were scanned with Pannoramic Desk machine (3D Histech, Budapest, Hungary) then analyzed by Pannoramic viewer software (3D Histech).

Neutral lipid staining

Mouse lung sections were made as described above. Cold acetone fixed sections were stained with anti-EpCAM1 antibody directly conjugated with FITC (ATCC clone G8.8), then the LipidTox (Life Technologies Inc.) staining was performed. Fluorescent images were captured and analyzed as described above.

Statistical analysis

If applicable, data are presented as mean ± standard deviation (SD), and the effects between various experimental groups were compared with the Student *t*-test. $P < 0.05$ was considered as significant.

Funding

PJE was supported by the European Union and the State of Hungary, co-financed by the European Social Fund in the framework of TÁMOP-4.2.4.A/ 2-11/1-2012-0001 'National Excellence Program'.

Author contributions

KT, CV, FD, ED, BD performed the experiments, KK prepared recombinant constructs. SG, JL and SV provided the lung tissue and performed stainings and analysis of primary human lung tissues, and PJE designed the studies, and KT, CV and PJE have written the manuscript.

Conflict of interest

None declared.

References

Baarsma HA, Spanjer AI, Haitsma G, Engelbertink LH, Meurs H, Jonker MR, Timens W, Postma DS, Kerstjens HA, Gosens R (2011) Activation of WNT/β-catenin signaling in pulmonary fibroblasts by TGF-β is increased in chronic obstructive pulmonary disease. *PLoS ONE* **6**, e25450.

Balogh P, Bebök Z, Németh P (1992) Cellular enzyme-linked immunocircle assay. A rapid assay of hybridomas produced against cell surface antigens. *J. Immunol. Methods* **153**, 141–149.

Barkauskas CE, Cronce MJ, Rackley CR, Bowie EJ, Keene DR, Stripp BR, Randell SH, Noble PW, Hogan BL (2013) Type 2 alveolar cells are stem cells in adult lung. *J. Clin. Invest.* **123**, 3025–3036.

Bartis D, Csongei V, Weich A, Kiss E, Barko S, Kovacs T, Avdicevic M, D'Souza VK, Rapp J, Kvell K, Jakab L, Nyitrai M, Molnar TF, Thickett DR, Laszlo T, Pongracz JE (2013) Down-regulation of canonical and up-regulation of non-canonical Wnt signalling in the carcinogenic process of squamous cell lung carcinoma. *PLoS ONE* **8**, e57393.

Bovia F, Salmon P, Matthes T, Kvell K, Nguyen TH, Werner-Favre C, Barnet M, Nagy M, Leuba F, Arrighi JF, Piguet V, Trono D, Zubler RH (2003) Efficient transduction of primary human B lymphocytes and nondividing myeloma B cells with HIV-1-derived lentiviral vectors. *Blood* **101**, 1727–1733.

Brack AS, Conboy MJ, Roy S, Lee M, Kuo CJ, Keller C, Rando TA (2007) Increased Wnt signaling during aging alters muscle stem cell fate and increases fibrosis. *Science* **317**, 807–810.

Briolay A, Lencel P, Bessueille L, Caverzasio J, Buchet R, Magne D (2013) Autocrine stimulation of osteoblast activity by Wnt5a in response to TNF-α in human mesenchymal stem cells. *Biochem. Biophys. Res. Commun.* **430**, 1072–1077.

Calvi CL, Podowski M, D'Alessio FR, Metzger SL, Misono K, Poonyagariyagorn H, Lopez-Mercado A, Ku T, Lauer T, Cheadle C, Talbot CC, Jie C, McGrath-Morrow S, King LS, Walston J, Neptune ER (2011) Critical transition in tissue homeostasis accompanies murine lung senescence. *PLoS ONE* **6**, e20712.

Chilosi M, Poletti V, Rossi A (2012) The pathogenesis of COPD and IPF: distinct horns of the same devil? *Respir. Res.* **13**, 3.

Crosby LM, Waters CM (2010) Epithelial repair mechanisms in the lung. *Am. J. Physiol. Lung Cell. Mol. Physiol.* **298**, L715–L731.

Engelhardt JF (2001) Stem cell niches in the mouse airway. *Am. J. Respir. Cell Mol. Biol.* **24**, 649–652.

Ferguson HE, Kulkarni A, Lehmann GM, Garcia-Bates TM, Thatcher TH, Huxlin KR, Phipps RP, Sime PJ (2009) Electrophilic peroxisome proliferator-activated receptor-gamma ligands have potent antifibrotic effects in human lung fibroblasts. *Am. J. Respir. Cell Mol. Biol.* **41**, 722–730.

Florian MC, Nattamai KJ, Dörr K, Marka G, Uberle B, Vas V, Eckl C, Andrä I, Schiemann M, Oostendorp RA, Scharffetter-Kochanek K, Kestler HA, Zheng Y, Geiger H (2013) A canonical to non-canonical Wnt signalling switch in haematopoietic stem-cell ageing. *Nature* **503**, 392–396.

Gao J, Serrero G (1999) Adipose differentiation related protein (ADRP) expressed in transfected COS-7 cells selectively stimulates long chain fatty acid uptake. *J. Biol. Chem.* **274**, 16825–16830.

Graham TA, Clements WK, Kimelman D, Xu W (2002) The crystal structure of the beta-catenin/ICAT complex reveals the inhibitory mechanism of ICAT. *Mol. Cell* **10**, 563–571.

Kazi AS, Tao JQ, Feinstein SI, Zhang L, Fisher AB, Bates SR (2010) Role of the PI3-kinase signaling pathway in trafficking of the surfactant protein A receptor P63 (CKAP4) on type II pneumocytes. *Am. J. Physiol. Lung Cell. Mol. Physiol.* **299**, L794–L807.

Königshoff M, Eickelberg O (2010) WNT signaling in lung disease: a failure or a regeneration signal? *Am. J. Respir. Cell Mol. Biol.* **42**, 21–31.

LeVine AM, Hartshorn K, Elliott J, Whitsett J, Korfhagen T (2002) Absence of SP-A modulates innate and adaptive defense responses to pulmonary influenza infection. *Am. J. Physiol. Lung Cell. Mol. Physiol.* **282**, L563–L572.

Li B, Zhong L, Yang X, Andersson T, Huang M, Tang SJ (2011) WNT5A signaling contributes to Aβ-induced neuroinflammation and neurotoxicity. *PLoS ONE* **6**, e22920.

Maina JN, West JB, Orgeig S, Foot NJ, Daniels CB, Kiama SG, Gehr P, Mühlfeld C, Blank F, Müller L, Lehmann A, Brandenberger C, Rothen-Rutishauser B (2010) Recent advances into understanding some aspects of the structure and function of mammalian and avian lungs. *Physiol. Biochem. Zool.* **83**, 792–807.

Meyer KC, Ershler W, Rosenthal NS, Lu XG, Peterson K (1996) Immune dysregulation in the aging human lung. *Am. J. Respir. Crit. Care Med.* **153**, 1072–1079.

Park KS, Wells JM, Zorn AM, Wert SE, Laubach VE, Fernandez LG, Whitsett JA (2006) Transdifferentiation of ciliated cells during repair of the respiratory epithelium. *Am. J. Respir. Cell Mol. Biol.* **34**, 151–157.

Paxson JA, Gruntman A, Parkin CD, Mazan MR, Davis A, Ingenito EP, Hoffman AM (2011) Age-dependent decline in mouse lung regeneration with loss of lung fibroblast clonogenicity and increased myofibroblastic differentiation. *PLoS ONE* **6**, e23232.

Polkey MI, Harris ML, Hughes PD, Hamnegärd CH, Lyons D, Green M, Moxham J (1997) The contractile properties of the elderly human diaphragm. *Am. J. Respir. Crit. Care Med.* **155**, 1560–1564.

Pongracz JE, Stockley RA (2006) Wnt signalling in lung development and diseases. *Respir. Res.* **7**, 15.

Rauner M, Stein N, Winzer M, Goettsch C, Zwerina J, Schett G, Distler JH, Albers J, Schulze J, Schinke T, Bornhäuser M, Platzbecker U, Hofbauer LC (2012) WNT5A is induced by inflammatory mediators in bone marrow stromal cells and regulates cytokine and chemokine production. *J. Bone Miner. Res.* **27**, 575–585.

Rehan VK, Torday JS (2012) PPARγ signaling mediates the evolution, development, homeostasis, and repair of the lung. *PPAR Res.* **2012**, 289867.

Rock JR, Barkauskas CE, Cronce MJ, Xue Y, Harris JR, Liang J, Noble PW, Hogan BL (2011) Multiple stromal populations contribute to pulmonary fibrosis without evidence for epithelial to mesenchymal transition. *Proc. Natl. Acad. Sci. U.S.A.* **108**, E1475–E1483.

Rooney SA, Young SL, Mendelson CR (1994) Molecular and cellular processing of lung surfactant. *FASEB J.* **8**, 957–967.

Schultz CJ, Torres E, Londos C, Torday JS (2002) Role of adipocyte differentiation-related protein in surfactant phospholipid synthesis by type II cells. *Am. J. Physiol. Lung Cell. Mol. Physiol.* **283**, L288–L296.

Sharma G, Goodwin J (2006) Effect of aging on respiratory system physiology and immunology. *Clin. Interv. Aging* **1**, 253–260.

Takada I, Kouzmenko AP, Kato S (2009) Wnt and PPARgamma signaling in osteoblastogenesis and adipogenesis. *Nat. Rev. Rheumatol.* **5**, 442–447.

Talaber G, Kvell K, Varecza Z, Boldizsar F, Parnell SM, Jenkinson EJ, Anderson G, Berki T, Pongracz JE (2011) Wnt-4 protects thymic epithelial cells against dexamethasone-induced senescence. *Rejuvenation Res.* **14**, 241–248.

Tolep K, Higgins N, Muza S, Criner G, Kelsen SG (1995) Comparison of diaphragm strength between healthy adult elderly and young men. *Am. J. Respir. Crit. Care Med.* **152**, 677–682.

Torday J, Hua J, Slavin R (1995) Metabolism and fate of neutral lipids of fetal lung fibroblast origin. *Biochim. Biophys. Acta* **1254**, 198–206.

Torday JS, Torres E, Rehan VK (2003) The role of fibroblast transdifferentiation in lung epithelial cell proliferation, differentiation, and repair *in vitro*. *Pediatr. Pathol. Mol. Med.* **22**, 189–207.

Varisco BM, Ambalavanan N, Whitsett JA, Hagood JS (2012) Thy-1 signals through PPARγ to promote lipofibroblast differentiation in the developing lung. *Am. J. Respir. Cell Mol. Biol.* **46**, 765–772.

Veldhuizen R, Possmayer F (2004) Phospholipid metabolism in lung surfactant. *Subcell. Biochem.* **37**, 359–388.

Verbeken EK, Cauberghs M, Mertens I, Lauweryns JM, Van de Woestijne KP (1992) Tissue and airway impedance of excised normal, senile, and emphysematous lungs. *J. Appl. Physiol. (1985)*, **73**, 2342–2353.

Vuga LJ, Ben-Yehudah A, Kovkarova-Naumovski E, Oriss T, Gibson KF, Feghali-Bostwick C, Kaminski N (2009) WNT5A is a regulator of fibroblast proliferation and resistance to apoptosis. *Am. J. Respir. Cell Mol. Biol.* **41**, 583–589.

Willis BC, Borok Z (2007) TGF-beta-induced EMT: mechanisms and implications for fibrotic lung disease. *Am. J. Physiol. Lung Cell. Mol. Physiol.* **293**, L525–L534.

Yee M, Vitiello PF, Roper JM, Staversky RJ, Wright TW, McGrath-Morrow SA, Maniscalco WM, Finkelstein JN, O'Reilly MA (2006) Type II epithelial cells are critical target for hyperoxia-mediated impairment of postnatal lung development. *Am. J. Physiol. Lung Cell. Mol. Physiol.* **291**, L1101–L1111.

Supporting Information

Additional Supporting Information may be found in the online version of this article at the publisher's web-site.

Fig. S1 The structure of the lung during aging presented by SkyScan micro Computed Tomograph; photographs of lungs of (A): 1–month-old and (B): 24-month-old Balb/c mice were obtained in 180 degree and converted to 3D by CTVol software (Skyscan).

Fig. S2 Characterization of 3D lung micro-tissue model.

Fig. S3 Inflammatory cytokines in 2D vs 3D tissues.

Fig S4 Pro-surfactant protein C expression following rhWnt5a treatment of the 3D human lung tissue model.

Short communication

Resveratrol is not the "magic bullet" of longevity when it comes to pulmonary senescence

Kovacs, T[1,5]; Ernszt, D[1,5], Rapp, J[1,5], Smuk, G[2], Sarosi, V[3]; Jakab, L[4], Kvell, K[1,5]; Pongracz, JE[1,5]

[1]Department of Pharmaceutical Biotechnology, [2] Department of Pathology, [3] Department of Pulmonology, [4]Department of Surgery, Faculty of Medicine, University of Pécs, [5] János Szentágothai Research Centre, University of Pécs, Pécs, Hungary,[6]

Corresponding author:
Dr JE Pongracz
Department of Pharmaceutical Biotechnology,
Faculty of Medicine,
University of Pecs
12 Szigeti Str
Pecs 7624
Szentágothai Research Centre
University of Pecs
Ifjúság útja 20.
Pecs 7622
Hungary
Tel: +36 30 435 7944

Resveratrol has been under investigation as a Sirtuin1 activator and consequent promoter of longevity. Sirtuin1, however, can down-regulate PPARγ, a central promoter of alveolar regeneration mechanism implying that resveratrol cannot constrain pulmonary senescence.

In our recent work (Kovacs *et al.* 2014) deregulation of the Wnt family of glyco-lipo-protein signaling cascades was established. The altered molecular microenvironment reduces regenerative capacity and facilitates the marked loss of tissue mass leading to significant decrease in lung capacity described as senile emphysema. One of the central players of the described pulmonary aging mechanism is the peroxisome proliferator-activated receptor gamma (PPARγ), a member of the nuclear hormone receptor superfamily, it regulates triglyceride uptake from the blood, maintains lipofibroblast differentiation that supports ATII function as well as surfactant production in the lung (Kovacs *et al.* 2014). In a constant quest to derail the aging program and to maintain healthy lung function for a considerably longer period of time, pharmacological Sirtuin1 (Sirt1) activators have been considered in recent studies (Rahman *et al.* 2012). Sirtuins (Silent Information Regulator) have been discovered in aging yeast, and this family of nicotinamide adenine dinucleotide NAD^+-dependent protein/histone deacetylase enzymes have been described to increase the life-span of several organisms . Mammals contain seven Sirtuins, Sirt1–7 with highly varied biological functions and diverse subcellular localizations (Haigis & Guarente 2006; Michan & Sinclair 2007). Sirt1 and Sirt7 have been shown to localize to the nucleus and also to modulate PPARγ activity. It has recently been discovered that Sirt1 represses PPARγ, therefore up-regulation of Sirt1 triggers lipolysis and leads to fat loss in white adipose tissue , while in contrast to Sirt1, Sirt7 promotes adipogenesis by directly binding to Sirt1 and suppressing Sirt1 activity (Bober *et al.* 2012). Amongst modulators of Sirt expression and function various small molecules including several plant polyphenols like resveratrol (Pervaiz & Holme 2009)) were investigated . As resveratrol is found in grapes and red wine it is popularly quoted to provide the beneficial effects of red wine consumption (Kopp 1998). In the light of our recent studies (Kovacs *et al.* 2014) describing a β-catenin dependent Wnt-signal regulated down-regulation of PPARγ as a central trigger for reduced regenerative capacity of the aging alveoli, it has become questionable whether Sirt1 activators would be beneficial to protect against pulmonary senescence.

In order to investigate, Sirt expression was analyzed in $EpCAM1^+$ epithelial and in $EpCAM1^-$ non-epithelial cells of 1 month and 24 months old young and aged Balb/c mice.

Lung cells were purified and sorted as described earlier (Kovacs *et al.* 2014). Interestingly, both Sirt1 and Sirt7 message levels increased with age, although Sirt7 showed a higher, nearly two fold increases in both epithelial and non-epithelial cell types (Figure 1A). As in literature Sirt1 and Sirt7 act differentially on PPARγ, it appeared that Sirt7 up-regulation in the aging lung is an attempt to counteract Sirt1- and Wnt4-induced down-regulation of PPARγ that leads to a drastic decline in lung function. However, as mouse studies are not always relevant to human tissues, protein levels of Sirt1 and Sirt7 were investigated in primary human lung tissue sections. Cryostat sections (7-9 μm) of young (21 yrs) and old (73 yrs) primary human lungs were stained with anti-Sirt1 or anti-Sirt7 specific antibodies. At protein level the difference between young (21 yrs) and old (73 yrs) lungs was more pronounced than at transcript level of aging Balb/c mice. In contrast to mRNA data of mouse studies, Sirt7 protein was undetectable in either young or old primary human lung samples (data not shown). Sirt1 protein, however, increased significantly in old human lung tissue (Figure 1B, 1C).

To compare the effects of Sirt1 and the β-catenin activator Wnt4 on PPARγ expression in human lungs, further experiments were performed in three dimensional (3D) human lung tissue aggregates (Kovacs *et al.* 2014). 3D human lung tissue aggregates were prepared from primary human small airway epithelial cells and primary human lung fibroblasts (Kovacs *et al.* 2014), then were treated with 10 nM resveratrol and the β-catenin pathway activator Wnt4 ias Wnt4 over-expressing cell line supernatant (Kovacs *et al.* 2014) for three days. To investigate the simultaneous effects of resveratrol and Wnt4, 3D tissue aggregates were also treated with the combination of the two compounds using the above described culture conditions. Both resveratrol and Wnt4 down-regulated PPARγ expression, and their effect was additive (Figure 1D).

Previously described molecular mechanisms also support our results. For example Holloway et al suggest that loss of Sirt1 protein leads to a significant decrease in the level of Dvl proteins, one of the signal transducer molecules from Wnt receptors. Following the reasoning along those lines, if Sirt1 is over-expressed and/or activated it renders Dvl proteins constitutively active leading to β-catenin accumulation in the cell nucleus and transcription of β-catenin dependent genes (Holloway *et al.* 2010) that can lead to reduction of PPARγ (Kovacs *et al.* 2014). Sirt1 interference with the β-catenin signaling pathway has also been reported in osteogenesis. In the osteogenic process Sirt1 promotes osteogenesis over

adipogenesis in mesenchymal stem cells (MSC) by deacetylating β-catenin which in turn accumulates in the nucleus and activates β-catenin dependent mechanisms.

In conclusion, while resveratrol/Sirt1, might effectively promote longevity in certain primitive organisms or specific tissue types (e.g. thymus), the lung may not benefit from activation of Sirt1 at all and "cost-benefit" has to be analyzed carefully before large doses of Sirt1 activators are taken systemically.

Ethical Statement

Following patient consent, lung tissue samples were collected anonymously during lung resections at the Department of Surgery and the project was approved both for the use of human samples and animal studies by the Ethical Committee of the University of Pécs.

Acknowledgments

PJE was supported by the European Union and the State of Hungary, co-financed by the European Social Fund in the framework of TÁMOP-4.2.4.A/ 2-11/1-2012-0001 'National Excellence Program'.

The authors declare no conflict of interest.

Figure

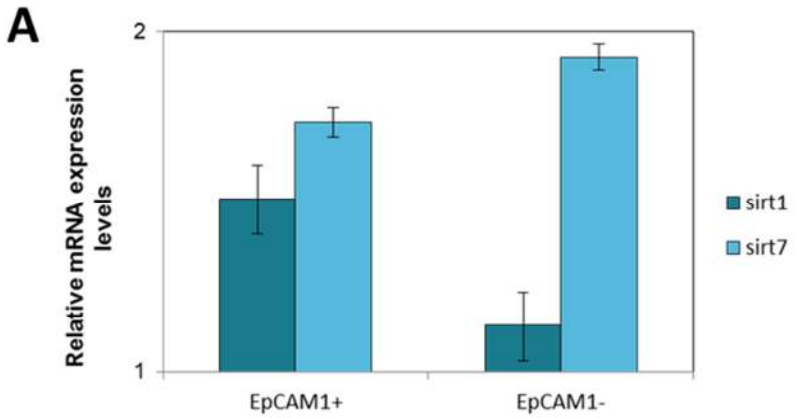

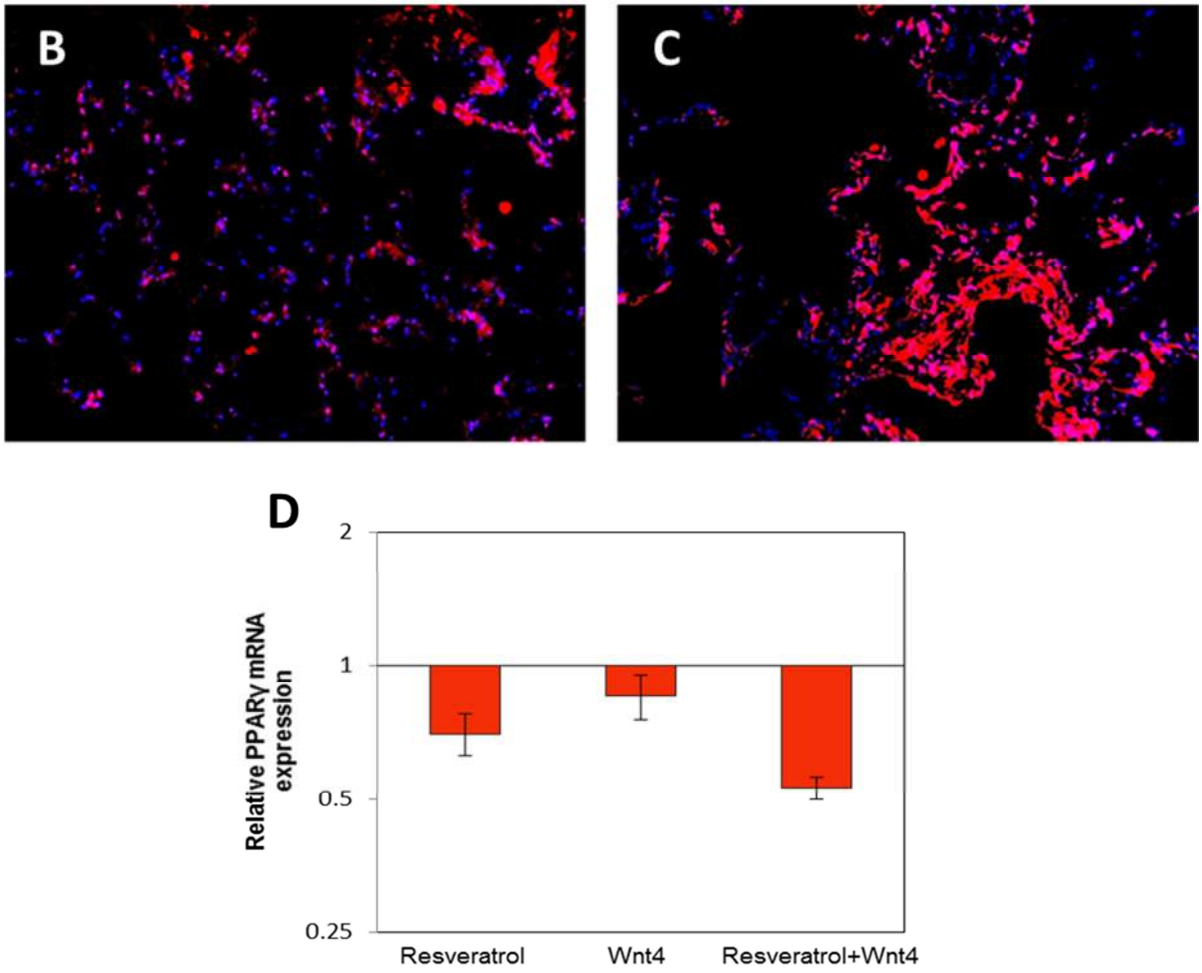

Figure legend

Figure 1. A: mRNA expression levels of Sirt1 (f: GACGATGACAGAACGTCACA; r: GATCGGTGCCAATCATGAGA) and Sirt7 (f: TGAGACAGAAGAGGCTGTCG; r: TGGATCCTGCCACCTATGTC) molecules in 24 months Balb/c mouse lung epithelial and non-epithelial cells were measured using qRT-PCR analysis and relative expression was determined to β-actin (f: TGGCGCTTTTGACTCAGGA; r: GGGAGGGTGAGGGACTTCC), then compared to Sirt1 and Sirt7 expression in test animals 1 month of age. Immunofluorescence staining of Sirt1 in **B:** 21 years old and **C:** 73 years old human lung tissue sections. Sirt1 (Santa Cruz, CA, USA) antibody was used as primary antibody. The secondary antibody was northern light anti-rabbit NL-557 (R&D systems, Minneapolis, MO, USA). The nuclei were counterstained with DAPI (Serva, Heidelberg, Germany). **D**: Relative PPARγ mRNA (f: GGTGGCCATCCGCATCT r: GCTTTTGGCATACTCTGTGATCTC) expression levels in 3D lung tissues following 1

week of 10 nM resveratrol and Wnt4 supernatant exposure. Human β-actin was used as inner control (f: GCGCGGCTACAGCTTCA r: CTTAATGTCACGCACGATTCC).

References

Bober E, Jian, Smolka C, Ianni A, Vakhrusheva O, Krüger M , Braun T (2012). Sirt7 promotes adipogenesis by binding to and inhibiting Sirt1ed^eds). *BMC Proceedings*.

Haigis MC , Guarente LP (2006). Mammalian sirtuins--emerging roles in physiology, aging, and calorie restriction. *Genes Dev*. **20**, 2913-2921.

Holloway KR, Calhoun TN, Saxena M, Metoyer CF, Kandler EF, Rivera CA , Pruitt K (2010). SIRT1 regulates Dishevelled proteins and promotes transient and constitutive Wnt signaling. *Proc Natl Acad Sci U S A*. **107**, 9216-9221.

Kopp P (1998). Resveratrol, a phytoestrogen found in red wine. A possible explanation for the conundrum of the 'French paradox'? *Eur J Endocrinol*. **138**, 619-620.

Kovacs T, Csongei V, Feller D, Ernszt D, Smuk G, Sarosi V, Jakab L, Kvell K, Bartis D , Pongracz JE (2014). Alteration in the Wnt microenvironment directly regulates molecular events leading to pulmonary senescence. *Aging Cell*. **13**, 838-849.

Michan S , Sinclair D (2007). Sirtuins in mammals: insights into their biological function. *Biochem J*. **404**, 1-13.

Pervaiz S , Holme AL (2009). Resveratrol: its biologic targets and functional activity. *Antioxid Redox Signal*. **11**, 2851-2897.

Rahman MA, Kim NH, Kim SH, Oh SM , Huh SO (2012). Antiproliferative and cytotoxic effects of resveratrol in mitochondria-mediated apoptosis in rat b103 neuroblastoma cells. *Korean J Physiol Pharmacol*. **16**, 321-326.